5-2013

PUMP CONTROLLER DESIGN FOR VARIABLE PRIMARY FLOW CONFIGURATION SYSTEMS

Yifan Shi
University of Nebraska, yifanshi@unomaha.edu

PUMP CONTROLLER DESIGN FOR VARIABLE PRIMARY FLOW CONFIGURATION SYSTEMS

by

Yifan Shi

A THESIS

Presented to the Faculty of

The Graduate College at the University of Nebraska

In Partial Fulfillment of Requirements

For the Degree of Master of Science

Major: Architectural Engineering

Under the Supervision of Professor Josephine Lau

Lincoln, Nebraska

May, 2013

PUMP CONTROLLER DESIGN FOR VARIABLE PRIMARY FLOW CONFIGURATION SYSTEMS

Yifan Shi, M.S.

University of Nebraska, 2013

Advisor: Josephine Lau

Pump systems are utilized widely in Heating, Ventilation and Air-Conditioning (HVAC) systems. There are mainly three configuration types: (1) the constant primary-only flow configuration, (2) the constant primary/variable secondary flow configuration, and (3) the variable primary-only flow configuration. This thesis focuses on finding the optimal control strategy for it and programming a controller for easy in-field usage.

In this thesis, the pump brake horse power (BHP) of the three pump configurations is simulated and compared using varying control methods. The best pump efficiency staging and DP reset control methods are implemented into the pump controller. A one month field experiment is performed in a chiller/boiler plant at the Western Nebraska Community College (WNCC) for the pump controller. The proposed control strategy is found to achieve an energy savings of 64.5% in comparison to the constant flow configuration.

ACKNOWLEDGEMENTS

I would like to express my deepest gratitude to my advisor Dr. Josephine Lau. She is very patient and has helped me with my research and course work over the last few years. Her encouragement and persistence has inspired me to be consistent and hard-working, traits that I believe will continue to help me throughout my career.

I would like to thank Dr. Siu-Kit Lau and Dr. Moe Alahmad for their support of my research. I am much honored to have them serve on my advisor committee. I would like to extend a special thank you to Dr. Mingsheng Liu for serving as my mentor, guiding me throughout the ins and outs of the research process. In addition, I would also like to thank the engineering team at WNCC as well as to my colleagues from Bes-Tech, Inc, including Zhan Wang, Yunhua Li, Bei Zhang, and Steve Lian for their help and support. Special thanks go to Emily Rieur and Ronald Ulmer for their hard work on editing the thesis.

Finally, I am very thankful and happy that my parents, my brother and my friends are always there to support me and encourage me in everything I do.

TABLE OF CONTENTS

LIST OF FIGURES

LIST OF TABLES

Chapter 1 Introduction

1.1 Introduction

Pump systems such as the chilled water loop pump system, the condenser water pump system, the cooling tower water pump system, and other boiler, and distribution pump systems are utilized widely in Heating, Ventilating and Air-Conditioning (HVAC) systems. Pursuing optimal pump system configurations and control methods is becoming increasingly important in efforts to ensure global environmental protection and to meet energy conservation goals. Pump configurations evolved from constant primary-only flow (CPF) systems, to constant primary/variable secondary flow (PSF) systems, and finally to variable primary-only flow (VPF) systems. The CPF configuration was used a lot in the past when saving energy was not as great of a concern. This is because the installation costs of the pumps are low, the control scheme is simple and the maintenance procedures are easy to implement. Since energy conservation is gradually becoming more of a concern, the PSF is developed and used to save pump energy in the last 20 years (Liu M. , 2002b). However, the PSF configuration has some drawbacks. These include: 1) higher initial cost, more pipes and pumps required compared to VPF and CPF; 2) more space consumed; 3) primary pump and chiller energy wasted (Bahnfleth & Peyer, 2004a). A lot of chiller systems in the PSF configuration suffer from the low delta-T syndrome, which is defined as the lower temperature difference

between the return and supplied chilled water when compared to design conditions. Taylor analyzed the causes of low delta-T and concluded that while a few can be avoided, the others cannot be mitigated (Taylor, 2002a). Thus the VPF configuration was proposed in order to save more energy and mitigate the effects of a low-delta-T. The PSF and VPF systems both have their share of proponents and critics. Proponents of the VPF configuration see it as a promising future replacement for the PSF (Kirsner, 1996); other scholars take more neutral positions. In simulations, Bahnfleth and Peyer proved that while the VPF saves more energy than the PSF, it is not a 'cure all' as technical difficulties, such as staging the chiller without a large flow fluctuation still needed to be solved (Bahnfleth & Peyer, 2004a). Taylor also does not doubt the VPF's many advantages (Taylor, 2002b). The author also believes that the VPF is promising in terms of both energy savings and for avoiding a low-delta-T and this thesis will discuss the control strategies for the VPF pump systems in detail.

1.2 Research Objective

Considering the potential benefits and increasing interest in VPFs, the research objective of this thesis is to develop an optimal pump controller for the variable primary pump system. The following key points are discussed herein:

1) Compare the energy consumption for the CPF, PSF and VPF using different control methods; compare the energy consumption of different control methods for the VPF configuration, and integrate the optimal control methods

together for the VPF pump system.

2) Implement the optimal control method from step 1) into an embedded control board.

3) Install the controller into a pump system and validate the control result.

Chapter 2 Literature Review

In Chapter 2, the operation, control as well as the advantages and disadvantages of the CPF, PSF, and VPF configurations are reviewed. Optimal pump control methods are also reviewed for the PSF and VPF configurations with multiple pumps. Finally, the parameter determination and the optimization for proportional-integral-differential (PID) control is reviewed considering that it is widely used to modulate the pump speed to maintain control expectations in both the PSF and VPF configurations. The optimal pump control methods will be integrated together to enable smoother, more efficient control of the variable primary only system in Chapter 3.

2.1 Three Pump System Configurations

The benefits, drawbacks and operation of the system are discussed in this section for the CPF, PSF, and VPF configurations.

2.1.1 Constant Primary Flow Configuration

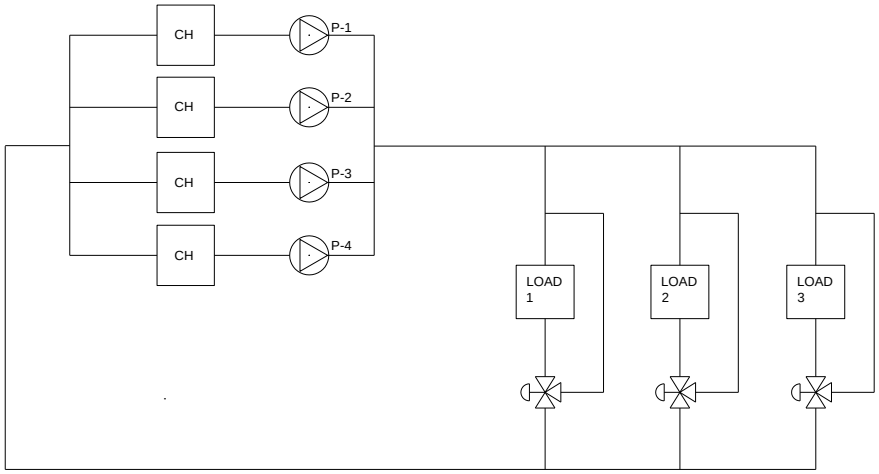

symbol	name	symbol	name
	pump		3-way valve

Figure 2-1: Constant Primary-Only Flow Configuration

The CPF is the simplest pump configuration. It consists of one set of pumps that operate at full speed to match the design chiller evaporator flow rates or boiler flow rate. 3-way valves are used at the load side to modulate the supply water flowing through the coils with the varying load. At high loads, less water is bypassed. The system resistance is considered constant when the 3-way valve effect is ignored. This configuration has the following benefits: 1) low installation costs with one set of pumps and no variable frequency drive (VFD); 2) much simpler control. The main drawback is that pump energy is wasted (Hubbard, 2011).

2.1.2 Constant Primary-Variable Secondary Flow configuration

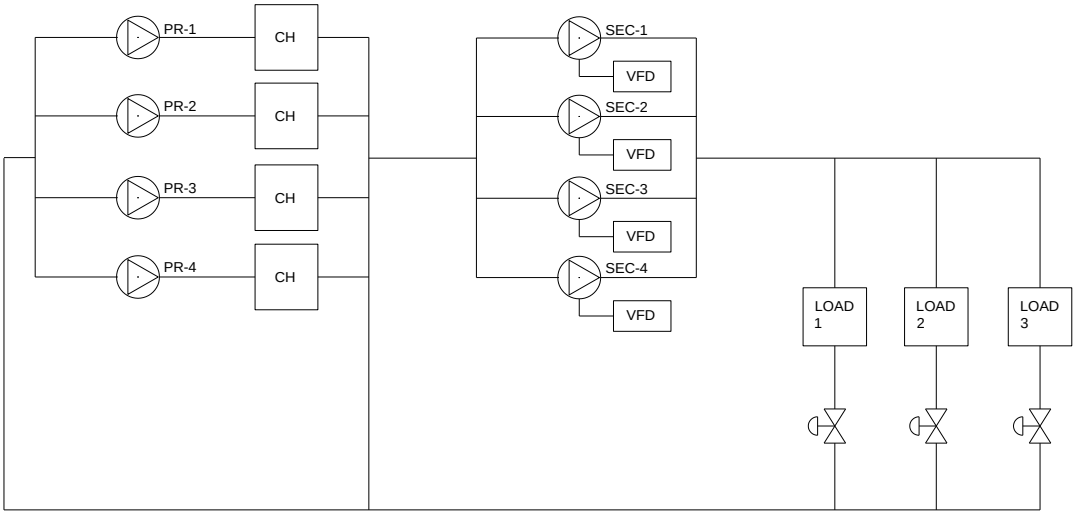

Figure 2-2: Constant Primary/Variable Secondary Flow Configuration

The constant primary variable secondary system (PSF configuraiton) has two sets of pumps consisting of two independent circuits separated by a decoupling bypass pipe. This decoupling pipe can have flow that travels in either direction. The primary side pump operates at a constant flow to match the design evaporator flow rates of the chillers or boilers which is similar to the pumps in the CPF configuration. The secondary side pump operates at a variable speed to maintain the loop differential pressure in a hydraulically remote location at the set point (which is called the independent differential pressure). The control valves at the load side are modulated to meet the cooling/heating load. One serious issue for the constant primary/variable secondary system is the “low delta-T syndrome”. When the cooling/heating load is lower than the chiller/boiler design load, the secondary side flow rate is lower than the primary side flow rate and more water thus flows through the decoupling bypass line from the supply to the return, increasing/decreasing the heating/cooling return water temperature. This

leads to a low delta-T.

Compared to the constant primary-only configuration, the PSF configuration has more installation requirements and thus higher installation costs. Since it uses secondary pumps and VFDs, and the configuration also occupies more physical space. However, there are some benefits to using the PSF configuration that some may argue make up for these disadvantages: secondary pump energy is saved, and the control scheme is simple.

2.1.3 Variable Primary Flow Configuration

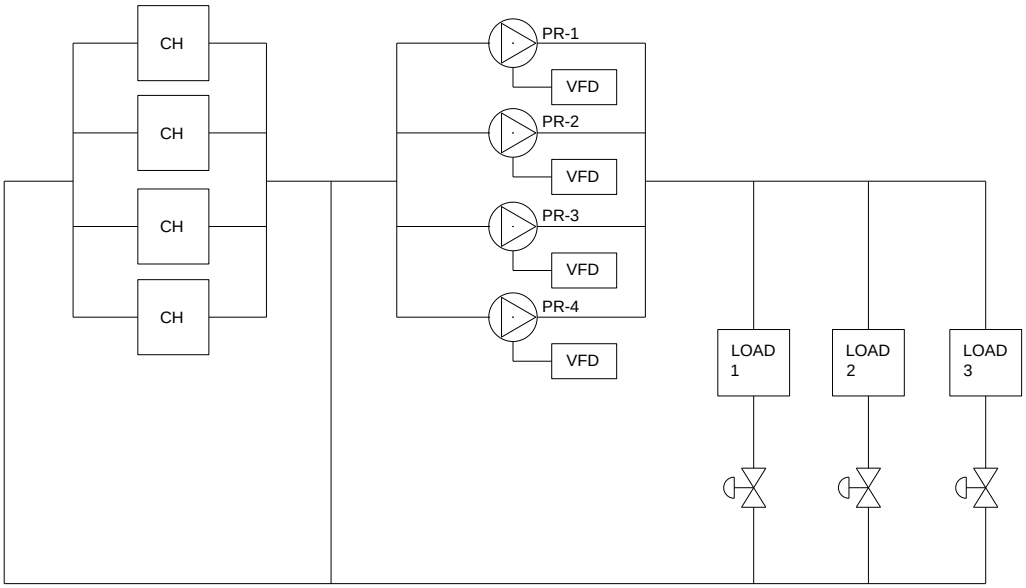

Figure 2-3: Variable Primary-Only Flow Configuration

An increasing number of scholars choose the variable primary-only system as a counterpart to the well-established PSF configuration (Behnfleth & Peyer, 2001 & 2003 & 2004b; Hubbard, 2011; Nonnemann & Flynn, 2010; Taylor, 2002b). Bahnfleth and Peyer provides four reasons for its growing popularity: 1) The variable primary configuration saves more pump energy than the PSF configuration; 2) The variable primary

configuration has a lower initial cost; 3) The PSF configuration has the “low delta-T syndrome” problem; and 4) current packaged chiller controls support the variable chiller flow rate (Bahnfleth & Peyer, 2003).

Similar to the constant primary flow configuration, there is only one set of pumps. A low-flow bypass line is added in parallel with the load lines in variable primary-only pump systems to meet the minimum chiller flow requirement, as shown in Figure 2-3. The low-flow bypass is normally closed and opens only under extreme low load conditions. This ensures that the minimum flow is maintained through the evaporators of the operating chillers. The low-flow bypass is not needed for boilers. The pumps are operated at a variable speed to maintain the distribution cooling/heating loads.

Taylor (2002b) compares the advantages and disadvantages of the VPF and PSF systems. He concludes that the VPF has four main advantages: Lower first costs, less required space, reduced motor design power and motor size, and lower pump power consumption. There are two key disadvantages: The complexity of the bypass control and the difficulties in chiller staging.

Bahnfleth and Peyer (2004a) investigated the potential benefits and issues of the variable primary flow chilled water pump system using model simulations and surveys and arrived at the same conclusion as Taylor. Five parameters were used in the system model: The system configuration, climate, chiller number, cooling load type, and delta T. Bahnfleth and Peyer summarized the following benefits of the VPF based on the simulation:

1) The variable primary configuration saves a total of 2-7 percent compared to the PSF configuration depending on the parameters;

2) Savings decrease with an increased chiller number;

3) Delta T affects savings;

4) Climate affects the amount of energy savings and, not the percentage.

43 designers, 4 chiller manufacturers, and 8 system owner/operators were also interviewed about their experiences engaging with the variable primary flow configuration. The authors conclude that the control scheme and system stability are the main VPF configuration issues that need to be solved.

2.2 Pump Speed Control Method

From the previous discussion it can be seen that the PSF and VPF configurations are more energy efficient in comparison to the CPF configuration. The PSF secondary side pump control is similar to the VPF pump control. In the following, both of the optimization control methods developed for the PSF and VPF are reviewed for the purpose of control of the VPF configuration with multiple parallel pumps. It is separated into two parts: pump staging control and pump speed modulation.

2.2.1 Pump Staging Control

The conventional pump staging control method is the maximum flow staging method. The principle is the following: (assume N pumps are running):

1) If the total water flow rate reaches the maximum flow of the pumps in

operation($\mathrm{Q_t} > \mathrm{N} * \mathrm{Q_{single_{des}}}$), an additional pump will be activated;

2) If the total pump flow rate reaches the low flow limit of the running pumps ($Q_t < (N-1) * Q_{single_{des}}$), one pump will be detracted. (Wang Z. , 2010)

Wang proposed what he terms the best efficiency staging control method and concluded that it saves more energy than the conventional maximum flow staging method. (Wang Z. , 2010).

In the Best efficiency method, the pump activates or deactivates to keep the pump continuously operate at a higher efficiency. The principle can be explained as follows: (assuming there are totally 2 pumps configured in parallel) (Wang Z. , 2010)

1) The pump operating speed and power is obtained from the variable frequency drive; while pump head is obtained from the differential pressure sensor installed at the pump inlet and outlet. (P for power, ω for speed ratio and H for pump head)

2) Calculate the water flow rate using equation [2-1] and [2-2];

   i. When the head scaled into full speed is higher than $\boldsymbol{H_{crit}}$, the flow rate is calculated by equation [2-2];

   ii. When it is lower than $\boldsymbol{H_{crit}}$, flow rate is calculated by equation [2-1].

$$\boldsymbol{if}\ \frac{H}{\omega} < \boldsymbol{H_{crit}}, \boldsymbol{then}\ \ \boldsymbol{Q_s} = \frac{-a_1*\omega-\sqrt{(a_1*\omega)^2-4*a_2*(a_0*\omega^2-H)}}{2*a_2} * \boldsymbol{n_{ext}} \qquad [2\text{-}1]$$

$$\boldsymbol{if}\ \frac{H}{\omega} > \boldsymbol{H_{crit}}, \boldsymbol{then}\ \ \boldsymbol{Q_s} = \frac{-b_1\omega^2+\sqrt{b_1^2\omega^4+4b_2\omega(b_0\omega^3-P/n_{ext})}}{2b_2\omega} * \boldsymbol{n_{ext}} \qquad [2\text{-}2]$$

Where,

a_0, a_1, a_2, b_0, b_1 and b_2, are coefficients of the pump pressure-flow curve and power-flow performance curves. They can be obtained with 2nd order polynomial equation regression.

n_{ext}, is the number of running pumps in the secondary loop;

H_{crit}, defines when the power-flow curve is used and when the pressure-flow curve is used to calculate the flow rate;

3) Calculate the current pump efficiency;

$$\boldsymbol{\eta_{ext} = Q_t * \frac{H}{P_{ext}} * C} \qquad [2\text{-}3]$$

Where,

C, is a constant, conversion factor.

4) Predict the pump speed in the other case:

A. If only 1 pump is in operation, predict the speed as if 2 pumps are running providing the same flow rate and head using equation [2-4]

B. When 2 pumps are in operation, predict the speed as if 1 pump is running providing the same flow rate and head using equation [2-4].

$$\boldsymbol{\omega_{pred} = \frac{-a_1 * Q_s/n_{pred} + \sqrt{(a_1 * Q_s/n_{pred})^2 - 4 * a_0 * (a_2 * (Q_s/n_{pred})^2 - H)}}{2 * a_0}} \qquad [2\text{-}4]$$

Where,

ω_{pred}, is the predicted pump speed ratio in the other case;

Q_s, is the total water flow rate in the secondary loop;

n_{pred}, is the predicted number of running pumps;

H, pump head;

5) Calculate the predicted pump efficiency using equations [2-5] and [2-6].

$$\boldsymbol{P_{pred} = \left(b_0 + b_1 * \frac{Q_s}{n_{pred}*\omega} + b_2 * \left(\frac{Q_s}{n_{pred}*\omega}\right)^2\right) * \omega_{pred}^3 * n_{pred}} \quad [2\text{-}5]$$

$$\boldsymbol{\eta_{prd} = Q_t * \frac{H}{P_{prd}} * C} \quad [2\text{-}6]$$

6) If the predicted efficiency is higher than the current efficiency, then change the operating pump number to n_{pred}:

   A. If $n_{pred} = 1$, then stop the 2nd pump;

   B. If $n_{pred} = 2$, then start the 2nd pump;

7) If the predicted efficiency is lower than the current efficiency, then keep the existing number of pumps on.

An energy comparison simulation of the two staging methods for the PSF and VPF is illustrated in Chapter 3. The optimal staging method is selected.

2.2.2 Pump Speed Control

In distribution pump systems in the PSF or VPF configurations, the remote loop differential pressure is normally controlled to save pump energy. The earliest and most commonly used principle is to maintain the remote differential pressure at a constant value by varying the pump speed with PID control. A differential pressure (DP) reset is

proposed to further save pump energy by reducing the system resistance. This resets the remote loop differential pressure so that it is proportional with the square of the water flow rate. Thus the remote loop differential pressure can be reset using the following equation:

$$\boldsymbol{H_{lp} = H_{lp_{des}} * \left(\frac{Q_t}{Q_{des}}\right)^2} \quad [2\text{-}7]$$

where,

H_{lp}, the remote loop differential pressure at flow Q_t;

$H_{lp_{des}}$, the remote design loop differential pressure;

Q_t, the current total water flow;

Q_{des}, the system total design water flow;

2.3 PID Control-Proportional, Integral, and Derivative

PID tuning is very important for field studies and measurements. It is also the key to achieving a stable, quick response in pump speed control. Since this thesis involves a field study, this section provides background on and addresses potential issues and determines PID parameters of PID control.

A general equation that describes the proportional, derivative and integral control is:

$$\boldsymbol{U = M + K_p * E + K_i * \int Edt + K_d * \frac{dE}{dt}} \quad [2\text{-}8]$$

where,

U, the controller output;

M, the controller offset;

K_p, the proportional gain;

K_i, the integral gain;

K_d, the derivative gain;

E, the difference between the actual controlled variable value and its set point;

The direct digital controller is considered to be a discrete system as it reads data and sends control commands at discrete time intervals. The PID algorithm is represented in discrete form as:

$$\boldsymbol{U = M + K_p * E + K_i * \sum E^n * T_s + K_d * \frac{E^n - E^{n-1}}{T_s}} \quad [2\text{-}9]$$

where,

T_s, the sampling time;

The P, PI and PID control can be categorized into two operation types: direct acting (DA) and reverse acting (RA). DA control increases the control output with an increased controlled variable; RA control decreases the control output with an increased controlled variable. Although PID control is very common, it is not always used in an optimal fashion. It has two offsets. One is the integrator windup issue; the other is the difficulty of obtain a proper control parameters in field.

2.3.1 Integrator Windup Issue

When there is a big difference between the controlled variable and its set point, the control signal starts to increase until reaches the saturation level. At that point, the

integral part continues to increase since the control error signal is still positive. The integral part starts to decrease when the controlled variable equals or is lower than the set point which takes time to decrease the control output and a large overshoot is created. This overshoot is called the integrator windup. Two anti-windup schemes have been developed as a way to counter the problem: conditional integration and tracking schemes.

Conditional integration is an integral action that occurs only when certain conditions are fulfilled. It is easy to implement, but discontinues the control. The tracking method ensures that the integral part is kept at a proper value when the actuator saturates so that the controller is ready to resume the actions as soon as the control error changes (Levine, 1995). The tracking method is utilized in the pump controller discussed in Chapter 3 and 4.

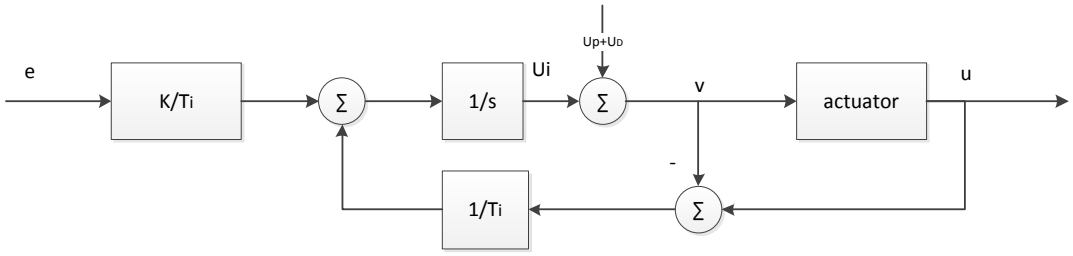

Figure 2-4: PID Controller that avoids windup by tracking (Levine, 1995)

2.3.2 PID Term Determination

A lot of prior work has focused on the method for finding proper PID control parameters. In 1942, Ziegler and Nichols presented two design methods for the PID controller. Their methods determine the dynamics process parameters: Static process

gain, process transport delay and process transport time. The first method is called reaction curve based method and is time-domain based. The method introduces a step change to the open loop plant input and records output with time. It then determines the gain and the time. The 2nd method is frequency-domain based (Ziegler & Nichols, 1942).

2.3.2.1 Time-Domain Based Ziegler-Nichols Method

The procedure of the reaction curve method is as the following:

1) With the plant in open loop, operate the plant in manual mode and wait until it stabilizes at a normal operating point. Say for example that the output settles at $y(t)=y_0$ with the input at $u(t)=u_0$.
2) At an initial time t_0, apply a step change to the plant input so that $u(t_0) = u_2$. The u_2 should be in the range of 10 to 20% of the full range.
3) Record the plant output change with the time until it settles to a new operating point, see Figure 2-5 for a reference plot.

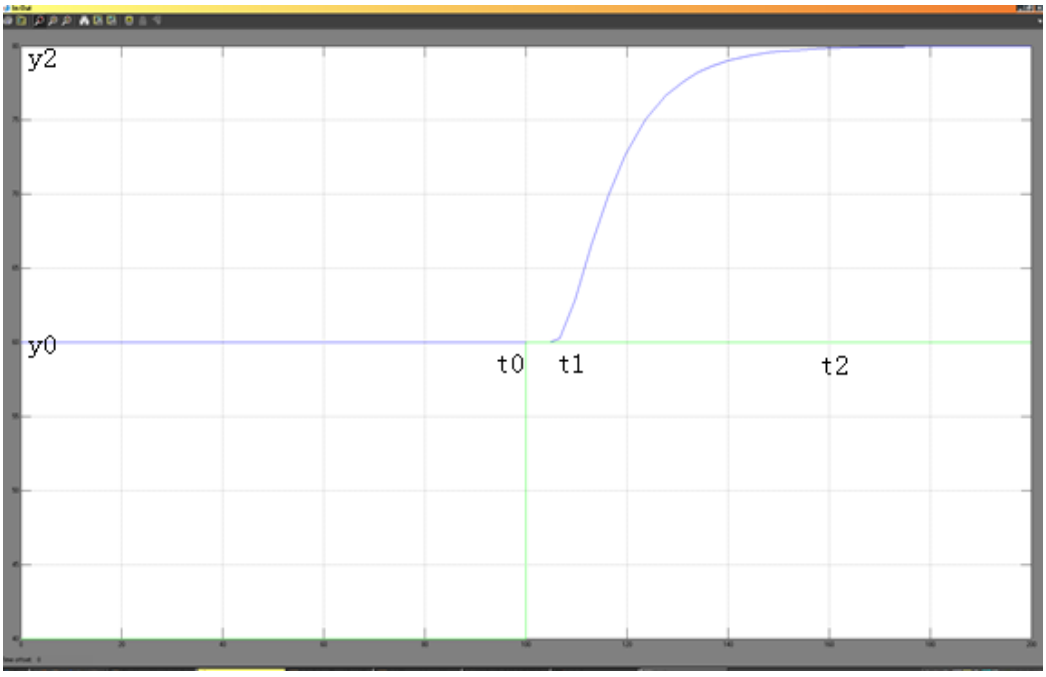

Figure 2-5: step response plot

4) Compute the gain and the time using the following equations:

$$K_0 = \frac{y_2 - y_0}{u_2 - u_0} \quad [2\text{-}10]$$

$$L = t_1 - t_0 \quad [2\text{-}11]$$

$$T = t_2 - t_1 \quad [2\text{-}12]$$

where,

K_0, the static process gain;

L, process transport delay;

T, the process time constant;

5) With the results acquired in step 4, calculate the PID terms according to Table 2-1.

Table 2-1: Ziegler-Nichols Process Reaction Curve based PID parameter determination ((Ziegler & Nichols, 1942)

Controller Type	K_p	T_i	T_D
P	$T/(K_{0*}L)$		
PI	$0.9T/(K_{0*}L)$	3L	
PID	$1.2\ T/(K_{0*}L)$	2L	0.5L

The Ziegler-Nichols process reaction curve based method can be used both in simulations and on-site, as long as the time constant and thus the sampling interval are large enough to record the reaction curve.

2.3.2.2 *Frequency-Domain Based Ziegler-Nichols Method*

This method can be used in simulations but is not practical for on-site use as it will damage the plant. The step-by-step procedure for this method is given in the following:

1) Connect a controller to the plant, set the controller to proportional control and set an initial p gain.
2) Increase the p gain gradually until the plant starts to oscillate.
3) Record the gain and cycle time when this occurs and use the collected values to calculate the PID control parameters.

2.3.2.3 CHR-Chien, Hrones and Reswick Proposed Method

The Ziegler-Nichols method gives unsatisfactory control as they result in closed loop loop systems with very poor damping. Then, in 1952, Chien, Hrones and Reswick modified the coefficients in the Ziegler-Nichols methods to allow for better damping (see

Table 2-2). They also recommended controller type selection using parameter R

(Table 2-3) (Chien, Hrones, & Reswick, 1952).

Table 2-2: CHR modified parameter coefficients from the Ziegler-Nichols method for aperiodic response

Controller Type	K_P	T_I	T_D
P	$0.3T/(K_0*L)$		
PI	$0.35\ T/(K_0*L)$	1.2T	
PID	$0.6\ T/(K_0*L)$	T	0.5L

Table 2-3: CHR recommendation for controller type selection based on parameter R

Controller Type	R = T/L
P	R>10
PI	7.5<R<10
PID parallel	3<R<7.5
Higher order	R<3

2.3.2.4 *Trial-and-Error Method*

Another simple practical method to find PID terms is the trial-and-error method. In this method, initial parameter values are assigned based on practical engineering experience and set guidelines (see Table 2-4) are then used to adjust the terms for proper system operation. This method is utilized in the experiments given in chapter 5.

Table 2-4: rules for tuning PID controller parameters

Response	Rise Time	Overshoot	Settling Time	Offset Error
$P(\uparrow K_P)$	↓	↑	First ↓ then↑	↓
$I(\uparrow K_I)$	↓	↑	First ↓ then↑	Zero
$D(\uparrow K_D)$	↓	↓	↓	No change

2.4 Summary

A review of the literature indicates that as far as is known in the prior art the CPF system is the most energy inefficient pump configuration. Conversely, the VPF system is considered the most energy efficient configuration. Wang (2010) performed both a simulation and a short-term (2 day) field test comparing the conventional maximum flow

pump staging and the best efficiency pump staging control with differential pressure (DP) reset PID modulation of the pump speed in the case of N chiller with N pumps and concluded that the latter one is more energy efficient than prior one (Wang Z. , 2010). The research done by Wang is encouraging but not enough. In this thesis, an energy simulation of multiple parameters is performed to find out the most energy efficient method for VPF systems. These include parameters for the pump configuration, the number of pumps, two pump staging methods and pump speed control methods. An optimal control algorithm obtained from the simulation is then integrated together for the VPF multiple pump configuration. The algorithm is programmed into an automated pump controller to save energy and to increase its ease of use.

Chapter 3 Control Strategy for the Pump Controller

This chapter illustrates the optimal control algorithm for the VPF (variable primary flow) system shown in Figure 3-1. In this system, two parallel pumps are implemented to provide the required load; and no bypass line is added. The Best Efficiency Pump Staging and Loop DP Reset Speed control is further improved upon and implemented into the optimal control algorithm. Energy consumption simulations are performed for all three pump configurations using the optimal algorithm and other control methods in order to help identify the optimal control algorithm for the VPF system.

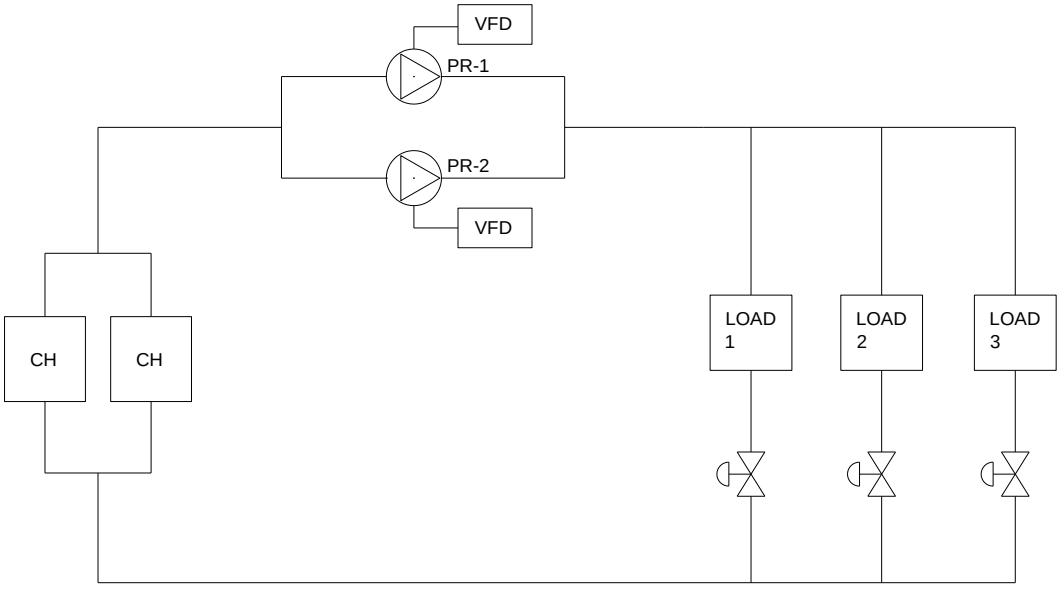

Figure 3-1: Variable Primary Flow without Bypass Line

3.1 Overview of the Control Strategy

In order to use the Best Efficiency staging control (as presented in section 2.2.1 or

section 3.2) and the DP Reset Speed control (as presented in section 2.2.2 or in section 3.3), the pump water flow rate must first be determined. A virtual flow meter developed by Bes-Tech, Inc. is implemented to perform the flow rate calculation. This flow meter has been installed and utilized in many buildings in both the USA and China. It integrates the flow calculation model developed by (Liu, G, 2006; Liu, M, 2002, 2005; Wang, 2007; Wang & Liu, 2007).

In their model, the relationship between the pump head & flow and the pump power & flow rate are expressed as 2nd order polynomial equations as shown in equations [3-1] and [3-2].

$$\frac{H}{\omega^2} = a_0 + a_1 * \left(\frac{Q}{\omega}\right) + a_2 * \left(\frac{Q}{\omega}\right)^2 \quad [3\text{-}1]$$

$$\frac{P}{\omega^3} = b_0 + b_1 * \left(\frac{Q}{\omega}\right) + b_2 * \left(\frac{Q}{\omega}\right)^2 \quad [3\text{-}2]$$

$$\omega = N/N_d \quad [3\text{-}3]$$

where,

Q = current pump water flow rate;

H = current pump inlet and outlet differential pressure;

P = current pump power consumption;

N = current pump speed;

N_d = pump design speed;

a_0, a_1, a_2 = pump head- flow 2nd order polynomial equation coefficients under design speed;

b_0, b_1, b_2 = pump power- flow 2nd order polynomial equation coefficients under design

speed;

ω = speed ratio between current speed and design speed;

The pump water flow rate is obtained by solving the root of the equations using the pump speed, pump head and pump power variables.

Figure 3-2 is a control diagram illustrating the logic of the pump controller. The required inputs are the pump power and pump head. The pump power is obtained from the variable frequency drive of the pump while the pump head is obtained from the water differential pressure sensor.

The control strategy is illustrated as follows: (Figure 3-2)

1) Generate the pump pressure & flow and the power & flow 2nd order polynomial equations;
2) Obtain the power and pressure input values;
3) Use the virtual flow meter to obtain the water flow rate;
4) Use the Best Efficiency method to control the pump ON/OFF;
5) Use the DP Reset PID control to modulate the pump speed;

The Best Efficiency Method and DP Reset PID control are discussed in more detail in the following two sections.

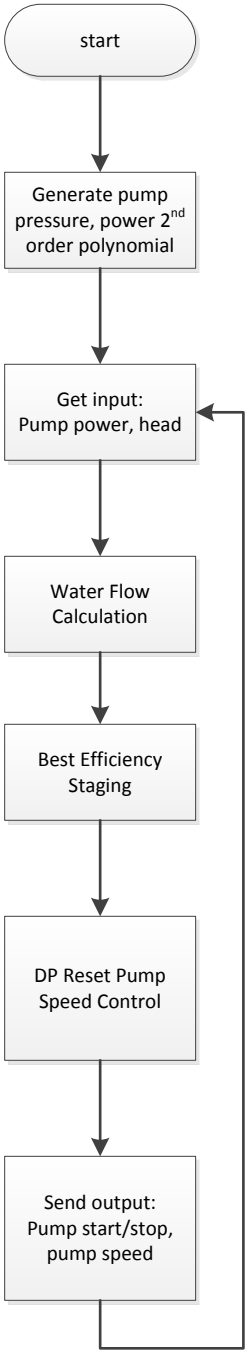

Figure 3-2: Control Diagram for the Pump Controller

3.2 Pump Staging Control

If the Best Efficiency Method is able to find out the equal efficiency point for a specific pump system, the pump staging control logic can be simplified as such: When

the flow rate is lower than the equal efficiency point, one pump runs; when the flow rate is higher than the equal efficiency point, then two pumps operate. As discussed in chapter 2, 6 equations need to be solved to get the equal efficiency point, with 3 of which are 2nd order polynomial equations. It is not applicable for implementation into the pump controller. The following part looks whether the efficiency curve can be illustrated as a 2nd order polynomial equation in order to simplify the control algorithm.

3.2.1 Efficiency Curve

The manufacturer curve for the pump consists of the Head-Flow (H-Q), Power-Flow (P-Q) and Efficiency-Flow (η-Q) curves. The pump efficiency-flow curve is regressed into a 2nd order polynomial equation in the same manner as that of the head and power curves in Liu's (2006) Pump Flow Model.

Take Taco Pump FI6013 as an example of the efficiency curve regression, which is used to verify the pressure-flow and power-flow equations in section 3.4.1. The result is plotted in Figure 3-3 and Figure 3-4. From Figure 3-3, it can be seen that the efficiency rate calculated by the 2nd order polynomial equations is much higher (the majority of the curve is 20% higher) than the actual efficiency (especially when the flow rate is higher than 700GPM as is the case for this particular pump). This difference between the efficiency and actual efficiency rates significantly mitigates the effects of the pump staging control. In Figure 3-4, the manufacture curve efficiency data is shown on the x-axis. The y-axis gives the calculated efficiency using the 2nd order polynomial equation

displayed in Figure 3-3. A linear regression curve that intercepts at zero is thus generated having a coefficient of 1.2413 and R-squared value of 0.557. The two values and the graph show that the calculated efficiency doesn't match the actual value that well. Therefore, it is evident that using a 2nd order polynomial equation for pump efficiency curve is not an optimal solution.

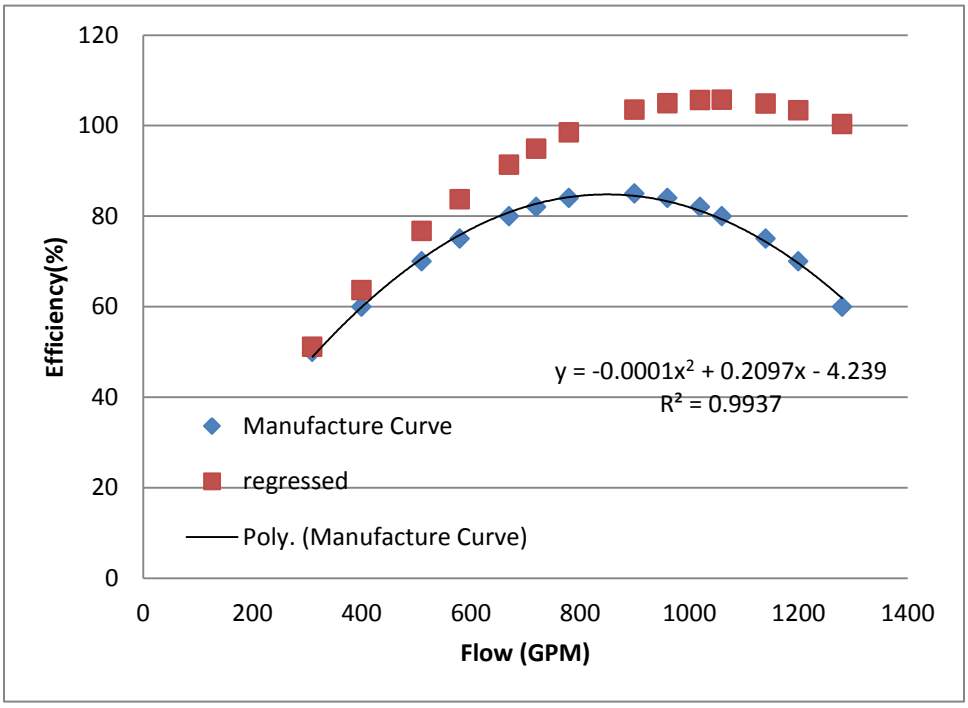

Figure 3-3: The Manufacturer's Efficiency Curve and Regressed Efficiency Curve (Model: FI6013, IN.DIA 11.25")

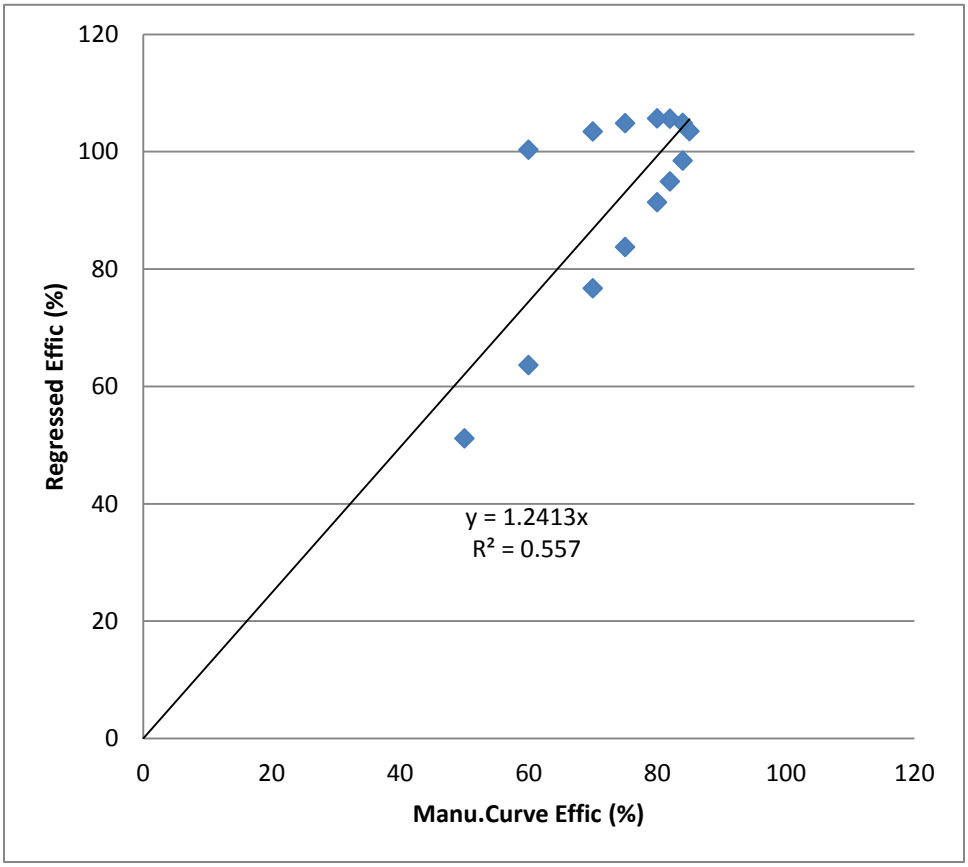

Figure 3-4: Comparison of the Manufacturer's Curve efficiency and Regressed Efficiency (Model: FI6013, IN.DIA 11.25")

The manufacturer's curves of other available impeller diameter pumps in the FI6013 series are analyzed and shown in Appendix A. Pumps that have smaller impeller diameters (9.5" and 10.375") have a regressed efficiency that deviates far from the manufacturer's curves which are similar to the 11.25" impeller diameter pump stated here. For pumps with larger impeller diameters (12.125" and 13"), the regressed efficiency is consistent with the efficiency of the manufacturer's curves. More research must be done to figure out the possible causes of this phenomenon.

In this manner, the pump staging control method introduced in chapter 2 is utilized. Figure 3-5 is a pump staging control diagram for pump staging. There are two points

added to simplify the control and to avoid system hunting:

1) When the pump efficiency is higher than a low limit, the pump staging algorithm is avoided;
2) A time dead band is added in the pump staging control that avoids the system pumps start/stop hunting.

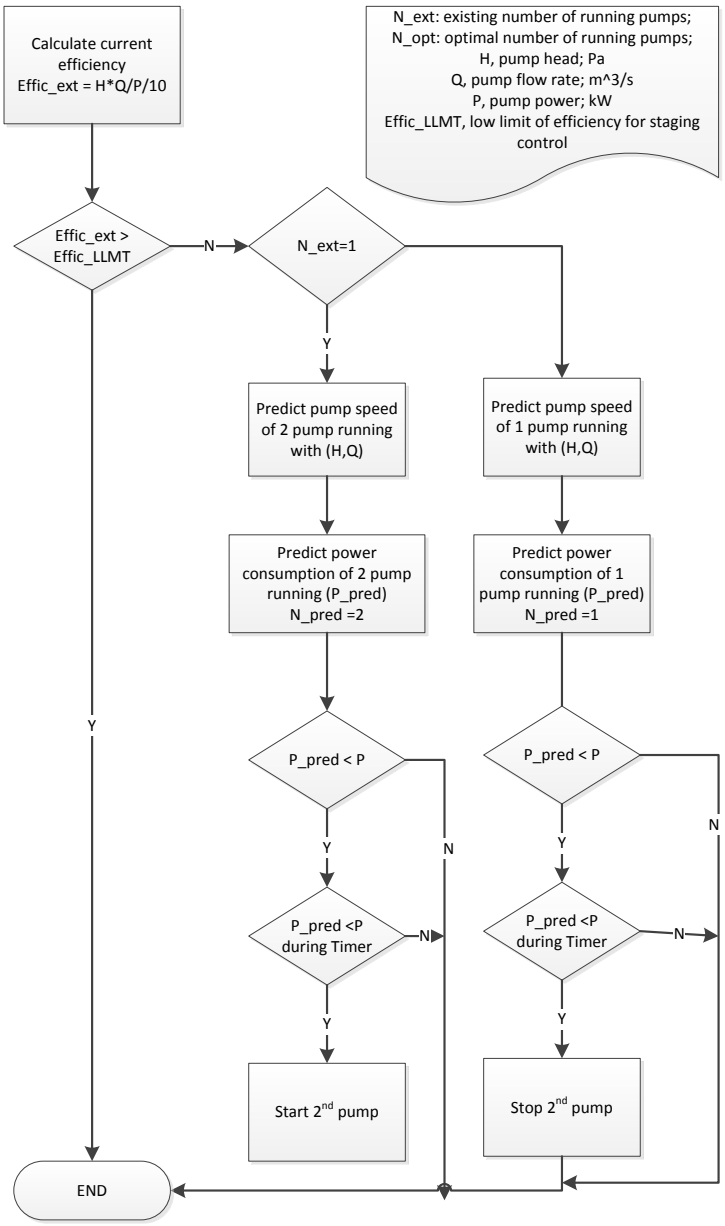

Figure 3-5: Pump Staging Control Diagram

3.3 Pump Speed Control

In this section the DP Reset PID control is illustrated. In terms of the DP reset, the system curve for the VPF system can be expressed in the following equation:

$$\boldsymbol{H} = (\mathbf{1} - \boldsymbol{\alpha_{des}}) * \boldsymbol{H_{des}} + \boldsymbol{\alpha_{des}} * \boldsymbol{H_{des}} * \left(\frac{\boldsymbol{Q_t}}{\boldsymbol{Q_{des}}}\right)^{\mathbf{2}} \quad [3\text{-}4]$$

The loop DP reset can be extracted as the following equation

$$\boldsymbol{H_{lp}} = \boldsymbol{\alpha_{des}} * \boldsymbol{H_{des}} * \left(\frac{\boldsymbol{Q_t}}{\boldsymbol{Q_{des}}}\right)^{\mathbf{2}} \quad [3\text{-}5]$$

where,

H_{lp}, remote loop differential pressure at flow Q_t;

α_{des}, ratio of the design loop differential pressure to the system total design head;

H_{des}, the system design head;

Q_t, the current total water flow;

Q_{des}, the system design water flow;

Substituting $\alpha_{des} * H_{des}$ to $\boldsymbol{H_{lp_{max}}}$, equation [3-5] can be rewritten as the following:

$$H_{lp_{spt}} = \boldsymbol{H_{lp_{max}}} * \left(\frac{Q_t}{Q_{des}}\right)^2\} \quad [3\text{-}6]$$

In order to ensure safe system operations, there is a low limit for the remote loop differential pressure. Thus the reset loop DP is expressed as the following:

$$\boldsymbol{H_{lp_{spt}}} = \left(\frac{\boldsymbol{Q_t}}{\boldsymbol{Q_{des}}}\right)^{\mathbf{2}} * \left(\boldsymbol{H_{lp_{max}}} - \boldsymbol{H_{lp_{min}}}\right) + \boldsymbol{H_{lp_{min}}} \quad [3\text{-}7]$$

where,

$\mathrm{H}_{lp_{spt}}$, loop differential pressure set point;

$\boldsymbol{Q_t}$, current system water flow rate;

Q_{des}, system design water flow rate;

$H_{lp_{max}}$, maximum loop differential pressure set point;

$H_{lp_{min}}$, minimum loop differential pressure set point;

The reverse acting PI control is utilized to modulate the pump speed, with a tracking method applied to avoid integrator wind up.

The control diagram for the speed control is shown in Figure 3-6. The tracking method is shown inside the blue rectangle.

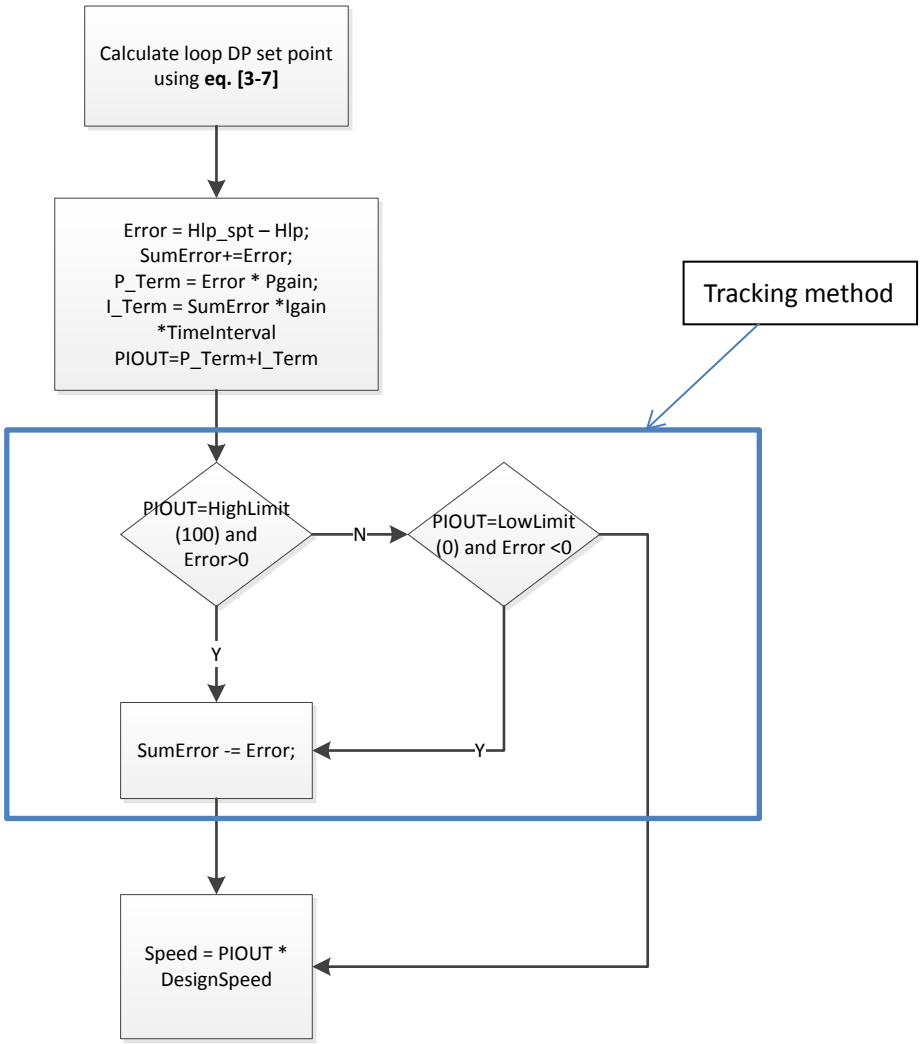

Figure 3-6: Control Diagram for DP Reset PI control

3.4 Simulation

The energy consumption rate is simulated and then compared for each pump configuration with different control methods in this section. This is done in order to verify that the optimal control algorithm proposed in the former section is the most energy efficient.

The pump model and the system pressure-flow model are built before simulation. The pump model determines the power consumed under a certain flow rate and pump head, while the system pressure model determines the system head needed to provide a certain water flow rate.

3.4.1 Pump Model

Liu.M, Liu.G and Wang's pump flow rate model (see section 3.1) is utilized to generate the pump model.

Taco pump FI6013 is used to verify the accuracy of the model. Figure 3-7 shows the manufacturer's pressure curve and displays the regressed 2^{nd} order polynomial equation of the manufacturer's pressure curve in which the R-squared value equals 0.9975.

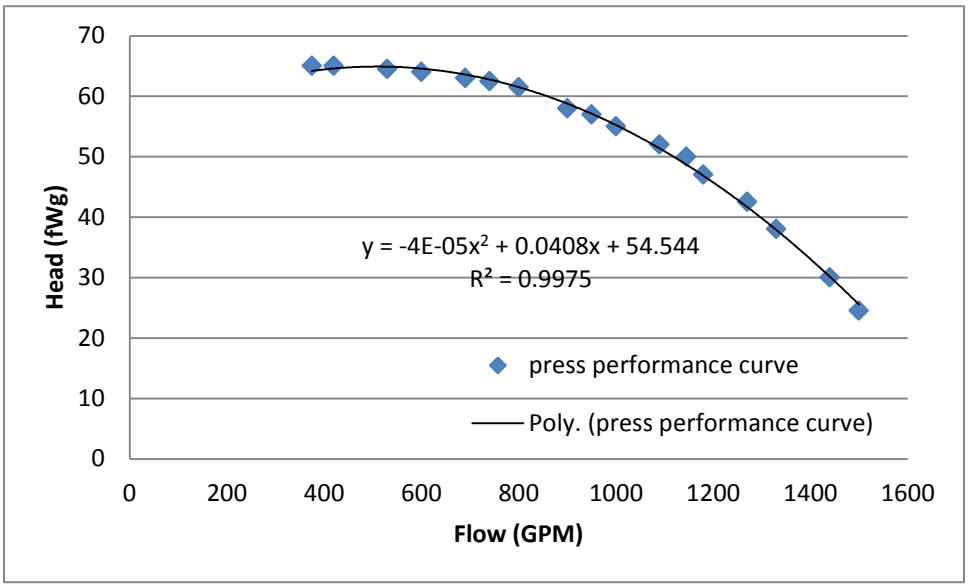

Figure 3-7: Pump Head-Flow Performance Curve (Model: FI6013, IN.DIA 11.25")

The x-axis in Figure 3-8 shows the pressure value obtained directly from the manufacture curve. The data plotted on the y-axis is the pressure value calculated using the 2nd order polynomial equation in Figure 3-7 under the same flow rate as the x-axis pressures. A linear trending line intercept at 0 is regressed. The linear coefficient is 1.0014 and the R-squared value is 0.9975. These values indicate that the 2nd order polynomial equation adequately illustrates the relationship between the pump pressure and the pump flow.

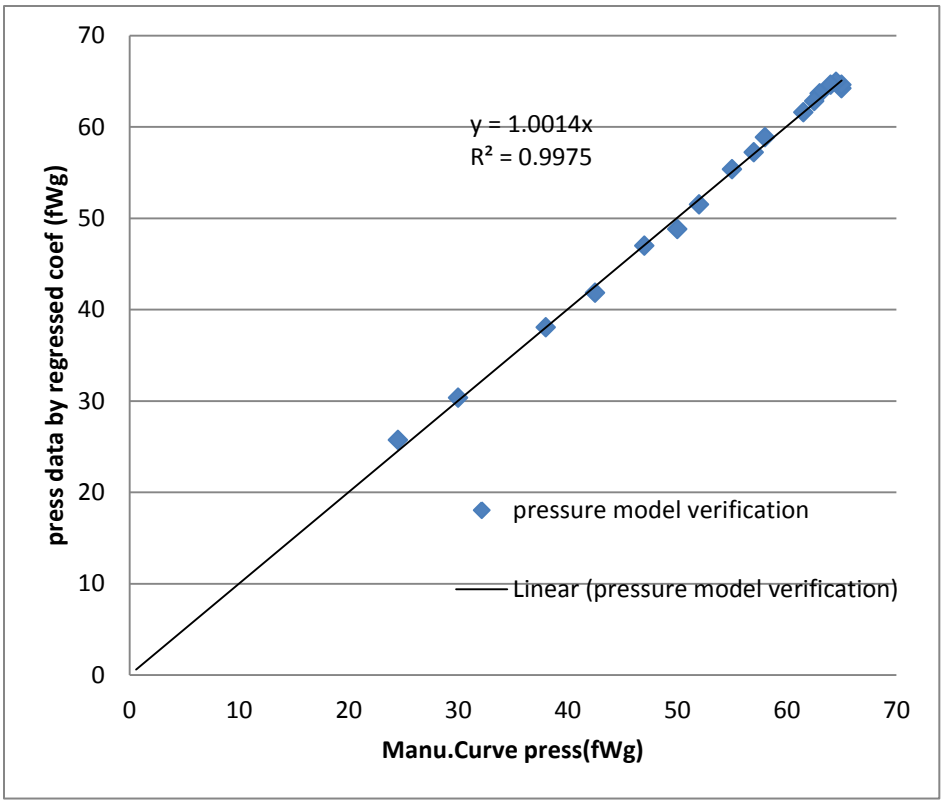

Figure 3-8: Pump Pressure Model Verification (Model: FI6013, IN.DIA 11.25")

Figure 3-9 shows the manufacturer's power curve and displays the regressed 2nd order polynomial equation for the manufacturer's power curve in which the R-squared value equals 0.9751.

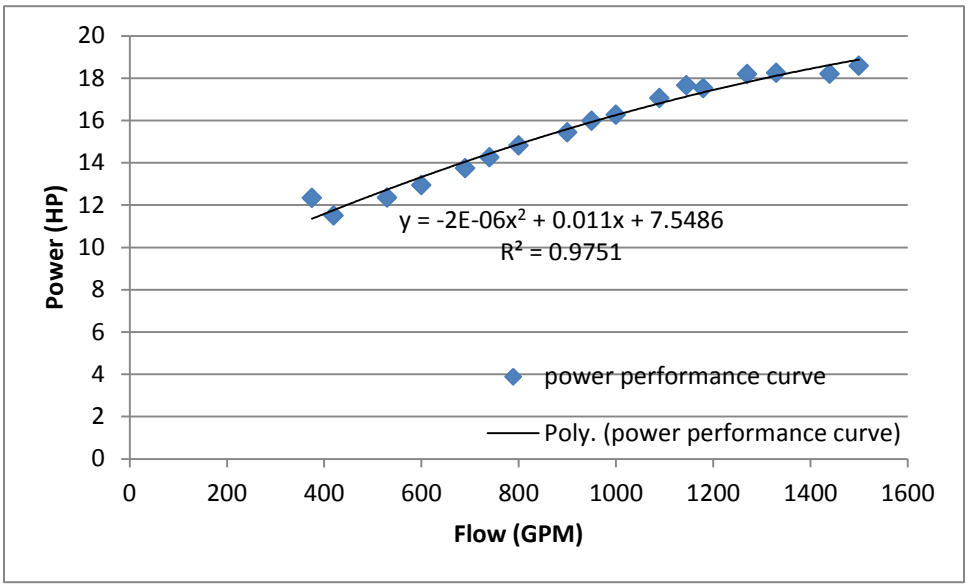

Figure 3-9: Pump Power-Flow Performance Curve (Model: FI6013, IN.DIA 11.25")

In Figure 3-10, the power value from the manufacture curve IS shown on the x-axis. The power value calculated using the 2nd order polynomial equation in Figure 3-9 (under the same flow rate as x-axis powers) is given on the y axis. A linear trending line intercept at zero is regressed. The linear coefficient is 1.0196 and the R-squared value is 0.9736. These values indicate that the 2nd order polynomial equation adequately illustrates the relationship between the pump power and the pump flow.

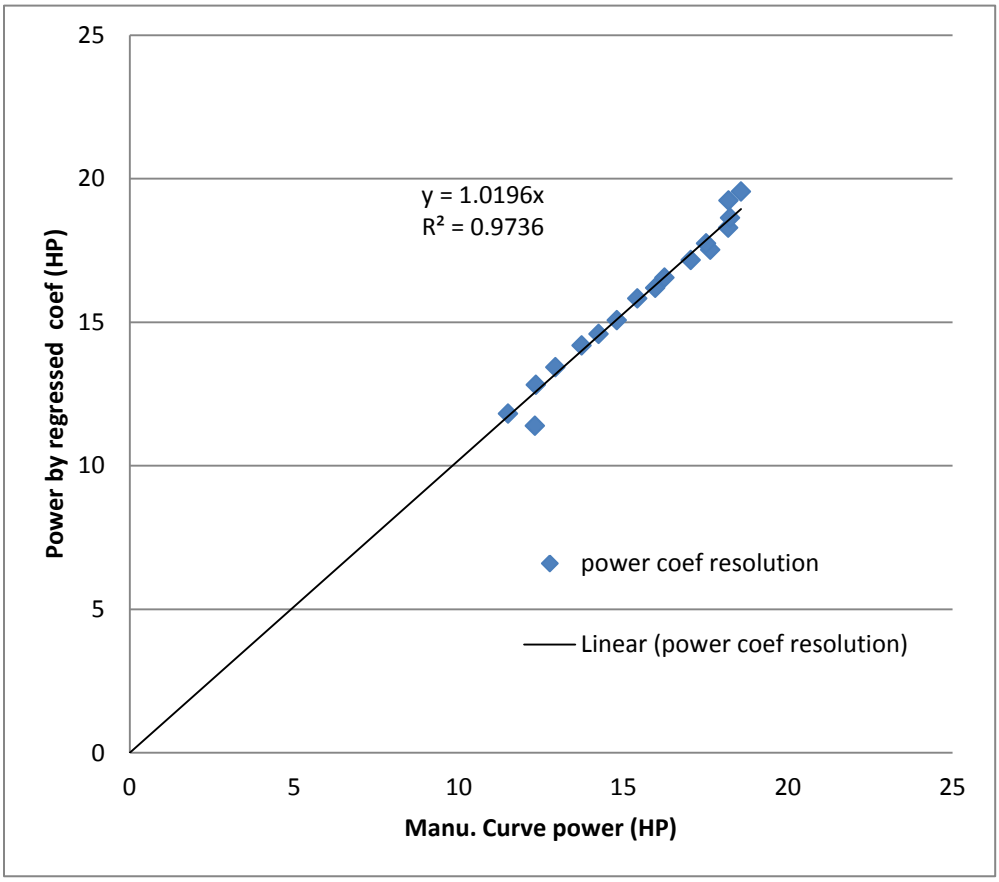

Figure 3-10: Pump Power Model Verification (Model: FI6013, IN.DIA 11.25")

3.4.2 Pump System Pressure Model

This model determines the pump head needed to provide for a specific water flow in a pump system.

The Bernoulli equation is considered the fundamental principle for the water flow system analysis in pipe systems, as shown in equation [**3-8**]

$$\frac{p}{\rho} + \frac{V^2}{2} + gz = constant \qquad [3\text{-}8]$$

where,

p, static pressure, lb/ft^2;

ρ, fluid density, lb/ft^3;

V, fluid average velocity over the cross section of the pipe, ft/s;

z, elevation head, ft;

g, acceleration of gravity, 32.2ft/s^2;

The Bernoulli equation is only valid for steady and incompressible fluid flow along a streamline with no friction. The elevation head is zero in a closed loop pump system. The Bernoulli equation can be simplified in the following for closed loop pump system:

$$\frac{p}{\rho} + \frac{V^2}{2} = \boldsymbol{constant} \qquad \textbf{[3-9]}$$

In a closed loop pump system, assuming that fluid flows from point 1 to point 2 without accessing the pump and with frictional head loss considered between these two points, then equation

[3-9] can be expressed as the following:

$$\frac{p_1}{\rho} + \frac{V_1^2}{2} = \frac{p_2}{\rho} + \frac{V_2^2}{2} + \Delta \boldsymbol{h_{friction}} * \boldsymbol{g} \qquad \textbf{[3-10]}$$

Equation

[3-10] can be converted to the following format revealing that the system pressure drop between point 1 and point 2 is equal to the frictional head.

$$\boldsymbol{H} = \frac{p_1 - p_2}{\rho * g} + \frac{V_1^2 - V_2^2}{2g} = \Delta \boldsymbol{h_{friction}} \qquad \textbf{[3-11]}$$

where,

H, the system head;

The Darcy-Weisbach equation describes the pressure drop caused by the friction of

a fluid flowing in a pipe, see equation

[3-12] below (ASHRAE, 2008).

$$\Delta \boldsymbol{p} = \boldsymbol{f} * \frac{\boldsymbol{L}}{\boldsymbol{D}} * \frac{\boldsymbol{\rho}}{\boldsymbol{g}} * \frac{\boldsymbol{V^2}}{\boldsymbol{2}} \quad \textbf{[3-12]}$$

where,

Δp, pressure drop, lb/ft^2

ρ, fluid density, lb/ft^3

f, friction factor, dimensionless

L, pipe length, ft

D, inside diameter of pipe, ft

V, fluid average velocity, ft/s

g, gravitational acceleration, 32.2 ft/s^2

The head loss can be obtained by dividing the fluid density ρ from both sides of equation

[3-12].

$$\Delta \boldsymbol{h} = \frac{\Delta \boldsymbol{p}}{\boldsymbol{\rho}} = \boldsymbol{f} * \frac{\boldsymbol{L}}{\boldsymbol{D}} * \frac{\boldsymbol{V^2}}{\boldsymbol{2 * g}} \quad [3\text{-}13]$$

where,

Δh, head loss through friction, ft (of fluid flowing)

Applying equation [3-13] into equation

[3-11], the system head equation is obtained:

$$\boldsymbol{H} = \boldsymbol{f} * \frac{\boldsymbol{L}}{\boldsymbol{D}} * \frac{\boldsymbol{V^2}}{\boldsymbol{2 * g}} \quad [3\text{-}14]$$

Through substituting the velocity in equation [3-14] for the fluid flow rate, the relationship between the system head and flow rate between the 2 different points without passing pumps is obtained:

$$\boldsymbol{H = (\frac{8}{\pi^2 * g}) f * \frac{L}{D^5} * Q^2} \quad [3\text{-}15]$$

In equation [3-15], the system pressure drop in the pipe line is proportional to the square of the fluid flow rate. The pipe line is considered as with constant system resistance. The chillers, boilers, and 3-way valves in the pump system are considered similar as a pipe line in system resistance, while the 2-way modulation valve has varying system resistance with varying open position. When system resistance is considered constant, the system head can be expressed as follows:

$$\boldsymbol{H = S * Q^2} \quad [3\text{-}16]$$

where,

S, system resistance;

3.4.3 CPF Configuration Simulation

3.4.3.1 Energy Consumption Simulation of 4 Parallel Pumps for CPF

Pump energy consumption for the CPF is simulated in this section. Assume that the chiller system has one chiller with constant primary only pumping. Four pumps serving the single chiller in parallel are introduced. The system requires a total water flow of 1800GPM and, a design system head of 140 feet. The pump operating point is also presented.

For identical parallel pumps, each pump will provide 450GPM water flow at the head of 140 feet. It is best to select the pump that satisfies the system design flow and design head at its best efficiency point. Using the Taco pump selection wizard, a pump performance curve for each pump is selected as shown in Figure 3-11. The red curve is the selected pump, and the red dot is the design working point.

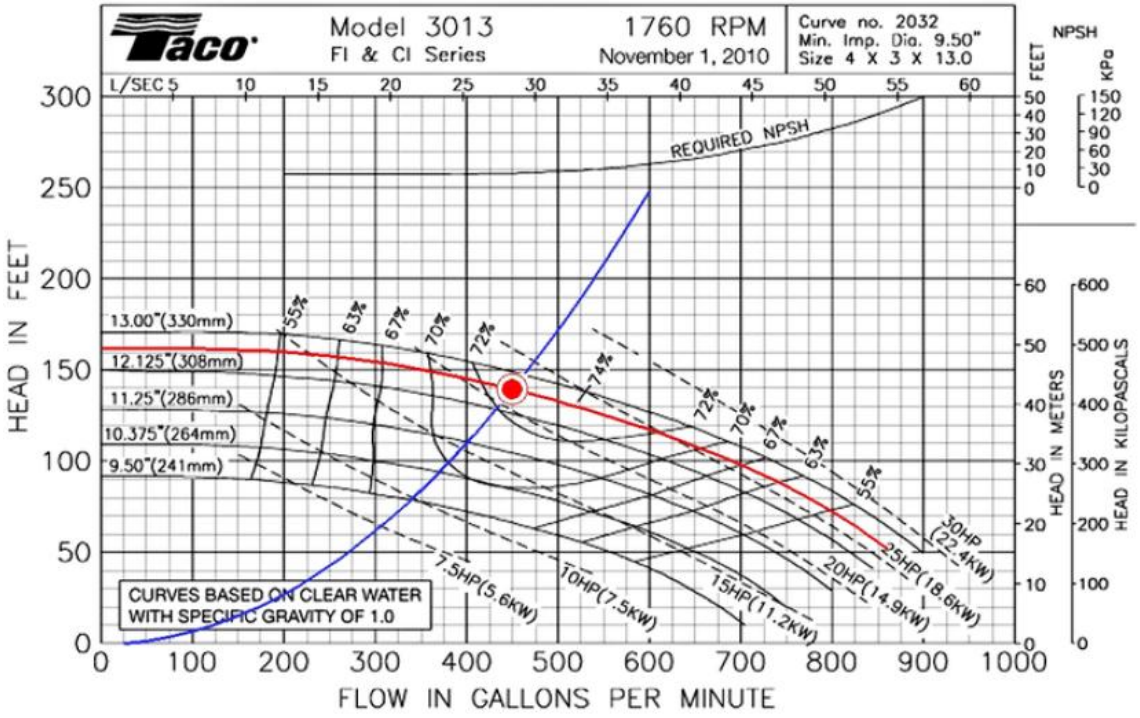

Figure 3-11: pump performance curve of Taco FI3013 series

The key parameters for the selected pump are listed in Table 3-2. The Pump curve is expressed as the following two 2nd order polynomial equations according to section 3.4.1:

$$\frac{H}{\omega^2} = a_0 + a_1 * \frac{Q}{\omega} + a_2 * \left(\frac{Q}{\omega}\right)^2 \quad [3\text{-}17]$$

$$\frac{P}{\omega^3} = b_0 + b_1 * \frac{Q}{\omega} + b_2 * \left(\frac{Q}{\omega}\right)^2 \quad [3\text{-}18]$$

Where,

$a_0 = 158.19653$;

$a_1 = 0.0442387$;

$a_2 = -0.0001894$;

$b_0 = 5.1284018$;

$b_1 = 0.0509092$;

$b_2 = -0.0000303$;

ω = speed ratio;

H, pump head, (unit is fWg);

P, pump power consumption, (unit is HP);

Q, pump flow, (unit is GPM)

Table 3-1: Parameters of Taco FI3013 Pump in CPF power consumption simulation

Manufacture	Model	Qty	Design Flow	Design Head	RPM	Imp Dia	Design Eff	HP	NOL HP
Taco, Inc	FI3013	4	450 GPM	140 feet	1760	12.7”	73%	21.86	27.63

For parallel pump configuration, the total flow rate, total power and total pump head can be expressed by the individual flow, power and pump head in the following equations:

$$\boldsymbol{Q_t = Q * 4} \quad [3\text{-}19]$$

$$\boldsymbol{P_t = P * 4} \quad [3\text{-}20]$$

$$\boldsymbol{H_t = H} \quad [3\text{-}21]$$

The pump performance curve for this CPF system can be expressed in the following

by applying equations [3-19] to [3-21] into equation [3-17] and [3-18]:

$$\frac{H_t}{\omega^2} = \boldsymbol{a_0} + (\boldsymbol{a_1/4}) * \frac{Q_t}{\omega} + (\boldsymbol{a_2/16}) * \left(\frac{Q_t}{\omega}\right)^2 \quad [3\text{-}22]$$

$$\frac{P_t}{\omega^3} = \boldsymbol{4b_0} + \boldsymbol{b_1} * \frac{Q_t}{\omega} + (\boldsymbol{b_2/4}) * \left(\frac{Q_t}{\omega}\right)^2 \quad [3\text{-}23]$$

For CPF system, the system resistance is constant. In this design, the pumps are operating at their design point to provide chiller system required flow and head. So the total power consumption can be calculated by substituting Q_t with 1800 and ω with 1 into equation [**3**-**23**]. The result is listed in the following table and illustrated in Figure 3-13. In Figure 3-12, the pump curve is the system pump performance curve, and the intersection between the pump curve and system curve is the operating point. There is only one working point for the CPF with no pump staging. If the number of pumps is the same as the number of chillers and the pumps are staged on/off with the specific chiller staging on/off, there will be N operating points for this system, where N is the number of chillers or staging.

Table 3-2: CPF power consumption with 4 parallel pumps

Operating point for CPF with 4 pumps			
$\boldsymbol{Q_t}$ **(GPM)**	H_t **(fWg)**	**P (HP)**	$\boldsymbol{P_t}$ **(HP)**
1800	139.75	21.90179	87.60717

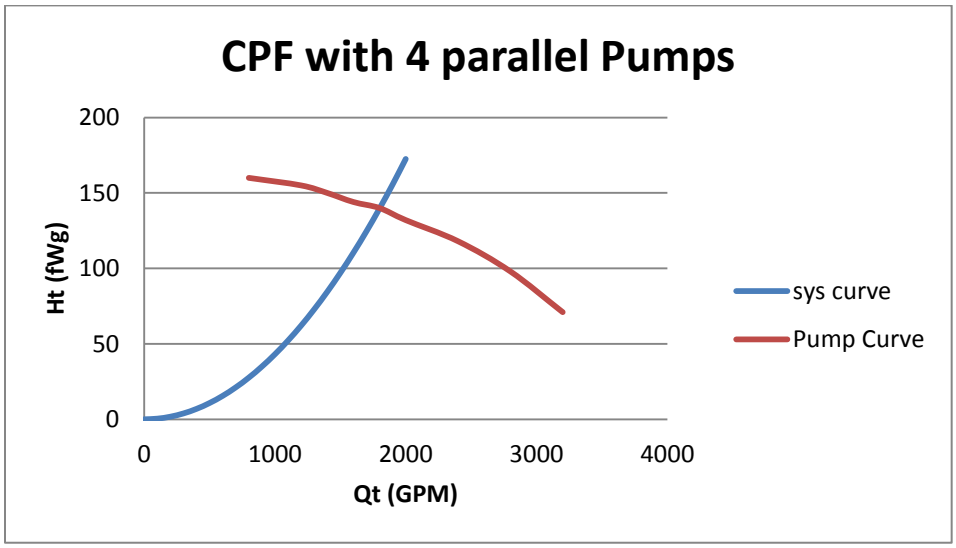

Figure 3-12: Pump performance curve and system curve plot in CPF with 4 pumps

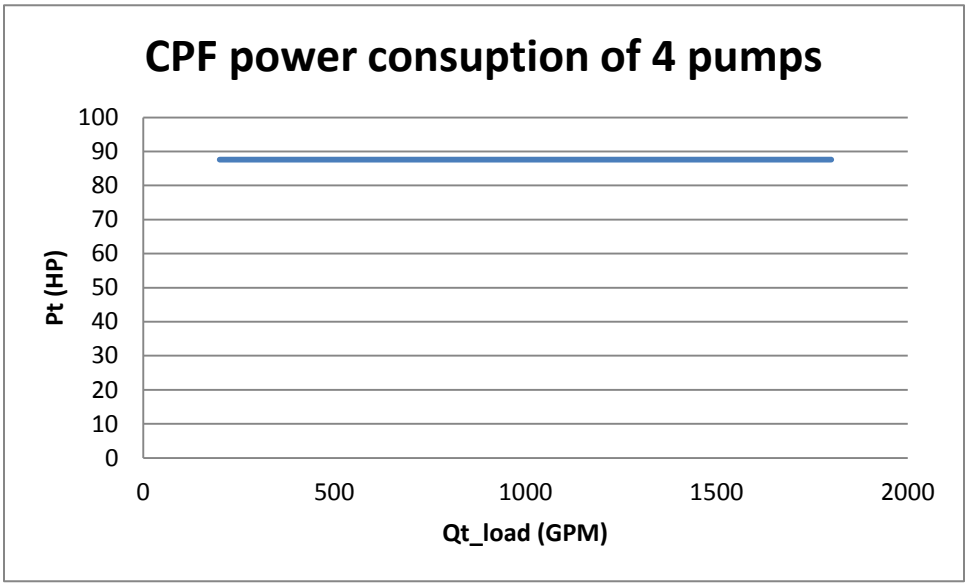

Figure 3-13: total power consumption with varying load flow in CPF with 4 pumps

3.4.3.2 Energy Consumption Simulation of 2 Parallel Pumps for CPF

When two parallel pumps are selected for the same chiller system in section 3.4.3.1, the Taco Model 5013 pump is selected. The manufacturer's curve of the pump and the key parameters are shown in Figure 3-14 and Table 3-3.

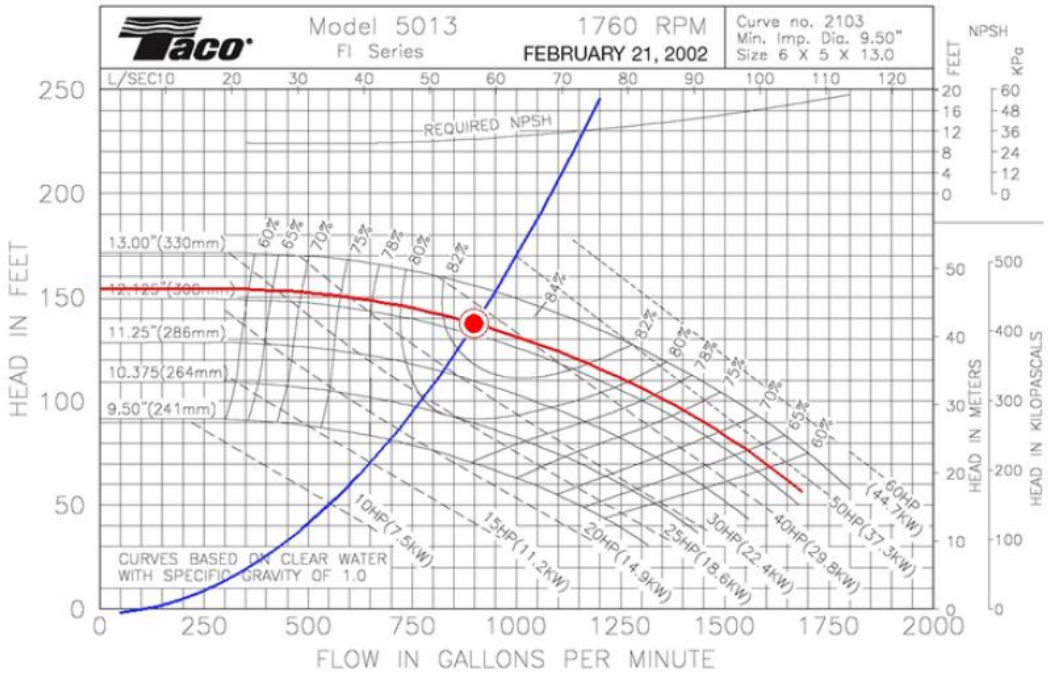

Figure 3-14: Pump Performance Curve of the Taco FI5013 series

Table 3-3: Parameters for the Taco FI5013 in CPF Power Consumption Simulation

Manufacture	Model	Qty	Design Flow	Design Head	RPM	Imp Dia	Design Eff	HP	NOL HP
Taco, Inc	FI5013	2	900 GPM	140 feet	1760	12.4”	83%	38.41	48.15

The same procedure of 4 pumps case in section 3.4.3.1 is performed, and the total power consumption is obtained and shown in Table 3-4.

The total power consumption is a little bit lower in this case than that in the 4 pump case shown in Table 3-2 and Table 3-4. The reason is that the FI5013 pump model has higher design efficiency than the PI3013 model used in the 4 pump case. Usually higher capacity pumps tend to have a higher efficiency, so the 2 pump case is a better choice when the total capacity is not too large.

Table 3-4: CPF power consumption with 2 parallel pumps

Operating point for CPF with 2 pumps			
Q_t (GPM)	H_t (fWg)	P (HP)	P_t (HP)
1800	139.0644	38.84834	77.69668

3.4.4 PSF configuration Simulation

To make it comparable with the CPF case, assume the same chiller system which has one chiller plant and requires a total design system flow of 1800GPM and design system head of 140 fWg. It is configured into the PSF configuration. Assume the primary side design head is 30% of the total system head and there are 2 pumps in the primary side and 2 pumps in the secondary side.

The system resistance for the PSF configuration can be divided into two parts: chiller side resistance and load side resistance. The short common line is ignored as it is always close to chiller/boiler and its length is very short.

3.4.4.1 Primary side energy simulation for PSF

Using Taco pump selection wizard, Model FI6013 is selected for primary side pumps. The pump performance curve and key parameter information are displayed in Figure 3-15 and Table 3-5.

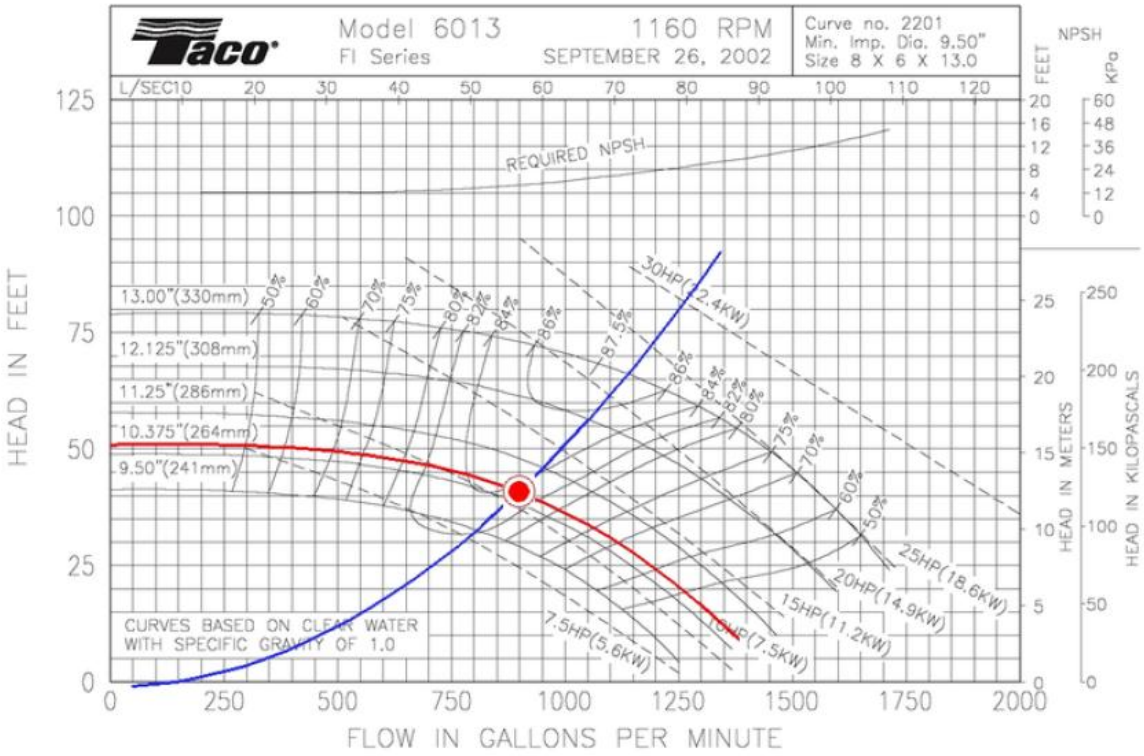

Figure 3-15: Pump performance curve for Taco FI6013

Table 3-5: Parameters of Taco FI6013 pump used in PSF primary loop

Manufacture	Model	Qty	Design Flow	Design Head	RPM	Imp Dia	Design Eff	HP	NOL HP
Taco, Inc	FI6013	2	900 GPM	42 feet	1160	10.7”	83%	11.44	12.93

The primary side pump operation is similar as the pumps in the CPF configuration. It is operated at the design working point to provide the chiller/boiler with the required design flow and its portion of the design head. The primary side power consumption is simulated and displayed in Table 3-6.

Table 3-6: primary side power consumption of PSF configuration

Primary side power consumption for PSF			
Q_t (GPM)	H_t (fWg)	P (HP)	P_t (HP)
1800	42	11.44	22.88

3.4.4.2 Secondary side energy simulation for PSF

Using the Taco pump selection wizard, Model FI5011 is selected for the secondary side pump. The performance curve and key parameters are displayed in Figure 3-16 and listed in Table 3-7.

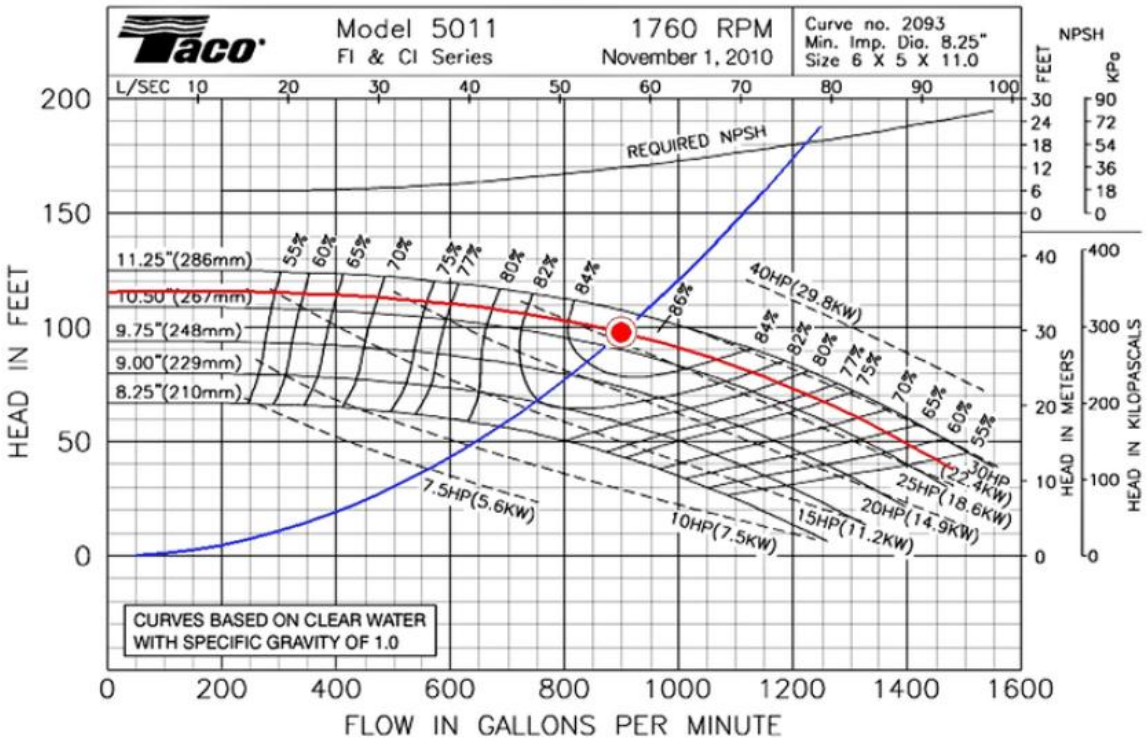

Figure 3-16: pump performance curve for Taco FI5011 pump

Table 3-7: Parameters for Taco FI5011 pump used in PSF secondary loop

Manufacture	Model	Qty	Design Flow	Design Head	RPM	Imp Dia	Design Eff	HP	NOL HP
Taco, Inc	FI5011	2	900 GPM	98 feet	1760	10.8”	85%	26.14	28.88

The system resistance in the secondary part can be expressed as the following equation when the constant independent head is to be maintained.

$$\boldsymbol{H_s = \left(\alpha_{des} + (1 - \alpha_{des}) * \left(\frac{Q_s}{Q_{s_{des}}}\right)^2\right) * H_{s_{des}}} \qquad [3\text{-}24]$$

Where,

H_s, is the system head in the secondary loop;

α_{des}, is the ratio of design independent head to the total design secodary head;

Q_s, is the total water flow rate in the secondary loop;

$Q_{s_{des}}$, is the design total water flow rate in the secondary loop;

$H_{s_{des}}$, is the design total head in the secondary loop;

Secondary side pump performance curve is expressed in the following two equations:

$$\boldsymbol{H_s/\omega^2 = a_0 + a_1 * \frac{Q_s}{n*\omega} + a_2 * \left(\frac{Q_s}{n*\omega}\right)^2} \quad [3\text{-}25]$$

$$\boldsymbol{\frac{P_s}{n*\omega^3} = b_0 + b_1 * \frac{Q_s}{n*\omega} + b_2 * \left(\frac{Q_s}{n*\omega}\right)^2} \quad [3\text{-}26]$$

Where,

a_0 =110.8448151;

a_1 =0.03285427;

a_2 =-0.0000541;

b_0 =6.41742809;

b_1 =0.03319862;

b_2 =-0.00001264;

H_s, Q_s, P_s, are secondary side system head, flow rate and power consumption;

n, is the number of pump running in the secondary loop;

ω, is the speed ratio of running speed to the design speed;

Here both methods are simulated for the secondary side pump. The equal efficiency point in the best efficiency method meets the following requirements. Assume the independent head is 20% of the total secondary design head. It is calculated by applying equation [3-27] to [3-29] into equation [3-25] to [3-26]. The equal efficiency point is shown in Table 3-8.

$$\boldsymbol{H_1 = H_2} \quad [3\text{-}27]$$

$$\boldsymbol{Q_1 = Q_2} \quad [3\text{-}28]$$

$$\boldsymbol{P_1 = P_2} \quad [3\text{-}29]$$

Table 3-8: the equal efficiency point for the secondary loop pumps

Q (GPM)	H(fWg)	P(HP)	ω_{single}	ω_{2pumps}
758.89	33.5357	8.0056	0.659726	0.55696

Note: ratio of independent head to secondary loop design head is 0.2.

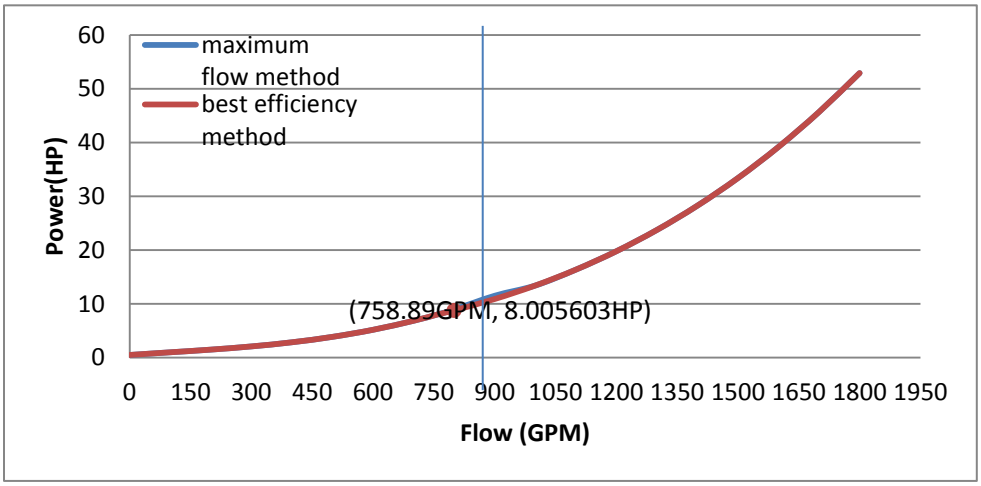

Figure 3-17: power consumption comparison of the two methods for PSF secondary pumps

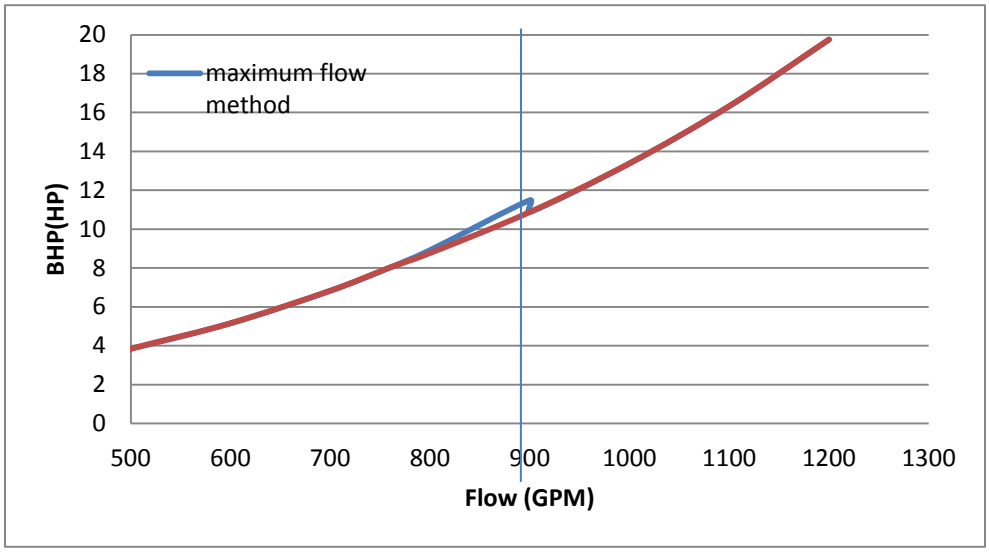

Figure 3-18: power consumption comparison within flow range of 500 to 1200 GPM for secondary loop

The power consumption comparison of these two methods in this case is shown in Figure 3-17. The red dot in the figure is the equal efficiency point. The power savings of the best efficiency method is not clear in Figure 3-17. By zooming the flow range to within 500~1200GPM, (as shown in Figure 3-18), it can be seen that some power saving does occur.

The total power consumption for the PSF configuration is the sum of the primary side power consumption and the secondary side power consumption (equation [3-30]). See Figure 3-19.

$$\boldsymbol{P_t = P_{pri} + P_{sec}} \qquad [3\text{-}30]$$

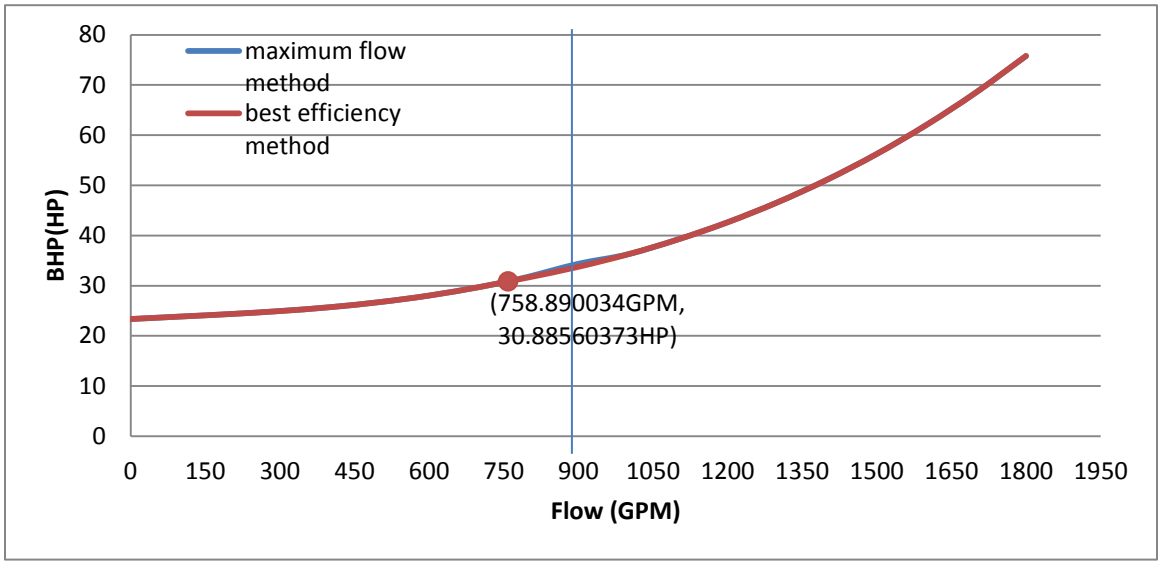

Figure 3-19: total power consumption plot of PSF configuration

3.4.5 VPF configuration Simulation

In this section, the VPF configuration is simulated for power consumption. Two sets of comparison are done herein. One is the Maximum flow staging and best efficiency staging control; the other one is the Constant DP Speed control and DP Reset Speed control. The former one is simulated under constant DP speed control, and the latter is simulated under the Best Efficiency staging control.

3.4.5.1 *Simulation of constant loop DP control with VPF configuration*

Assume the same chiller system requirement as in the cases for the PSF and CPF configurations. There is one chiller requiring a total design flow rate of 1800 GPM and a total design head of 140 fWg in the chiller system. The chiller is configured as a variable primary only system. Two pumps are required.

The system design is the same as in the 2 pump CPF case. The only difference is that 2 variable frequency drives are added to allow for speed modulation. So the pump

model is FI5013. See Figure 3-14 and Table 3-3.

Similarly, the maximum flow method and best efficiency methods are simulated for the constant independent DP as in that PSF configuration. The system curve for the VPF is expressed in equation [3-31]. Assume the design independent head ratio occupies 14% of the total design ratio ($\alpha_{des} = 0.14$).

$$\boldsymbol{H = \left(\alpha_{des} + (1 - \alpha_{des}) * \left(\frac{Q_t}{Q_{t_{des}}}\right)^2\right) * H_{des}} \quad [3\text{-}31]$$

Where,

α_{des}, the ratio of design independent head to the total system design head;

Q_t, the total water flow rate;

$Q_{t_{des}}$, the design water flow rate; herein it is 1800GPM;

H_{des}, the design system head; herein it is 140 fWg;

The pump performance curve is expressed in the following two 2nd order polynomial equations according to section 3.4.1.

$$\boldsymbol{H/\omega^2 = a_0 + a_1 * \frac{Q_t}{n*\omega} + a_2 * \left(\frac{Q_t}{n*\omega}\right)^2} \quad [3\text{-}32]$$

$$\boldsymbol{\frac{P}{n*\omega^3} = b_0 + b_1 * \frac{Q_t}{n*\omega} + b_2 * \left(\frac{Q_t}{n*\omega}\right)^2} \quad [3\text{-}33]$$

Where,

a_0 =153.5998564;

a_1 =0.0255499;

a_2 =-0.0000462;

b_0 =12.9142112;

b_1 =0.0343057;

b_2 =-0.0000061;

H, Q_t, P, are system head, flow rate and power consumption;

n, is the number of running pumps;

ω, is the speed ratio of running speed to the design speed;

By applying equation [3-31] and [3-32], the system performance curve and pump performance curve can be plotted in Figure 3-20. The green dot is the design working point.

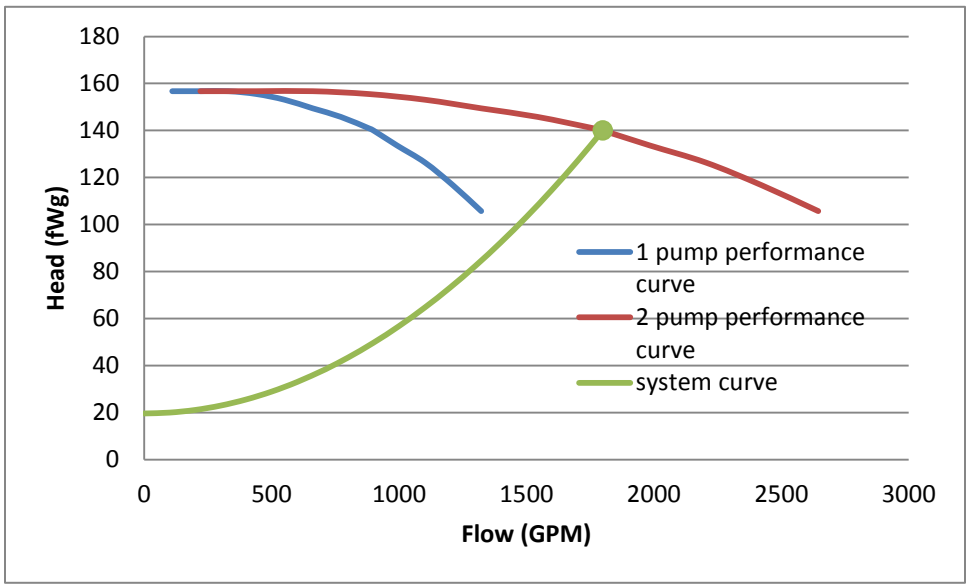

Figure 3-20: VPF system performance curve

The equal efficiency point for 1 pump operation and 2 pump operation is found out by applying the following equations into equation [3-32] to equation [3-33]. The result is displayed in Table 3-9.

$$\boldsymbol{P_1 = P_2} \qquad [3\text{-}34]$$

$$\boldsymbol{H_1 = H_2} \quad [3\text{-}35]$$

$$\boldsymbol{Q_1 = Q_2} \quad [3\text{-}36]$$

Table 3-9: the equal efficiency point for the VPF configuration

Q (GPM)	H(fWg)	P(HP)	$\boldsymbol{\omega_{single}}$	$\boldsymbol{\omega_{2pumps}}$
723.254	39.03852	9.17637	0.58414	0.512506

Note: ratio of independent head to design head is 0.14.

In the maximum flow method, in the range of 0-900GPM flow, 1 pump is operated; in the range of 900-1800GPM flow, the 2nd pump is started. Given a flow rate, the pump head can be calculated using equation [3-31]; then the pump speed is solved using equation [3-37] which is obtained by solving the root of equation [3-32]. Finally power consumption is obtained by applying the calculated speed ratio and the given flow rate into equation [2-23]. In best efficiency method, in the range of 0-723.254GPM flow, 1 pump is operated; in the range of 723.254-1800GPM flow, the 2nd pump is started. The power consumption is obtained similarly as in the maximum flow method. The power consumption plot for both methods is displayed in Figure 3-21 and Figure 3-22. The power savings of the best efficiency method can be seen in Figure 3-22.

$$\omega = \frac{-a_1 * Q_t/n + \sqrt{(a_1 * Q_t/n)^2 - 4 * a_0 * (a_2 * (Q_t/n)^2 - H)}}{2 * a_0} \quad [3\text{-}37]$$

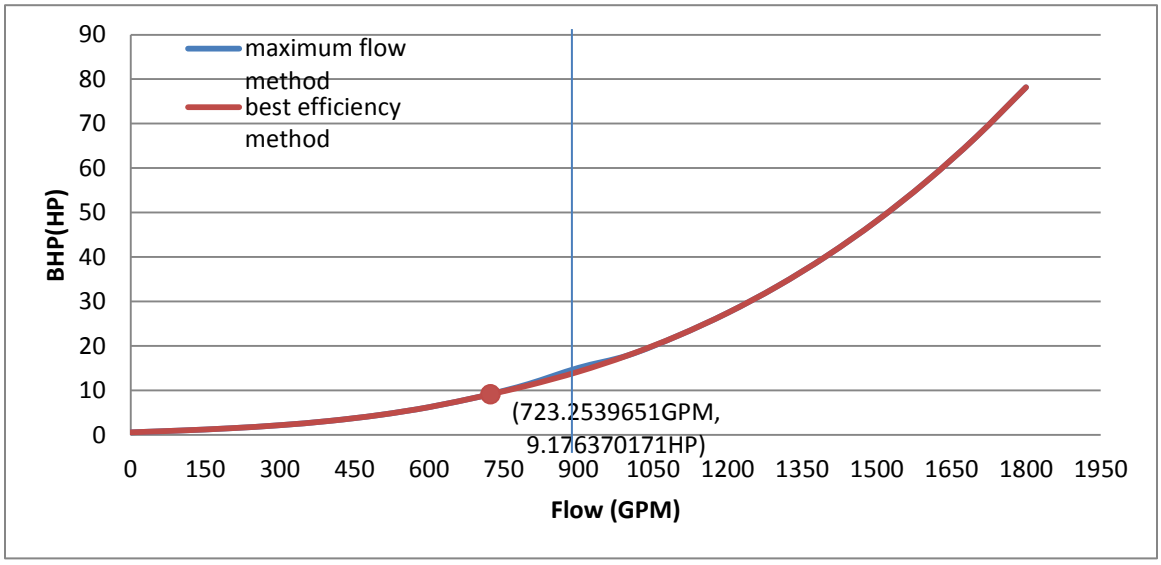

Figure 3-21: maximum flow and best efficiency methods' power comparison in VPF case

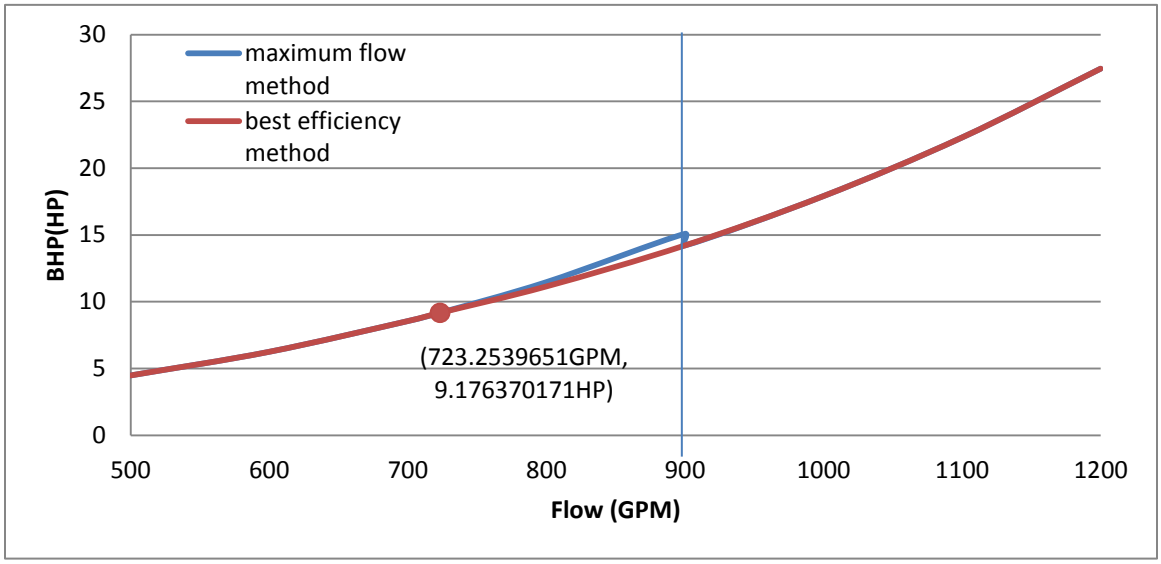

Figure 3-22: maximum flow and best efficiency methods' power comparison in VPF case-range 500 to 1200GPM

3.4.5.2 *Simulation of DP Reset Control with VPF configuration*

In this section, the loop DP reset control in the VPF configuration is simulated. The reset loop DP can be expressed as the following equation

$$H_{lp} = \alpha_{des} * H_{des} * \left(\frac{Q_t}{Q_{des}}\right)^2 \qquad [3\text{-}38]$$

where,

H_{lp}, remote loop differential pressure at flow Q_t;

α_{des}, ratio of design loop differential pressure to the system total design head;

H_{des}, the system total design head;

Q_t, the current total water flow;

Q_{des}, the system total design water flow;

Then the real time independent head ratio to total system design head can be generated as the following equation:

$$\boldsymbol{\alpha = \frac{H_{lp}}{H_{des}} = \alpha_{des} * \left(\frac{Q_t}{Q_{des}}\right)^2} \quad [3\text{-}39]$$

In order to ensure safe system operations, a low limit is given for the remote loop differential pressure. So the independent head ratio α is finalized as follows:

$$\alpha = \max\{\alpha_{min},\ \alpha_{des} * \left(\frac{Q_t}{Q_{des}}\right)^2\} \quad [3\text{-}40]$$

where,

α_{min}, the minimum value of the independent head ratio to the total design system head;

The system curve for the DP reset control is expressed in the following equation:

$$\boldsymbol{H = \left(\alpha + (1 - \alpha_{des}) * \left(\frac{Q_t}{Q_{des}}\right)^2\right) * H_{des}} \quad [3\text{-}41]$$

The constant DP control is simulated in section 3.4.5.1, therefore only the DP reset is simulated. Assuming that the minimum independent head ratio is 0.05, and then the best efficiency staging method is simulated for the loop DP set.

Figure 3-23 displays the system performance curve for both the constant DP control and the DP reset control methods. It can be seen that the system head in DP

reset is much lower than that in the Constant DP method.

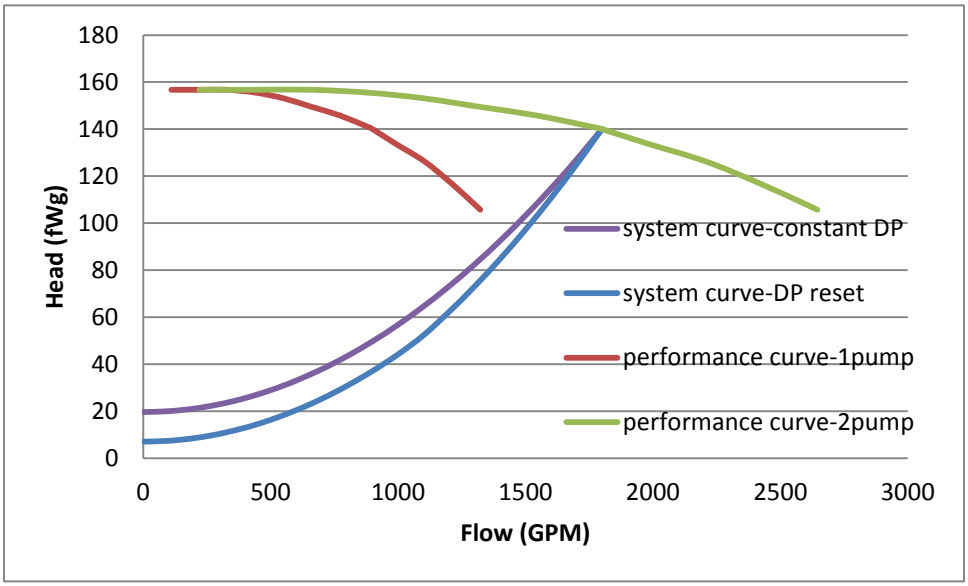

Figure 3-23: VPF system performance curve for Constant DP control and DP Reset Control ($\alpha = 0.14, \alpha_{min} = 0.05$)

Figure 3-24 illustrates the power consumption comparison of these two pump speed control methods with the best efficiency staging control applied.

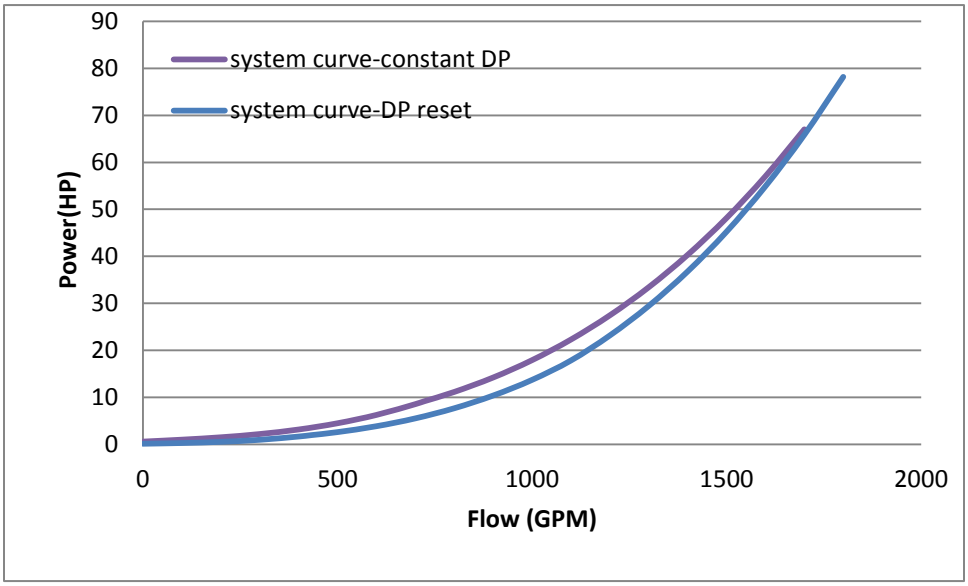

Figure 3-24: Power comparison of the Constant DP control and DP Reset control for the VPF configuration ($\alpha = 0.14, \alpha_{min} = 0.05$)

3.4.6 Energy Consumption Prediction for all Three Pump Configurations

The power consumption for each system configuration is simulated and plotted in the previous sections. In this section, the potential power savings of the PSF and VPF to CPF configuration is predicted using the Integrated Part Load Method.

The Integrated Part Load Method was originally developed by Air Conditioning, Heating and Refrigeration Institute (AHRI) to predict the chiller efficiency at the rating points. Zhan Wang utilized it to predict pump power consumptions in his dissertation for on chiller plant pump systems. (Wang Z. , 2010) Here it also is utilized to predict the energy consumptions of the 3 pump system configurations. It is shown below:

$$\boldsymbol{P_{IPL} = 0.01A + 0.42B + 0.45C + 0.12D} \quad [3\text{-}42]$$

Where,

A- Pump power consumption at 100% load;

B- Pump power consumption at 75% load;

C- Pump power consumption at 50% load;

D- Pump power consumption at 25% load;

Table 3-10 displays the power comparison of the three system configurations. The following points can be acquired:

1) In the CPF configuration, the 2 pump system saves 11.3% more power than the 4 pumps system due to the fact that larger capacity pumps have a much higher efficiency.

2) In the PSF configuration, an additional 48.7% of power is saved using maximum

flow staging control, compared with the 2 pump CPF configuration. When the best efficiency method is applied to this, 0.69% more power is saved.

3) In the VPF configuration, 40.7% of the power is saved compared to the PSF configuration. The Best efficiency method saves 1.67% of power compared to the maximum flow method which is higher than in the PSF case. When the DP reset is applied, 15.2% more power is saved compared with the constant DP.

A smaller amount of savings between the best efficiency method and the maximum flow method is predicted in the PSF and VPF configurations compared to savings in Wang's dissertation. This is because there is only one chiller in the simulations here while there are multiple chillers and the same number of pumps in Wang's simulation. The chiller staging off under lower load can further reduce the system head and help save more pump power.

Table 3-10: Power Comparison of the CPF, PSF and VPF by the IPL Load Prediction Method

System	Number of Pump	Control Method	A(HP)	B(HP)	C(HP)	D(HP)	P_{IPL}(HP)	% saved to base	% saved to prior
CPF	4		87.60717	87.60717	87.60717	87.60717	**87.60717**	**0**	**0**
CPF	2		77.6967	77.6967	77.6967	77.6967	**77.6967**	**11.312%**	**11.312%**
PSF	2 primary+ 2 secondary	Max Flow staging	75.77604	48.783	34.3673	26.185447	**39.85416**	**54.508%**	**48.705%**
PSF	2 primary+ 2 secondary	Best Effic staging	75.77604	48.783	33.75663	26.185447	**39.57936**	**54.822%**	**0.690%**
VPF	2	Max Flow +constant DP	78.17577	36.75176	15.08675	3.774826	**23.45951**	**73.222%**	**40.728%**
VPF	2	Best Effic+ constant DP	78.17577	36.75176	14.2176	3.774826	**23.06839**	**73.668%**	**1.667%**
VPF	2	Best Effic+ Reset DP	78.17577	32.9804	10.38449	2.113791	**19.5602**	**77.673%**	**15.208%**

Figure 3-25 shows the power comparison for the CPF, PSF and VPF configurations. It is seen that around a flow of 1800GPM, the PSF consumes less power than the VPF. This is due to the higher secondary pump efficiency in the PSF configuration than the pumps in the VPF configuration.

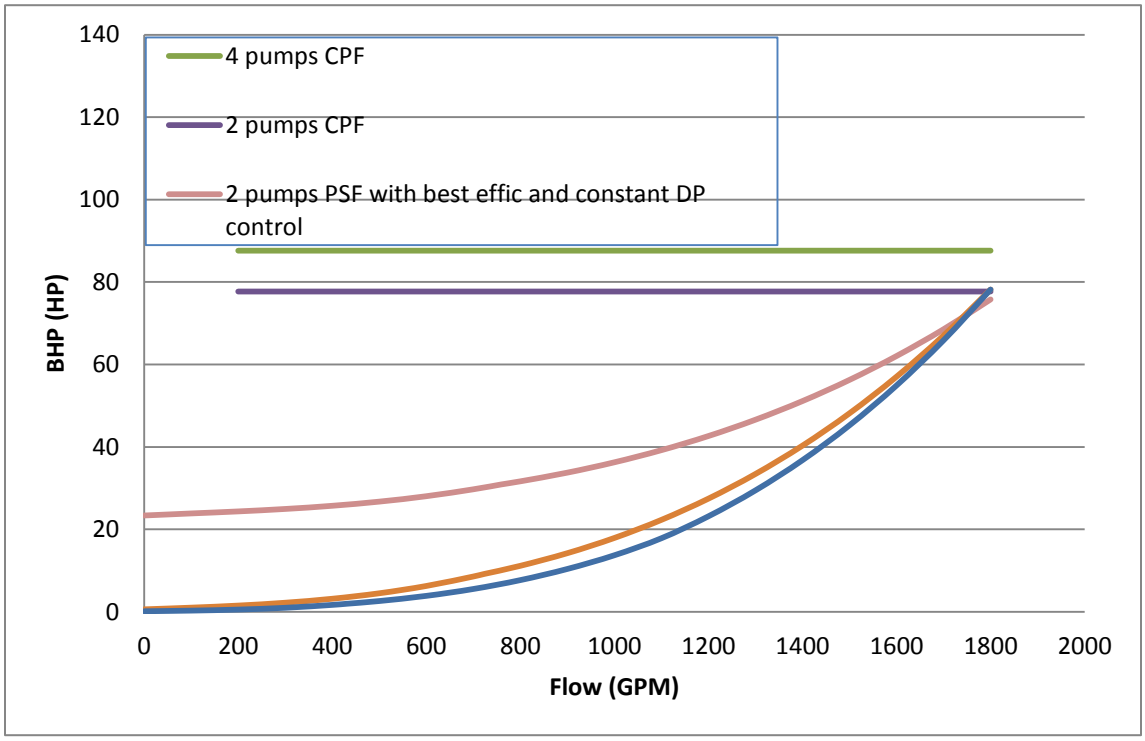

Figure 3-25: Comparison of BHP between CPF, PSF, and VPF

From the simulations, it can be concluded that the VPF configuration is the most energy efficient compared to the: CPF and PSF. It can also be concluded that when both the best efficiency method and the loop DP Reset control are applied to the VPF configuration, the largest amount of power saving occurs.

3.5 Summary

In this chapter, the optimal control algorithms were integrated together for the pump controller. The power consumption simulation was also done for the CPF, PSF, and

VPF configurations with varying control methods. The following conclusion is drawn:

1) The VPF configuration is the most energy efficient compared to the PSF and CPF. CPF is the least efficient of the three configurations.
2) The best efficiency staging method saves 0.7% to 1.67% of energy compared to the conventional maximum flow staging method.
3) The loop differential pressure reset PID control saves 15% of energy compared to the constant DP PID control in the VPF configuration.

Chapter 4 Controller Design

In Chapter 3, the optimal control strategy for a pump controller was proposed and simulated. Chapter 4 introduces the hardware components. Figure 4-1 shows a typical wiring diagram of the pump controller for pump systems.

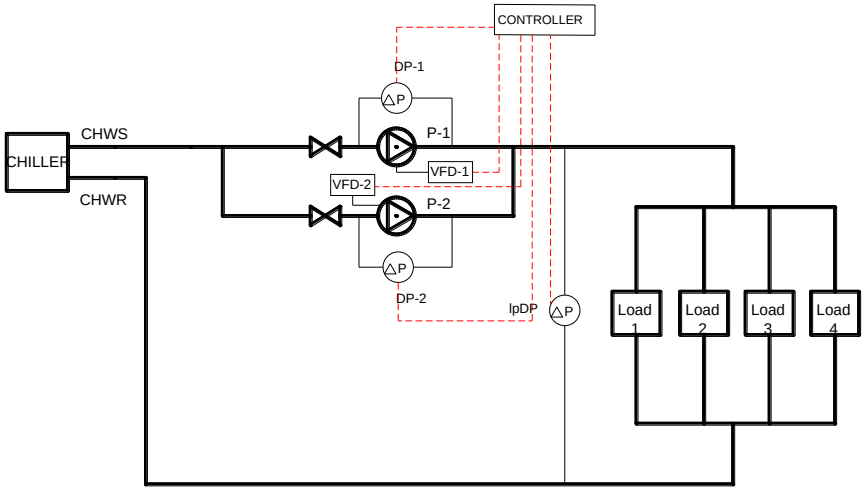

Figure 4-1: System Configuration with Pump Controller

4.1 Hardware

The components required for the pump controller are:

1) Three water differential pressure sensors (DP sensor).

2) An input/output board: IOS1018

3) Programming board: PMC (short for programmable microprocessor controller) with 4×20 LCD (short for Liquid Crystal Display) and 4×4 Keypad.

The PMC board (shown in Figure 4-2) is the programming board that holds all the control algorithms. The IOS1018 board (shown in Figure 4-2) accepts the analog input

signals and sends out analog output signals. It communicates with the PMC board using digital communication (Modbus RTU Protocol). The water side DP sensors measure pump 1 head, pump 2 head and loop differential pressure. The measured analog signals are transmitted to IOS1018 board via analog input ports. The PMC controller then retrieves them from IOS1018 board.

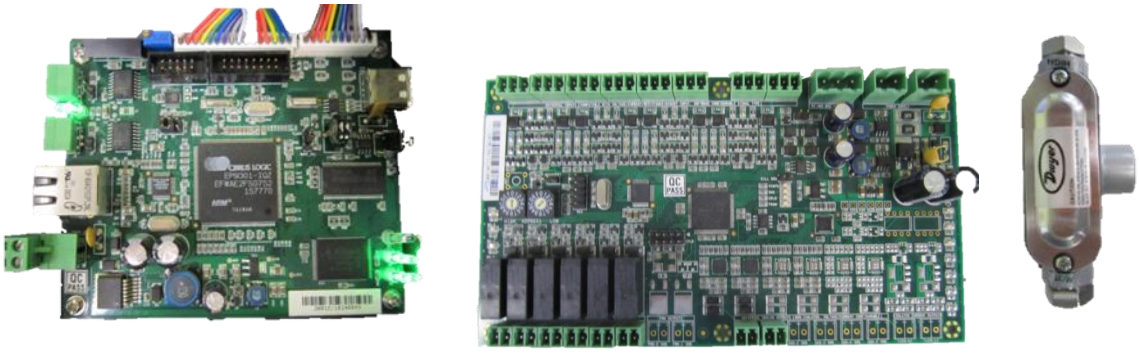

PMC: Programming Board IOS1018: Input/Ouput Board DP Sensor

Figure 4-2: Required Components for Pump Controller

4.1.1 PMC Board

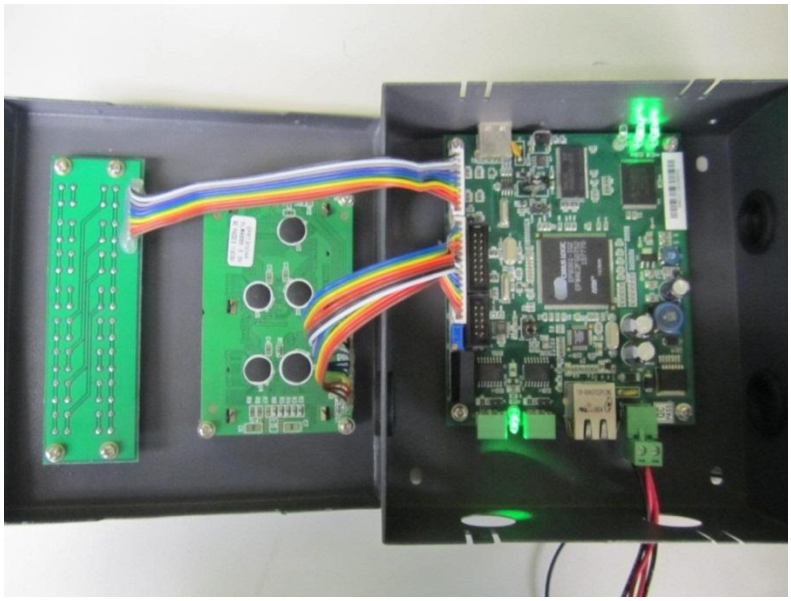

Figure 4-3: LCD and Keyboard connection with control board

The PMC board is implemented with a 4×20 LCD display and 4×4 keypad, as shown in Figure 4-3.

The PMC board's microprocessor is CIRRUS LOGIC ARM chip EP9301. A small Linux Crater system resides on the PMC board, along with the features shown in Figure 4-4.

- Two (2) RS485 ports for serial communication
- One (1) RS232 port for board flashing
- One Ethernet port for internet access
- One (1) power port for 24VDC power supply
- One (1) USB 2.0 port for file transfer to USB drive
- Support LCD display and Keypad operation

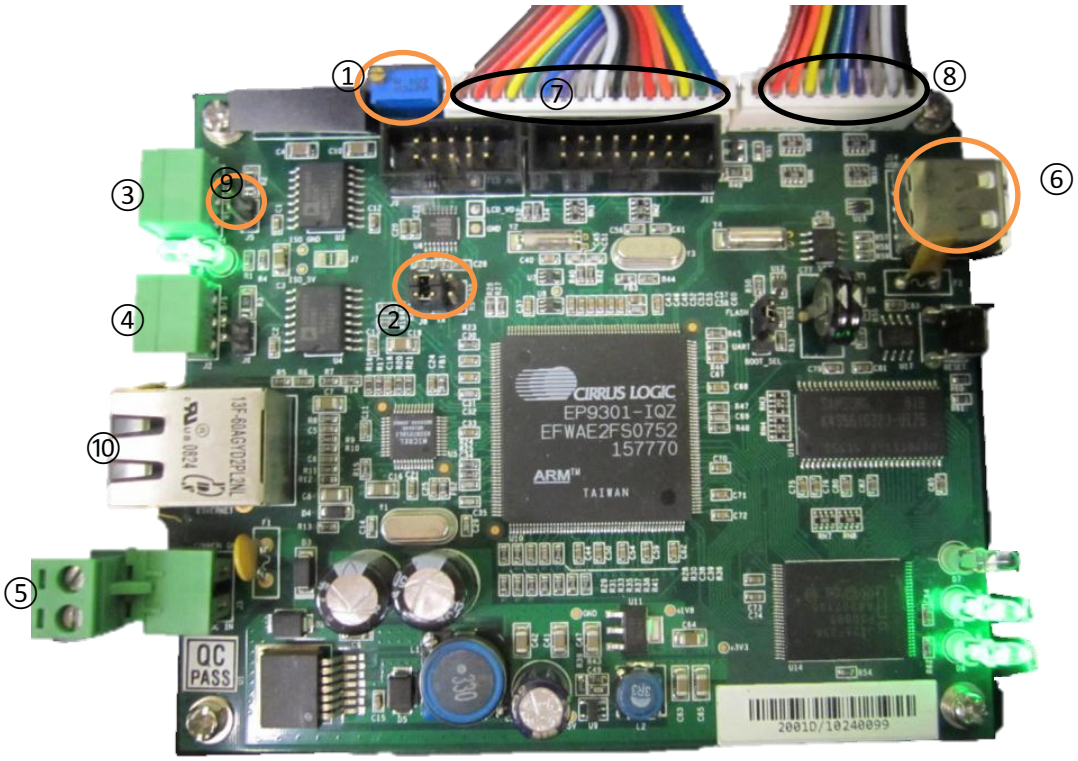

① - LCD Brightness Ratio Modification Resistor

② - RS485 Selection Jumper, left 2 pins shorted for Tier 2 Modbus Communication, as shown in the figure

③ - RS485 Port for Tier 2 Modbus Communication

④ - RS485 port for Tier 1 Modbus Communication

⑤ - Power Supply Port

⑥- USB Port used to download/upload the OFC File, and to download the Trend File

⑦ - Connector to LCD Screen

⑧ - Connector to Keyboard

⑨- Termination Jumper for Tier 2

⑩ - Ethernet Port

Figure 4-4: PMC Board

4.1.2 IOS1018 Board

IOS1018 board supports Modbus RTU communication via RS485 port. It consists of eight universal inputs (UI), six binary outputs (BO) and two analog outputs (AO). See Figure 4-5. Each universal input can be configured to accept 0-10V voltage, 4-20mA, dry contact, or resistance signals. While each analog output can be configured to send out

0-10V or 4-20mA signals. The configuration uses USB-to-RS485 conversion cable and MCT software provided by Bes-Tech, Inc.

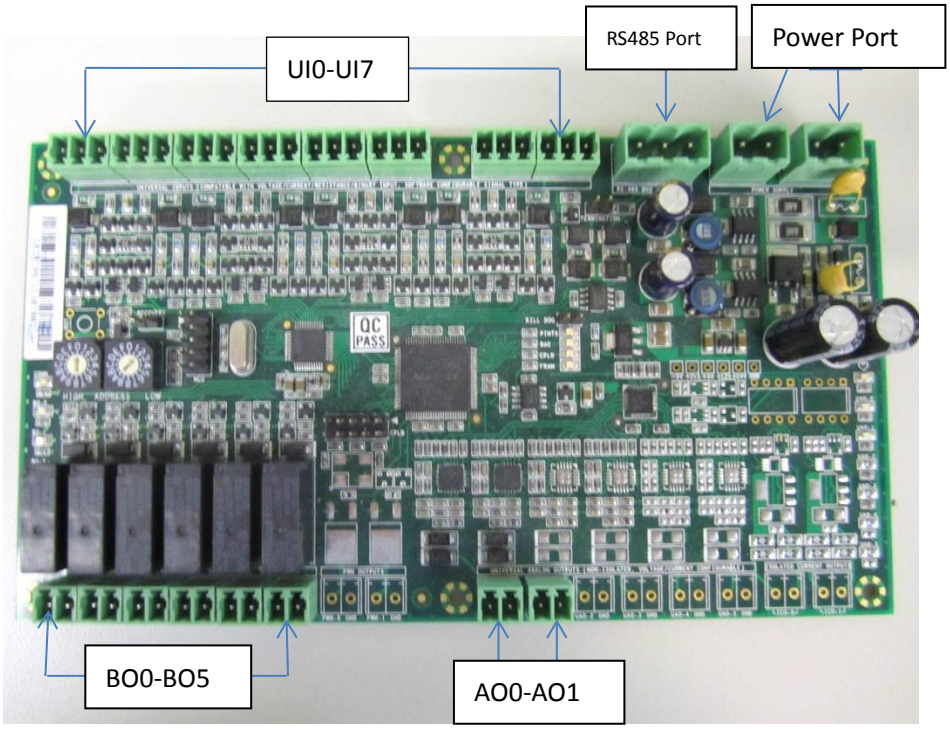

Figure 4-5: I/O board (IOS1018 from Bes-Tech, Inc.)

The first three universal inputs (UI0-UI2) receive the loop differential pressure, pump 1 head and pump 2 head signals. If VFD (variable frequency drive) for pump 1 and pump 2 supports Modbus RTU communication, then the pump controller communicates with the VFDs to start/stop pumps and to modulate the pumps' speed. Otherwise, the pump controller communicates with the IOS1018 board to control pump start/stop and to modulate the pump speed. Assign the unoccupied UIs to the speed feedback and pump fault code; assign the BOs to the pump start/stop command; assign the AOs to the speed command, as shown in Figure 4-6.

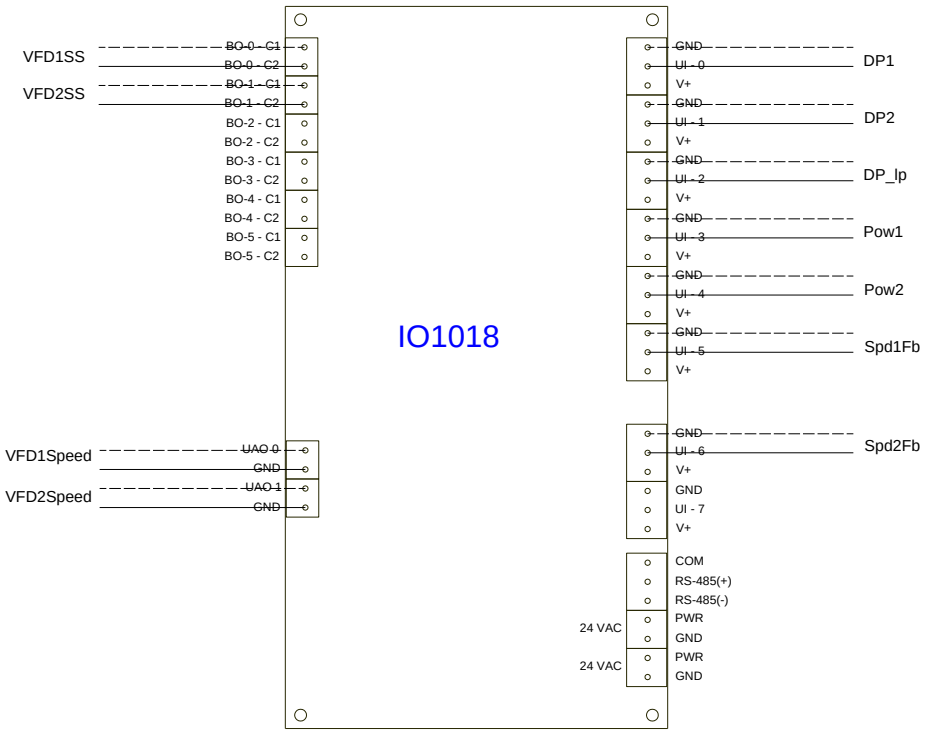

Figure 4-6: Input and Output Signals on IOS1018 Board

4.1.3 DP Sensor

This study utilized a Dwyer wet/wet differential pressure transmitter Series 629 for pump head and loop differential pressure measurements, as shown in Figure 4-2. It provides ±0.5% F.S. (full range) accuracy and outputs 4-20 mA current signal or optional 0-5 or 0-10 VDC voltage signal.

4.2 Control Points and Control Parameter Definition

Table 4-1 lists all the control points required for the pump controller, and Table 4-2 lists all the input and output points defined in the pump controller mentioned in Table 4-1.

Table 4-1: Control Point List for the Pump Controller

Point	Type	Location
Loop Differential Pressure	AI	IOS1018
Pump 1 Head	AI	IOS1018
Pump 2 Head	AI	IOS1018
Pump 1 Power	AI(Modbus)	IOS1018(VFD-1)
Pump 1 Speed Feedback	AI(Modbus)	IOS1018(VFD-1)
Pump 1 Start/Stop Command	BO(Modbus)	IOS1018(VFD-1)
Pump 1 Speed Command	AO(Modbus)	IOS1018(VFD-1)
Pump 2 Power	AI(Modbus)	IOS1018(VFD-2)
Pump 2 Speed Feedback	AI(Modbus)	IOS1018(VFD-2)
Pump 2 Start/Stop Command	BO(Modbus)	IOS1018(VFD-2)
Pump 2 Speed Command	AO(Modbus)	IOS1018(VFD-2)

Table 4-2: I/0 Points for the Pump Controller

Signal from IOS1018		
Name	**Readable Name**	**Value**
LDP	End User Loop Differential Pressure	PSI
P1Press	Pump 1 Head	PSI
P2Press	Pump 2 Head	PSI
Pow1	Pump 1 Power	kW
Pow2	Pump 2 Power	kW
Spd1Fb	Pump 1 Speed Feedback	Hz
Spd2Fb	Pump 2 Speed Feedback	Hz
Signal to IOS1018		
Name	**Readable Name**	**Value**
Spd1	Pump 1 Speed Command	Hz
Spd2	Pump 2 Speed Command	Hz
P1cmd	Pump 1 Start/Stop Command	N/A
P2cmd	Pump 2 Start/Stop Command	N/A

Table 4-3 lists the required control parameters for the control logic defined in Chapter 3. Use LDPmin, LDPmax and Qdes to reset loop differential pressure set point; Pgain and Igain define the proportional gain and integral gain for the PI speed control; and SpdMin defines the minimum pump running speed.

Table 4-3: Default set points in the Pump Controller

Parameters		
Name	**Readable Name**	**Value**
LDPmin	Loop DP Minimum Set Point	30PSI
LDPmax	Loop DP Maximum Set Point	150PSI
Qdes	System Design Flow Rate	1800GPM
Efficlowlimit	Efficiency Low Limit to Escape from Pump Staging Control	75%
Pgain	Pump Speed Control Proportional Gain	0.1
Igain	Pump Speed Control Integral Gain	0.001
SpdMin	Pump Minimum Speed	25Hz

Figure 4-7 illustrates the wiring among the components. The grey and purple wires are RS485 communication wires between PMC board and IOS1018 board; the protocol used is Modbus RTU communication. The red and blue wires are the power supply wires. They provide the 24VAC power to all the component boards. The blue wires are the signal wires between IOS1018 board and the DP sensors and the red wires provide the 24 volt power supply to the DP sensors.

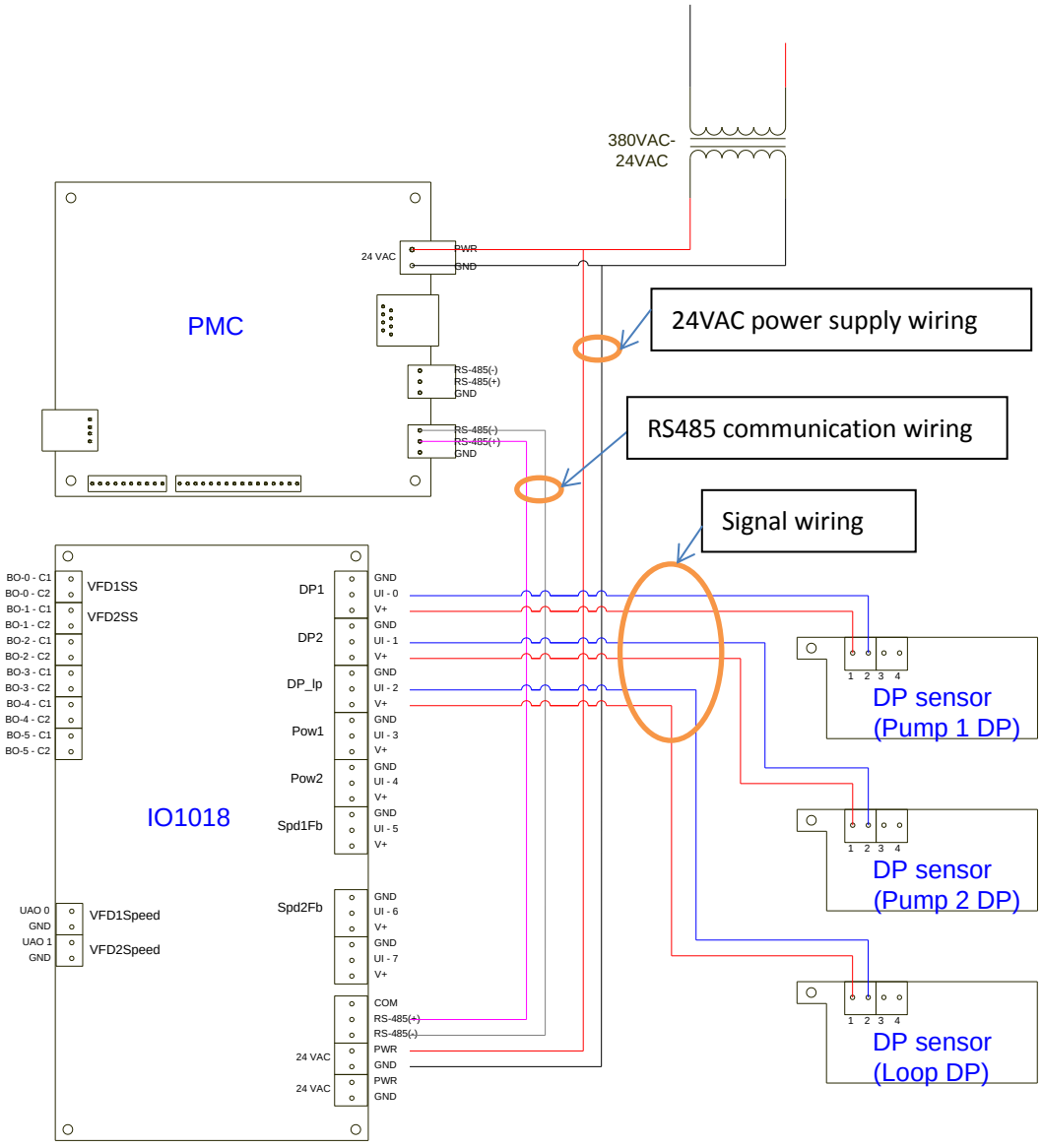

Figure 4-7: Wiring Diagram of Pump Controller

Chapter 5 Experiments

In Chapter 5, the pump controller developed in Chapter 4, is applied to a chiller plant and the operation data after the pump controller implementation is analyzed and compared with the energy savings before the controller implementation.

5.1 Chiller/Boiler Pump System Description

The experiment was done on the chiller/boiler plant in the Main Building of Western-Nebraska Community College, which is located at 1601 East 27th St, Scottsbluff, NE69361. WNCC is post-secondary community college. The main building was erected in 1969 with a gross floor area of 160,239 square feet. The building's 596 occupants utilize the facility for about 83 hours per week. HVAC systems consist of mainly chiller and Roof Top Units. The chiller is cycled on/off and the Roof Top Units run continuously. 95% of the building is covered for cooling and heating with gas being the heat source.

5.2 Pump System before Renovation

The chiller and boiler share the same pipe system. Two manual 3-way valves in main supply pipe and return pipe are used to switch between hot water and chilled water flow There are four pumps that run in parallel to distribute the water to Air Handler Units (AHU), locker room, handball court, and primary pump feedings separately (see Figure 5-1). The pumps run at a constant speed continuously, even though the chiller/boilers cycle on and off. 3-way valves and bypass pipes are used to

modulate loads fed to the heating/cooling coils of the heating/cooling coil water supply and return pipes (see Figure 5-2).

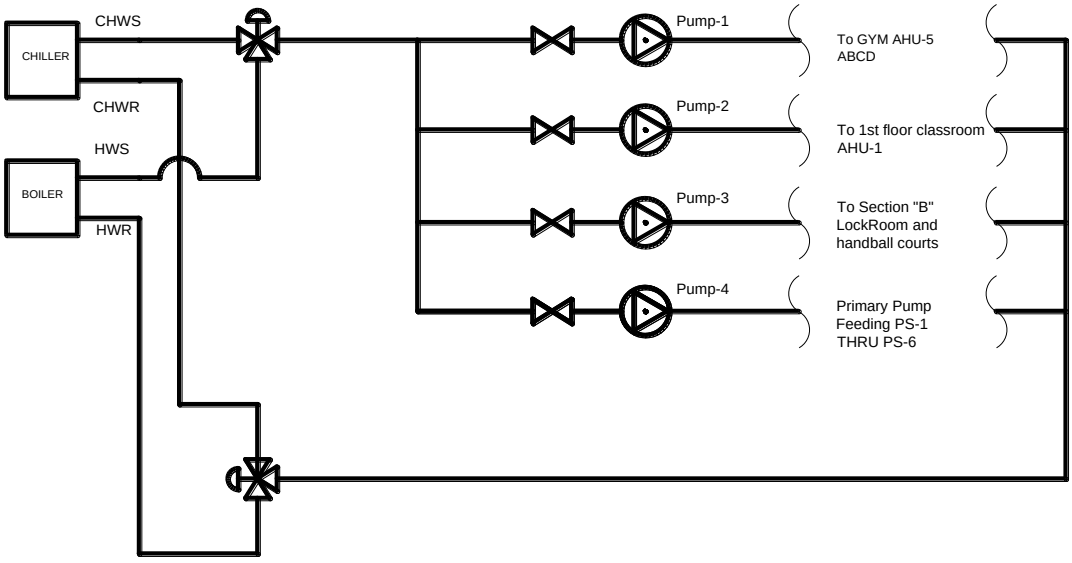

Figure 5-1: Chiller/Boiler Side Pump System Diagram before Renovation

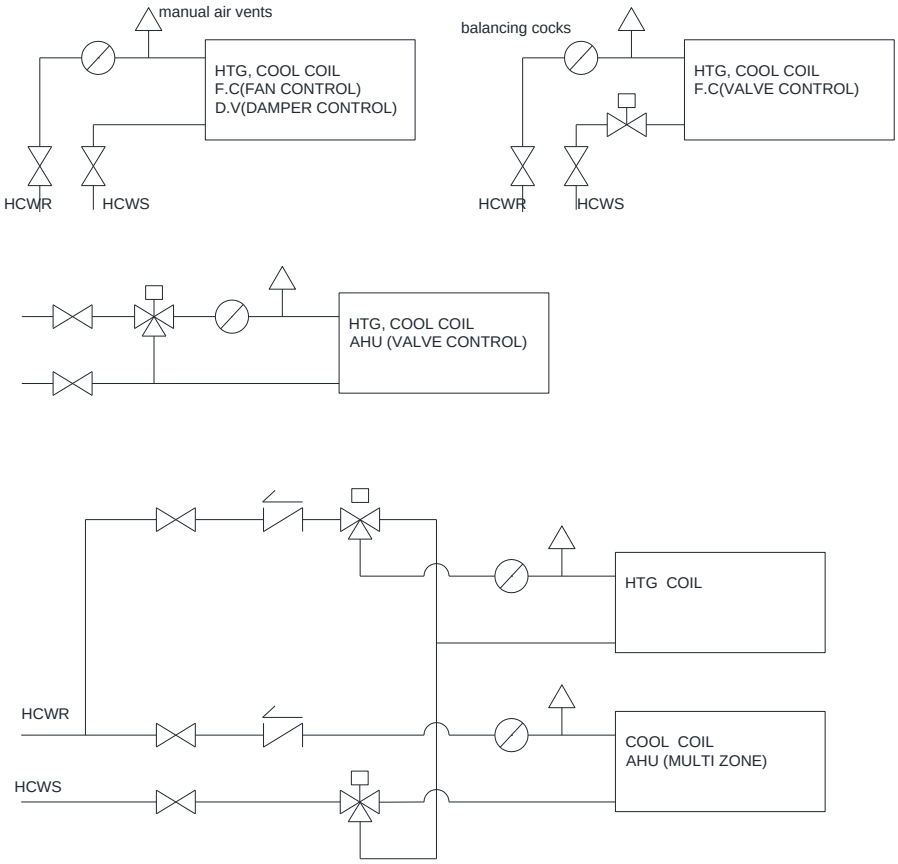

Figure 5-2: Coil Piping Diagram before Renovation

With this system configuration and control logic, when load is varied and low, a lot of water is bypassed and directed back to the chiller/boiler without passing any loads, so chiller/boiler efficiency is low under low conditions. Also the pump energy is wasted under partial loads.

Table 5-1 lists the pump schedule of the original system. The manufacturer curves of these 4 pumps are not available. To predict the total pump consumption of this system, a design efficiency of 75% and the motor design efficiency of 78% is assumed and used. Then the pump power consumed is predicted using the following equation:

$$\boldsymbol{P_{pump} = Q_{des} * \frac{H_{des}}{\eta_p} * C} \qquad \textbf{[5-1]}$$

$$\boldsymbol{P_{motor} = P_{pump}/\eta_m} \quad \textbf{[5-2]}$$

where,

C, the unit conversion factor;

η_p, pump efficiency;

η_m, motor efficiency;

Table 5-1: pump schedule before renovation

PUMP SCHEDULE BEFORE RENOVATION									
MARK	USE	MFG	CAT	GPM	HEAD FT.	MOTOR			
						H.P	V.	φ	RPM
P-1	AHU 5A. 5B. 5C & 5D GYM	THRUSH	4 TV-10	300	65	10	208	3	1725
P-2	1st FL SEC. "B"	THRUSH	4 TV-10	235	70	10	208	3	1725
P-3	G.FL. SEC"B" 1st FL. FLMTO. FC. LOCKER RM'S & HANDBALL	THRUSH	3 TV-5	155	70	5	208	3	1725
P-4	PRIMARY FOR PUMPS PS-1 TO PS-5	THRUSH	4 TV-10	380	65	10	208	3	1725

Table 5-2 lists the predicted pump power consumption. When motor loss is not considered, the total power consumption is 17.98kW; when motor loss is considered with a motor efficiency of 78%, total power consumption is 23.05kW.

Table 5-2: Pump Power Consumption before System Renovation

Pump	**Flow (GPM)**	**Pump Power (kW)**	**Power with Motor Loss Included(kW)**
P-1	300	4.903086	6.286008
P-2	235	4.136193	5.302812
P-3	155	2.728127	3.497599
P-4	380	6.210576	7.962276
Total	1070	17.97798	23.04869

5.3 Pump System after Renovation

The system is retrofitted to variable flow configuration for the purpose of energy efficiency. Figure 5-3 shows the new configuration. The four smaller size parallel pumps are replaced with two (2) larger size pumps (Table 5-3) and the corresponding pipes are modified accordingly. The 3-way control valves on the load side are replaced with 2-way modulation valves. Variable frequency drives are added for the pumps (Table 5-4) and three (3) differential pressure sensors are installed to measure both pump heads and loop differential pressure for control purposes.

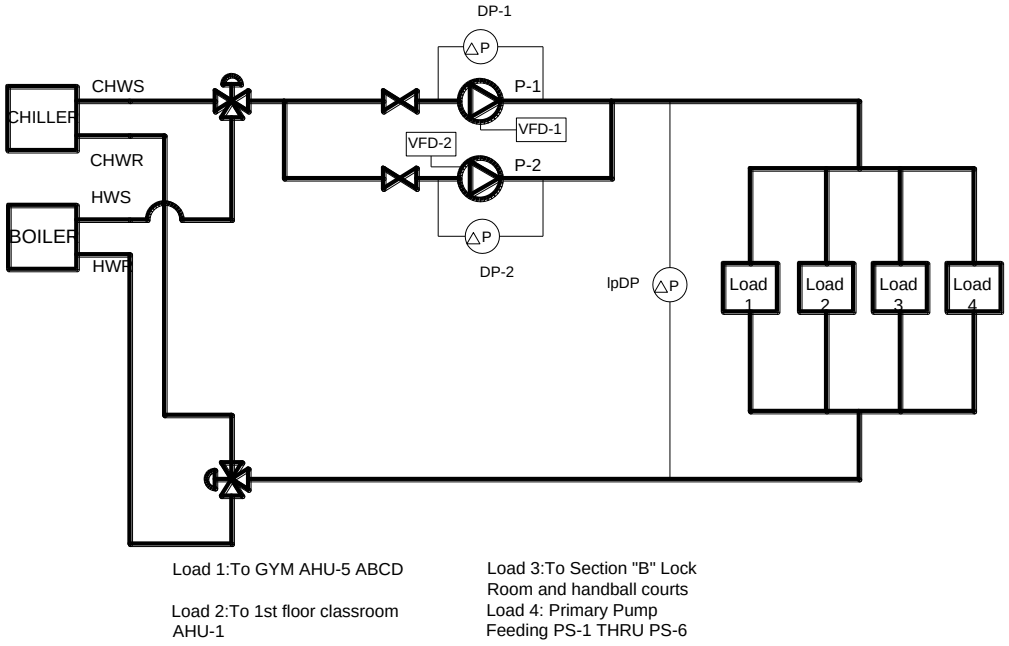

Figure 5-3: Chiller/Boiler Side Pump System Diagram after Renovation

Table 5-3 lists the information of the two new pumps. The design working point for each pump is 900GPM with 140 feet head.

Table 5-3: Replaced Pump General Information

MANU	MODEL	SIZE	IMP.DIAM/IN	GPM	TDH	ELECTRICAL	HP
TACO	FI5013	6”×5”	12.4”	900	140’	208/3/60/1750	50

Table 5-4 lists the information of VFD (PowerFlex 700 from Allen Bradley). It has a rated efficiency of 97.5% and power factor of 0.98. Figure 5-4 plots VFD efficiency change with speed and load variation. Its efficiency is considered constant with speed variation (98%) and is above 95% when load is above 40%.

Table 5-4: Variable Frequency Drive Selected

MANU	MODEL	Efficiency at rated Amps	Power Factor
Allen Bradley	PowerFlex 700	97.5%	0.98

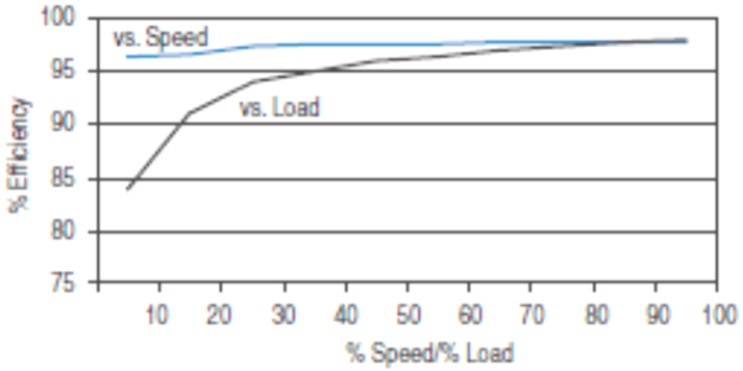

Figure 5-4: Efficiency Derating Plot of PowerFlex 700

Table 5-5 and Table 5-6 list the pump motor information. It is ODP (Open-Drip-Proof) premium efficiency motor. The motor efficiency is considered 95% when the load is above 50%.

Table 5-5: Pump Motor (EM2543T) Efficiency and PF Information

Load	1/2	3/4	Full load
Efficiency %	94.9	95.4	95.0
Power Factor %	75	83	87

Table 5-6: Pump Motor (EM2543T) NAMEPLATE data from Baldor Reliance

CAT.NO EM2543T	**CLASS** F	**Hz** 60	**PF** 87%
SPEC 42F056W387	**PH** 3	**DES** B	**SER F** 1.15
RATING 40C AMB_CONT	**CODE** G	**Usable at** 208 121A	**FRAME** 326T
VOLTS 230/460	**RPM** 1775	**AMPS** 114/57	**HP** 50
NEMA NOM EFF 94.5%			

5.3.1 Pump Controller Installation

The controller is installed according to the wiring diagram in Figure 4-7. For VFD signals such as speed command, start/stop command, power signal, and speed feedback wiring to the IOS1018 board, refer to the wiring diagram below.

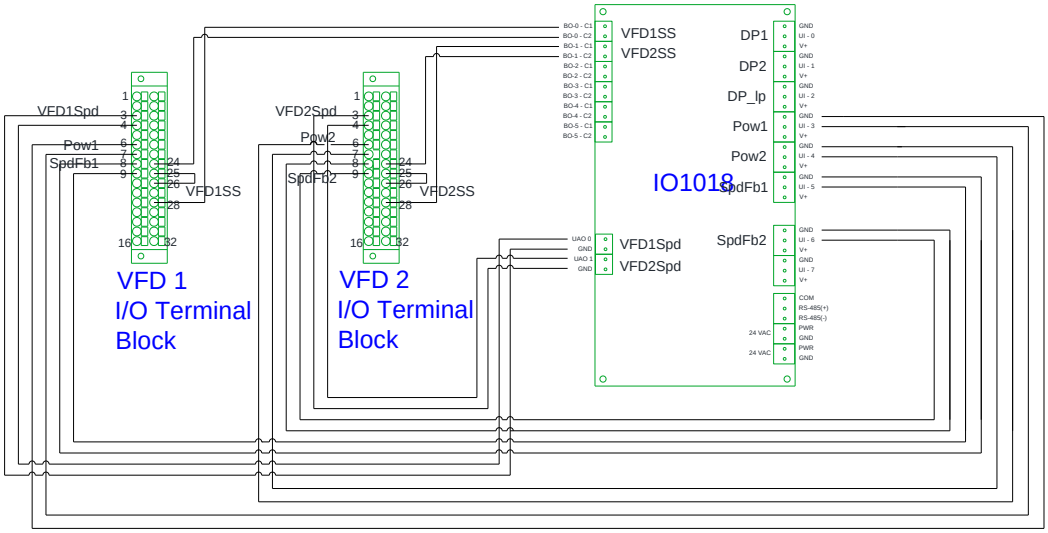

Figure 5-5: VFD signal wiring to Pump Controller ISO1018 Board

5.3.2 Pump Controller Set up

Configuration of the control parameters are listed in Table 5-7. The loop differential pressure maximum and minimum values are 60 PSI and 10 PSI respectively. The system design water flow is 1800 gallon per minute. PID control proportional gain and integral gain are 0.02 and 0.001 respectively.

Table 5-7: Parameter Settings in Pump Controller

Parameter	Value	Parameter	Value
P_gain	0.02	I_gain	0.001
LpDPmax	60	lpDPmin	10
Design Flow	1800		

5.4 System Operation Analysis with Pump Controller

Pump system operation data is analyzed in this part. The trending data is projected to other months with the use of cooling degree days and thus to predict the annual operation of the system with pump controller implemented.

5.4.1 Operation Data Analysis

The new system with pump controller operation data from Jun 11th to Jun 29th 2012 was trended; see Appendix B for the trending data plot. During this period, the water flow range is 580 to 800 GPM (gallon per minute); Pump 1 is running. Pump speed is varied from 33Hz to 45 Hz, and provides the required system head with a high efficiency of 78%. The average flow rate and average power consumption are calculated using the trending data (see Table 5-8). The average water flow rate is 688.53 gallon per minute and the power consumption is 7.762 kW. Compared with the pump system before renovation, it saves 66.32% energy. When VFD power loss is considered (VFD efficiency 95%), the power saving is 64.55%.

Table 5-8: Power Consumption Comparison between Before and After renovation of the Pump System

System	Flow	Power	% saving to base
Before renovation	1070 GPM	23.048kW	0%
After renovation	688.53 GPM	7.762kW	66.32%
		8.171kW (VFD loss added)	64.55%

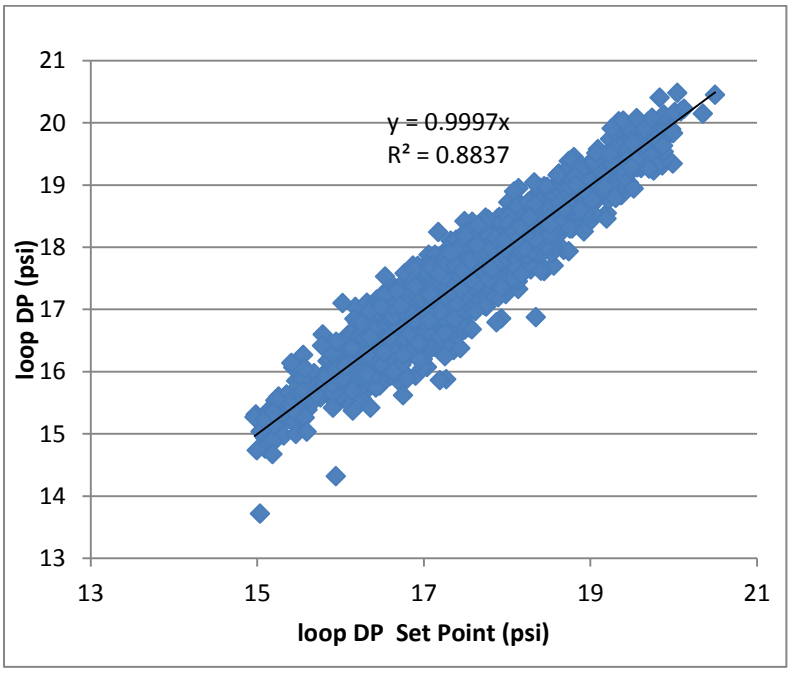

Figure 5-6: Loop Differential Pressure vs. Its Set Point plot during Jun 11th to Jun 29th

In Figure 5-6, x axis is the loop differential pressure set point; y axis is the loop differential pressure. The plot lists all the trending data during Jun 11th to Jun 19th. A linear trend line is plotted to see how well loop DP is consistent with its set point. The linear coefficient is 0.9997 and the R squared value is 0.8837. Both values show that loop DP is modulated well and is consistent with its set point.

Trending data on June 16th is analyzed in the following section.

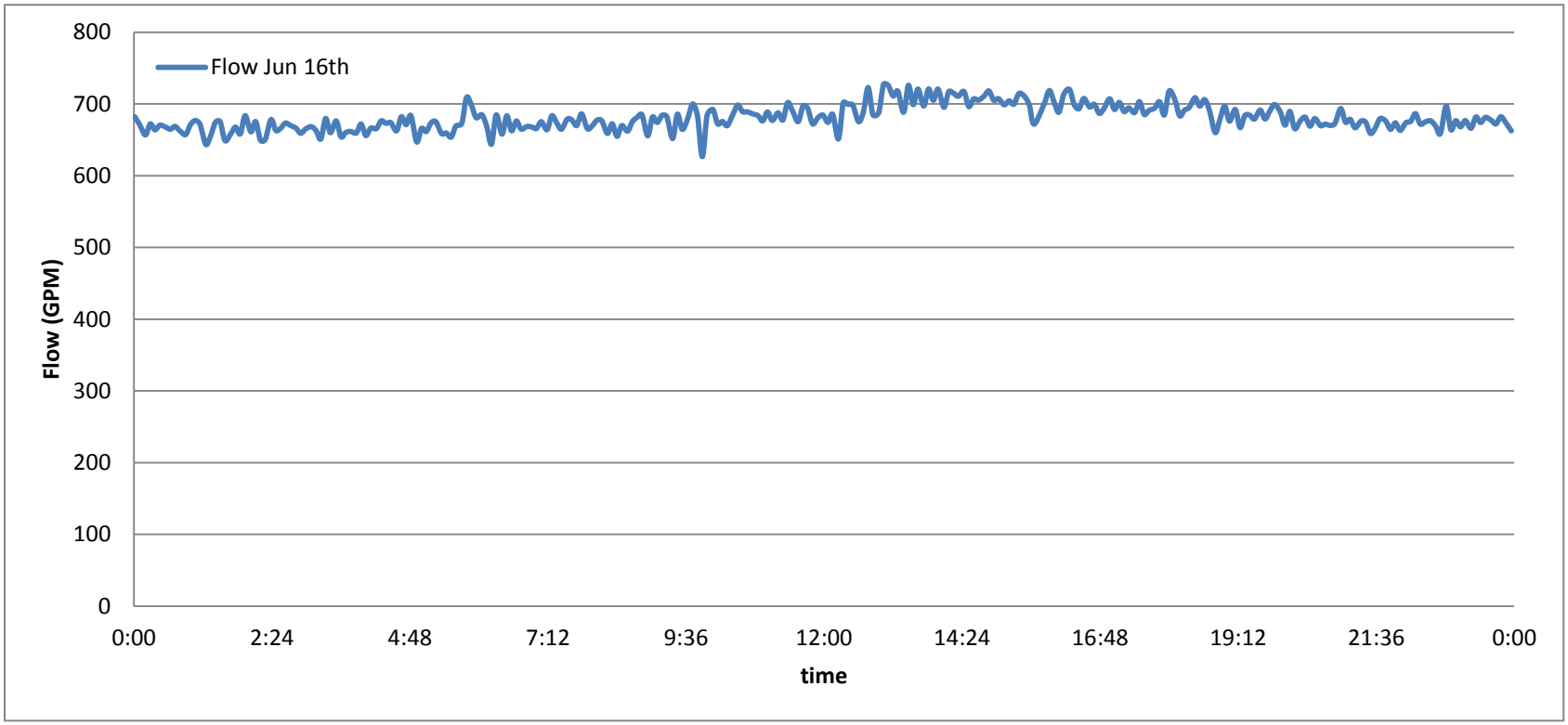

Figure 5-7: Flow Trending Plot on Jun 16th (trending sampling time is 5 minutes)

Figure 5-7 plots the flow trending data on June 16th. The flow rate is around 600 to 750 GPM. The flow variation is smooth without interrupt change.

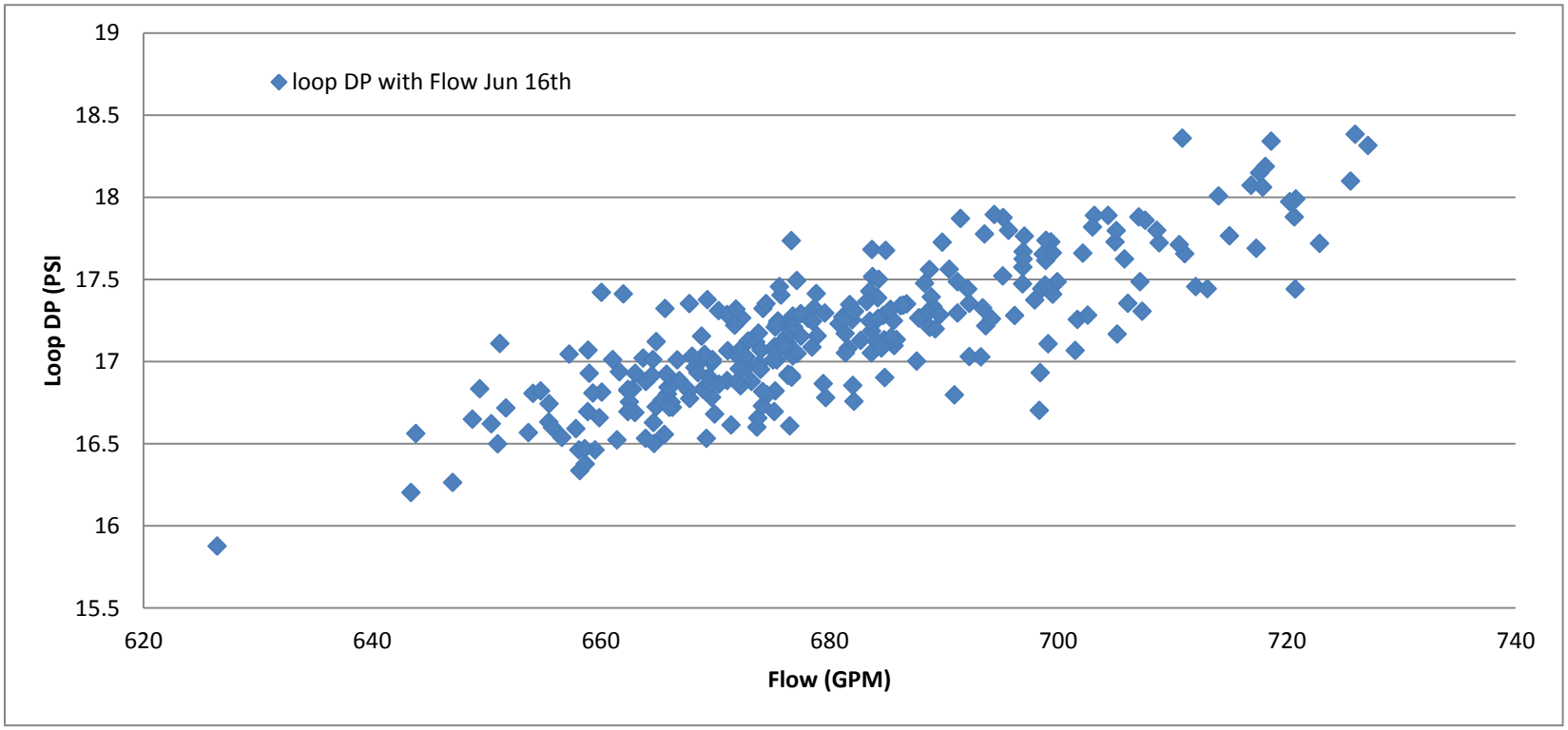

Figure 5-8: Loop Differential Pressure vs. Flow Plot on Jun 16th

Figure 5-8 plots the relationship of loop differential pressure with flow on June 16th. For flow of 640 to 730 GPM, the loop differential pressure is 16.2 to 18.5 PSI. For a specific flow, the loop differential pressure is 1 PSI varied.

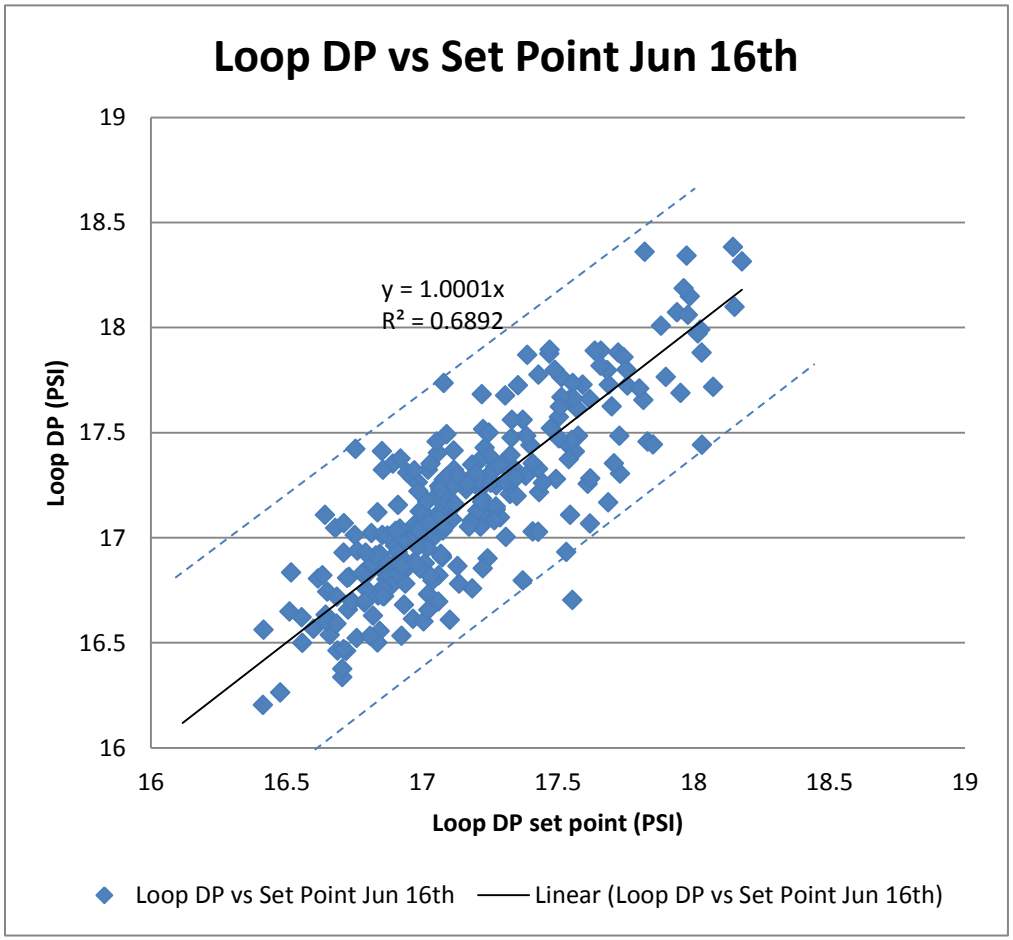

Figure 5-9: Loop Differential Pressure vs. Its Set Point Plot of Jun 16th

Figure 5-9 displays the relationship of loop differential pressure with its set point. A linear trend line is plotted to tell how well

they are matched. The linear coefficient is 1.0001 with R squared value of 0.6892. The dashed blue lines show the upper and lower limit and tell how much loop DP differs from its set point. It is ±0.5 PSI. Both the trend line and dashed blue lines show that loop DP is consistent with its set point and the control is good.

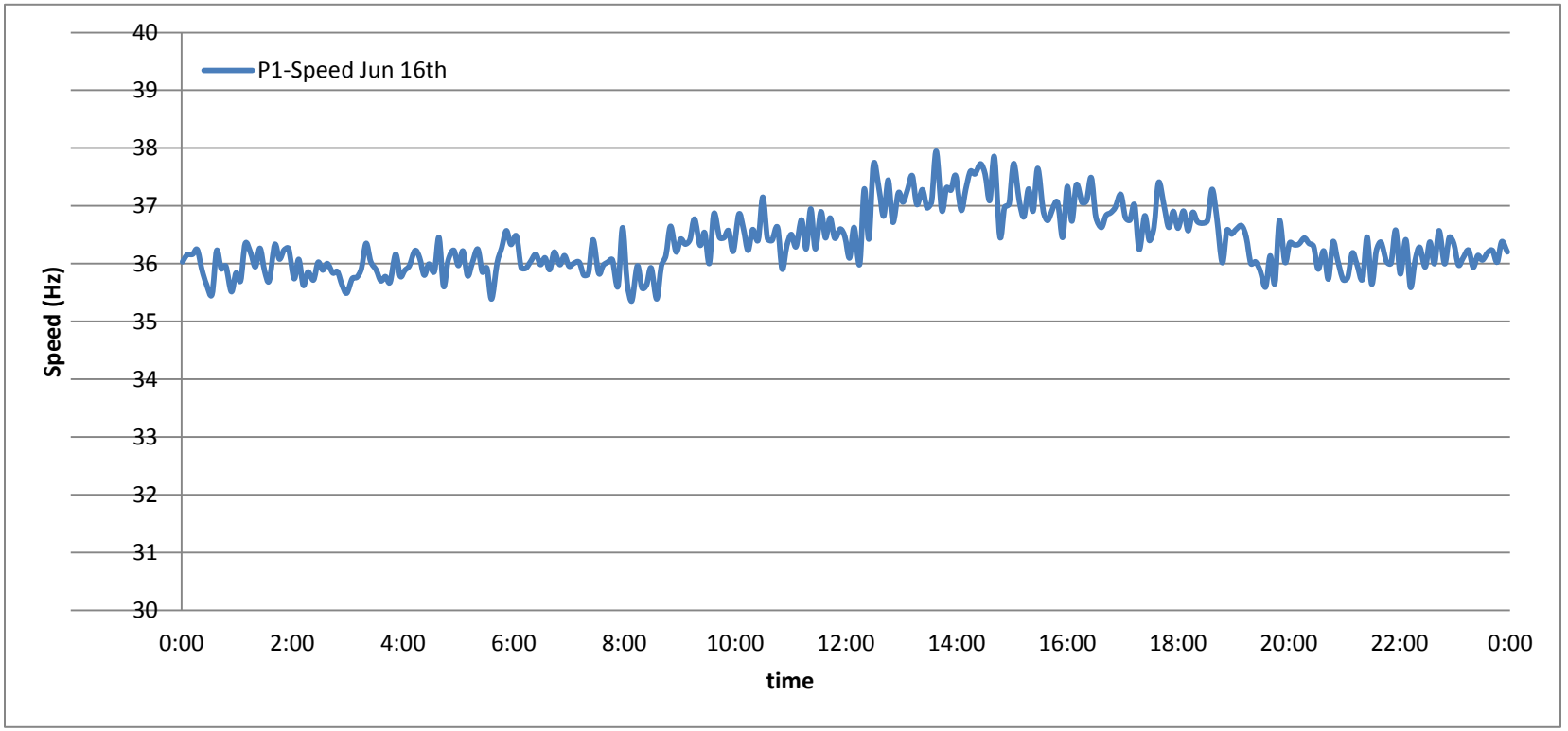

Figure 5-10: Pump 1 Speed Trend Plot on Jun 16th (sampling time interval 5 minutes)

Figure 5-10 plots the pump speed variation with time on June 16th. The speed is varied from 35 Hz to 38 Hz smoothly which is good for pump system operation and chiller operation.

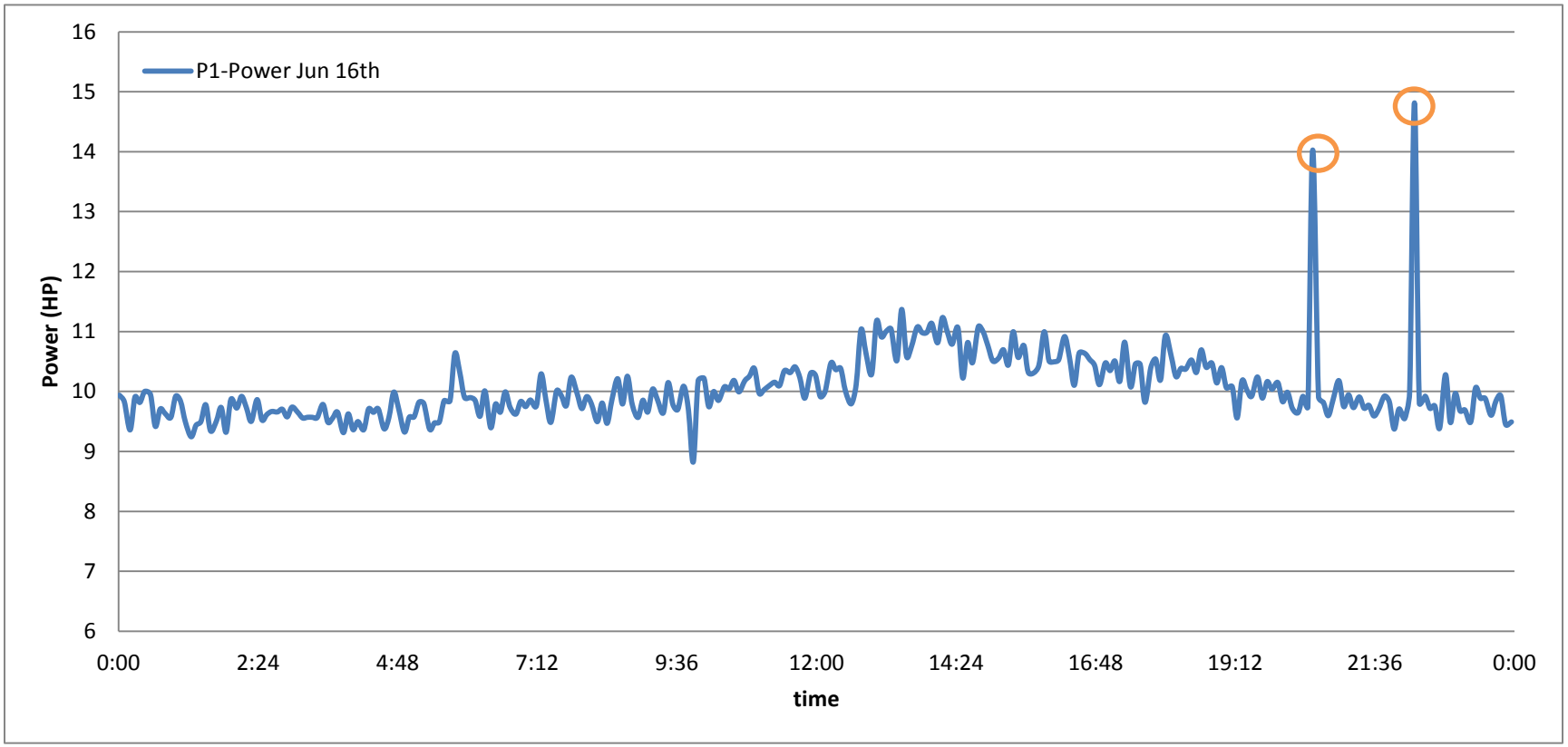

Figure 5-11: Pump 1 Power Trend Plot on Jun 16th (sampling time interval 5 minutes)

Figure 5-11 shows the pump power consumption trending data plot on June 16th. There are two extremely high peak values which are circled in orange. When the flow rate, pump head, and pump speed are in normal values, the pump power should not be that high, so these two data points are considered incorrect data. The power consumption varied from 9 to 11.5 HP.

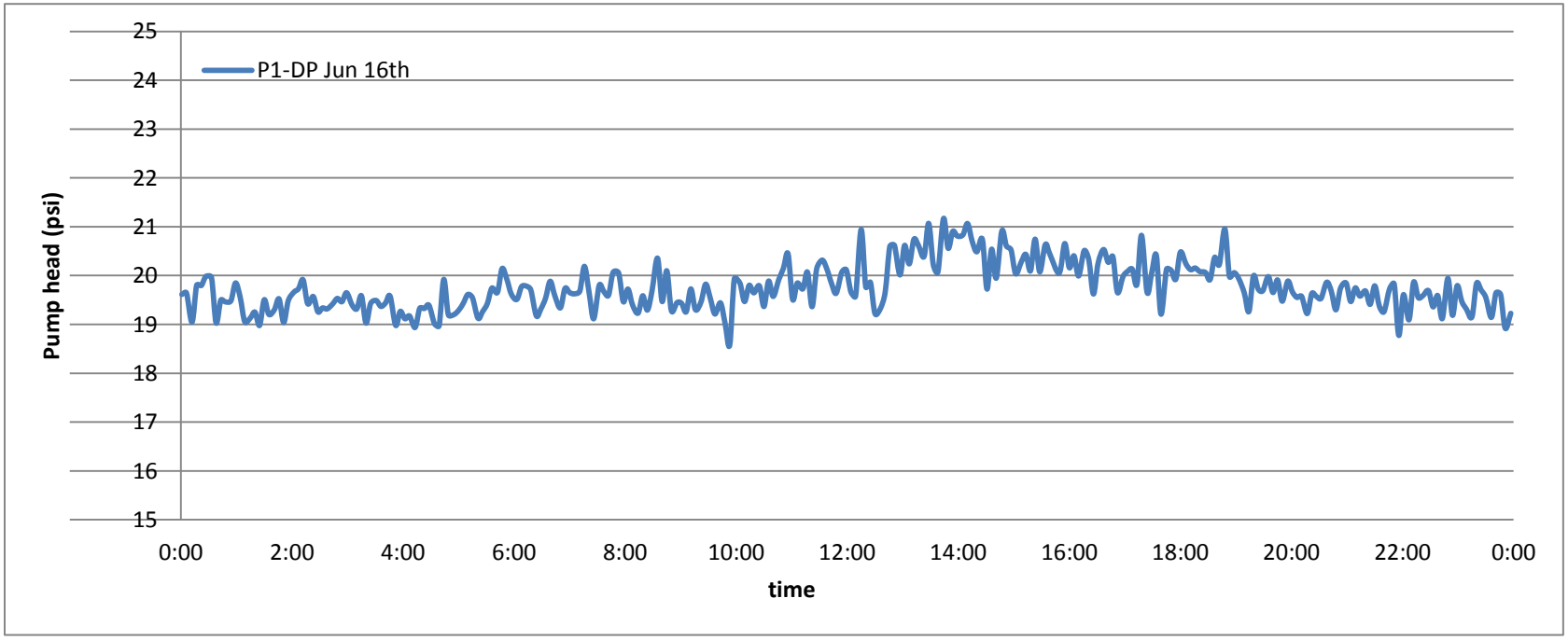

Figure 5-12: Pump 1 Head Trend Plot of Jun 16th (sampling time interval 5 minutes)

Figure 5-12 plots pump head variation with time on June 16th. The pump head varied in the range of 18.5PSI to 21PSI.

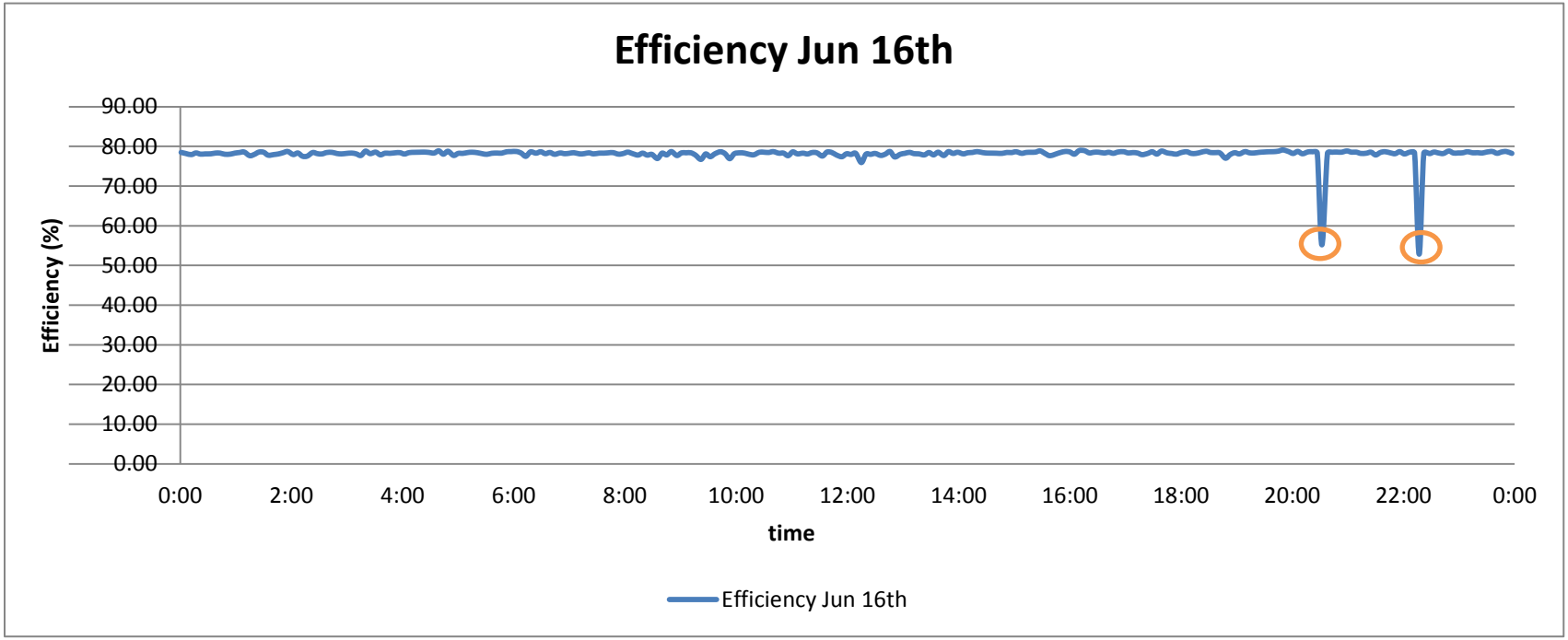

Figure 5-13: Pump 1 Efficiency Trend Plot of Jun 16th (sampling time interval 5 minutes)

Figure 5-13 plots pump efficiency variation with time on June 16th. There are two extremely low peaks in the plot. These two points are consistent with the two high peaks in the power plot in Figure 5-11 and are ignored for the same reason. The efficiency is about 78%.

5.4.2 Monthly Operation Prediction

Assume that the temperate difference between supply water temperature and return water temperature is constant (10^{o}F). The monthly water flow rate is considered proportional to the cooling degree days. With the monthly cooling degree days (base temperature is 65 ^{o}F) and the average water flow rate in June, other months' flow rate can be predicted with the following equation:

$$\boldsymbol{Q' = Q * CDD'/CDD} \qquad \textbf{[5-3]}$$

Where,

Q', average water flow rate of the predicted month;

Q, average water flow rate in June 2012, 688.5GPM;

CDD', monthly cooling degree days of the predicted month as Q';

CDD, monthly cooling degree days of June 2012;

Figure 5-14 plots the predicted monthly water flow rate from March to October for cooling. The higher cooling load stays in June to August.

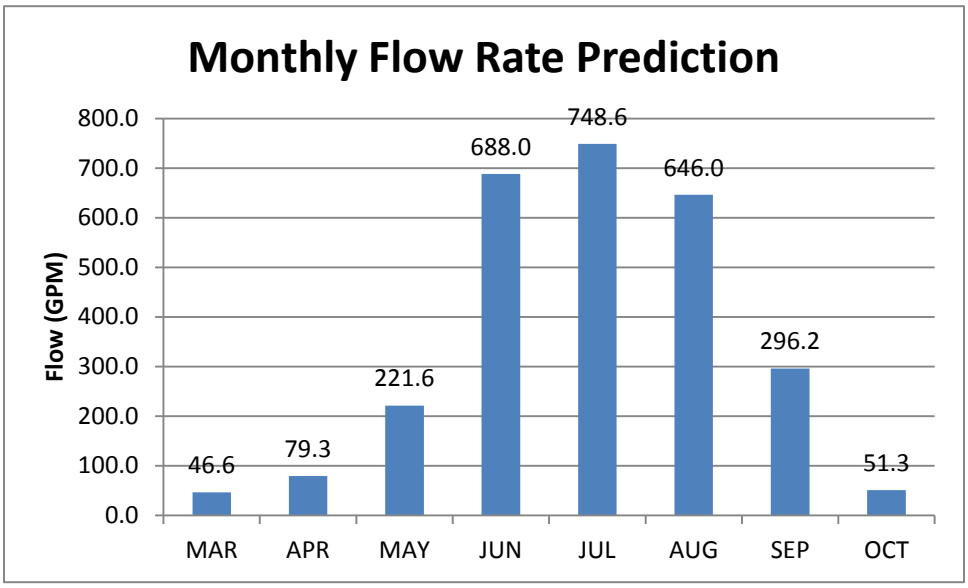

Figure 5-14: predicted water flow rate in other months for cooling

The average ratio of loop DP to pump 1 DP is 0.861. It is obtained by applying the trending data in June to the following equation:

$$\boldsymbol{Z = (\sum_{n}^{1} \frac{lpDPi}{P1DP_i})/n} \qquad \textbf{[5-4]}$$

Where,

Z, ratio of loop DP to Pump 1 DP;

$lpDPi$, the ith data point of loop DP;

$1DP_i$, the ith data point of Pump 1 DP;

n, number of data points;

Then the loop DP is calculated by applying the water flow rate into the following equation which is utilized to calculate the loop DP set point in the pump controller.

$$\boldsymbol{lpDP = (lpDP_{max} - lpDP_{min}) * \left(\frac{Q}{Q_{des}}\right)^2 + lpDP_{min}} \quad \textbf{[5-5]}$$

Where,

$lpDP_{max} = 60psi; lpDP_{min} = 10psi; Q_{des} = 1800GPM$

Then the pump head can be calculated as the following:

$$\boldsymbol{P1DP = lpDP/Z} \quad \textbf{[5-6]}$$

Where,

$P1DP$, pump 1 head;

$lpDP$, loop DP;

Z, ratio of $lpDP$ to $P1DP$ (0.861);

Then the pump speed and power are calculated using equations [5-7] and [5-8]. Figure 5-15 shows the predicted monthly power consumption. The annual power consumption is then 3.96kW.

$$\boldsymbol{\omega 1 = \frac{-a_1 * Q + \sqrt{(a_1 * Q)^2 - 4 * a_0 * (a_2 * Q^2 - H)}}{2 * a_0}} \quad \textbf{[5-7]}$$

$$\boldsymbol{P1 = \left(b_0 + \frac{Q}{\omega 1} * b_1 + \left(\frac{Q}{\omega 1}\right)^2 * b_2\right) * \omega 1^3} \quad \textbf{[5-8]}$$

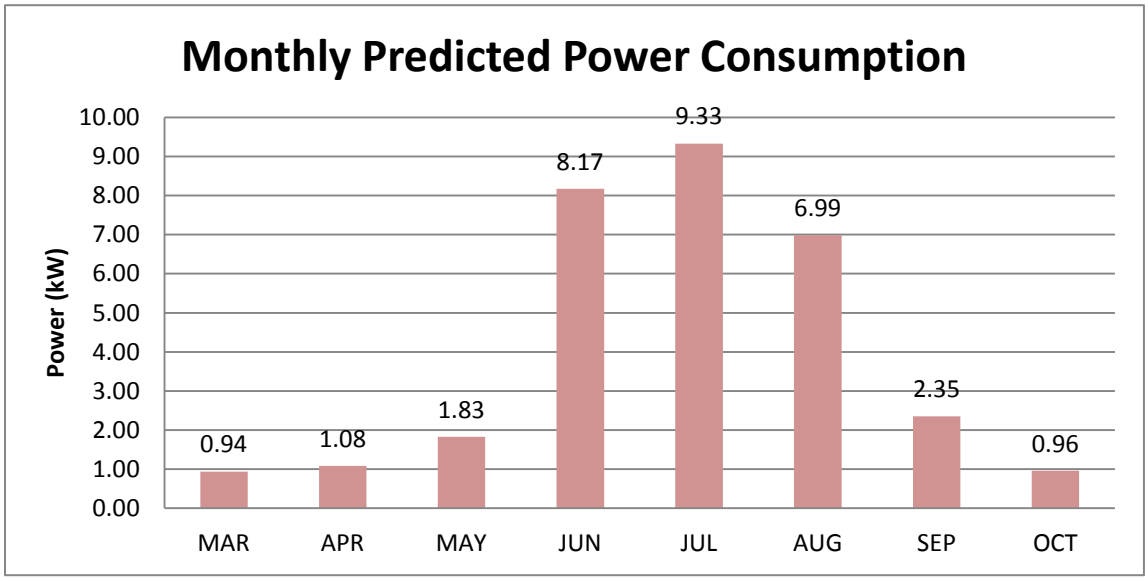

Figure 5-15: Predicted Monthly Power Consumption for cooling

5.5 Summary

The pump system in WNCC was originally running four pumps at constant speed to feed individual AHUs and local loads. It is renovated to variable primary flow configuration with two pumps. The following conclusions are generated using the analysis in the former sections and based on the operation trending data of Jun 11th to Jun 29th:

1) Power savings of 64.5% is achieved compared to the original constant primary system.
2) Loop differential pressure is consistent with its set point.
3) The system operation is stable and energy efficient.

Chapter 6 Conclusion and Future Work

6.1 Conclusion

This thesis presented the design of a pump controller for a variable primary flow configuration pump system. The Best efficiency staging and the loop DP reset were implemented into the pump controller. It was installed and operated in the chiller/boiler plant of WNCC to verify the control effects. Conclusions of the study are listed below:

1) According to the simulation in Chapter 3, the variable primary system has a 40% energy savings when compared to constant primary-variable secondary system; an extra 15% savings is achieved when the pump controller algorithm is implemented.
2) The pump controller potentially provides pump energy savings of 64.5% when compared to constant primary flow system as is verified in WNCC experiment.
3) The system operation with the pump controller is stable.

6.2 Future Work

The following future work is to be done to improve the pump controller:

1) Install and operate the pump controller in more sites to collect more data, especially multiple pump operation data and analyze the energy consumption and system operation status.
2) Add the pump lead/lag switch to the pump controller to equalize pump

operation time.

Reference

Andreasen, B. (2011, April). three keys to hydronic system control. *HPAC Engineering*.

ASHRAE. (2007). *ASHRAE Handbook-HVAC Applications.* Atlanta,GA: American Society of Heating, Refrigerating and Air-Conditioning Engineers,Inc.

ASHRAE. (2008). *ASHRAE Handbook-Systems and Equipment.* Atlanta,GA: American Society of Heating,Refrigerating and Air-Conditioning Engineers, Inc.

Avery, G. (1993). Designing & Commissioning Variable Flow Hydronic Systems. *ASHRAE Journal*.

Avery, G. (2001). Improving the efficiency of Chilled Water Plant. *ASHRAE Journal*, 14-18.

Behnfleth, W., & Peyer, E. (2001). Comparative analysis of variable and constant Primary-Flow Chilled-Water-Plant Performance. *HPAC Engineering 73, no.4*, P41-P50.

Bahnfleth, W., & Peyer, E. (2003). Energy Use Characteristics of Variable Primary Flow Chilled Water Pumping Systems. *International Congress of Refrigeration 2003.* Washington,D.C.

Bahnfleth, W., & Peyer, E. (2004a). *Variable-primary flow chilled water systems: potential benefits and application issues.* Energy Efficiency Research, Arlington, Virginia: Air-Conditioning, Heating, and Refrigeration Institute.

Bahnfleth, W., & Peyer, E. (2004b). Varying Views on Variable-Primary Flow Chilled-Water Systems. *HPAC Engineering 76, no.3*, S5-S9.

Bernier, M., & Bourret, B. (1999). Pumping Energy And Variable Frequency Drives. *ASHRAE*.

BizEE Degree Days Weather Data for Energy Professionals. (n.d.). Retrieved from http://www.degreedays.net/

Chien, K., Hrones, J., & Reswick, J. (1952). On the automatic control of generalized passive systems. *Trans. ASME, 74*, 175.

Clark, D., Hurley, C., & Hill, C. (1985). Dynamic Models for HVAC System Components. In *ASHRAE Transaction, Vol.91,Part 1B* (pp. 737-750).

Erpelding, B. (2006). Ultraefficient All-Variable-Speed Chilled-Water Plants. *HPAC Engineering*, 35-43.

Hartman, T. (2001). Ultra-Efficient Cooling with Demand-Based Control. *HPAC Engineering* , 29-35.

Hegberg, M. C. (2000). Control Valve Selection for Hydronic Systems. *ASHRAE Jounal*.

Hsu, J., Kueck, J., & etc. (1998, Jan/Feb). Comparison of Induction Motor Field Efficiency Evaluation Methods. *IEEE Transactions on Industry Applications. Vol.34, No.1*.

Hubbard, R. S. (2011). Energy Impacts of Chilled-Water-Piping Configuration. *HPAC Engineering*, 20-26.

Kirsner, W. (1996). The demise of the primary-secondary pumping paradigm for chilled water plant design. *HPAC*, 73-78.

Levine, W. (1995). *The control handbook.* CRC Press.

Liu, G. (2006). *Development and Applications of fan air flow station and pump water flow station in heating, ventilating and air-conditioning (HVAC) systems.* University of Nebraska.

Liu, M. (2002a). Variable Speed Drive Volumetric Tracking (VSDVT) for Airflow Control in Variable Air Volume (VAV) Systems. *Solar Energy Engineering*, 318-323.

Liu, M. (2002b). Variable Water Flow Pumping for Central Chilled Water Systems. *Journal of Solar Energy Engineering 124, no. 3*, 300-304.

Liu, M., Liu.G., Joo, I., Song, L. & Wang G. (2005). Development of In-situ Fan Curve Measurement for VAV AHU Systems. *Solar Energy Engineering*, 287-293.

NEMA. (2004). *Motors and generators, Standard MG 1-2003, Rev.1-2004.* Rosslyn, VA.: National Electrical Manufacturers Association.

Nonnenmann, J. J., & Flynn, D. J. (2010). Improving Efficiency with Variable-Primary Flow. *HPAC Engineering*, 0-45.

SMACNA. (2010). In SMACNA, *HVAC Systems Application 2nd Edition* (p. 17.2). Chantilly,VA: Sheet Metal and Air Conditioning Contractors' National Association,Inc.

Taylor, S. T. (2002a). Degrading Chilled Water Plant Delta-T: Causes and Mitigation. *ASHRAE Transactions V108, Pt.1*, 1-13.

Taylor, S. T. (2002b). Primary-Only vs. Primary-Secondary Variable Flow Systems. *ASHRAE Journal 44, no. 2*, 25-29.

Taylor, S. T. (2006). Chilled Water Plant Rotrofit-A Case Study. *ASHRAE Transactions 112*, 187-197.

Taylor, S. T., & Stein, J. (2002). Balancing Variable Flow Hydronic Systems. *ASHRAE Journal*, 17-24.

Wang, G., & Liu, M. (2007). Development of Motor Powe Based Fan Airflow Station. *Proceedings of Energy Sustainability*.

Wang, Z. (2010). *PhD Dissertation:Two-Pump Systems for central plant-innovative pump design and operation.* Lincoln: University of Nebraska-Lincoln (230).

Ziegler, J., & Nichols, N. (1942). Optimum settings for automatic controllers. In *Trans. ASME, 64,* (p. 759).

Appendix – A: Pump Efficiency Regression

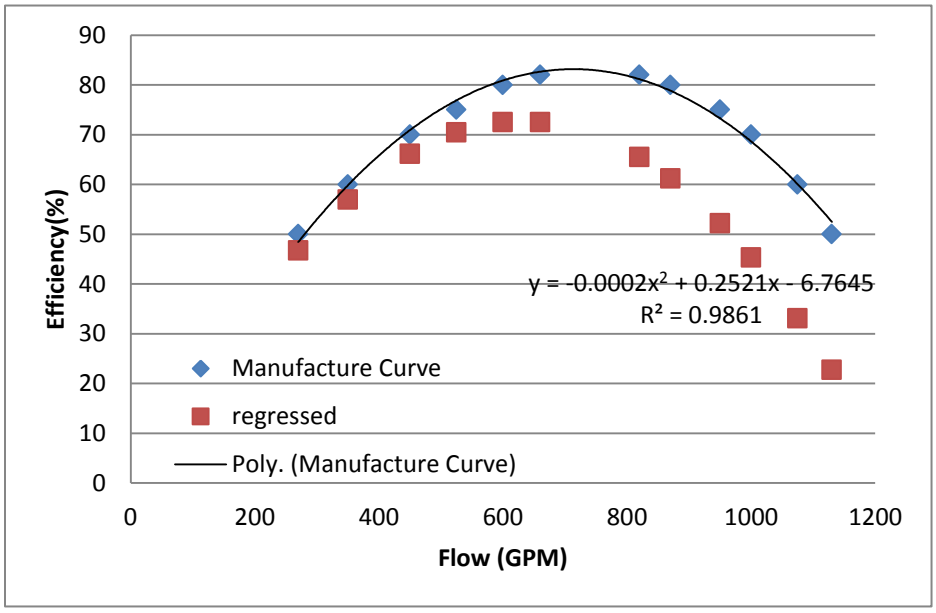

Figure A-1: Manufacture Efficiency Curve and Regressed Efficiency Curve (Model: FI6013, IN.DIA 9.5")

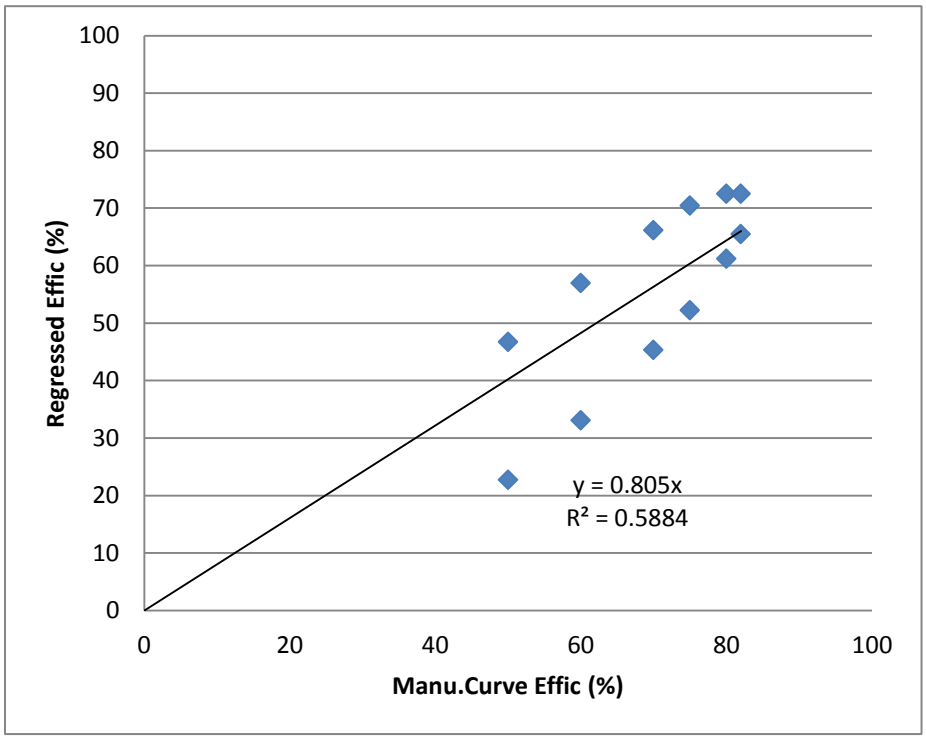

Figure A-2: Manu. Curve efficiency and regressed efficiency comparison (Model: FI6013, IN.DIA 9.5")

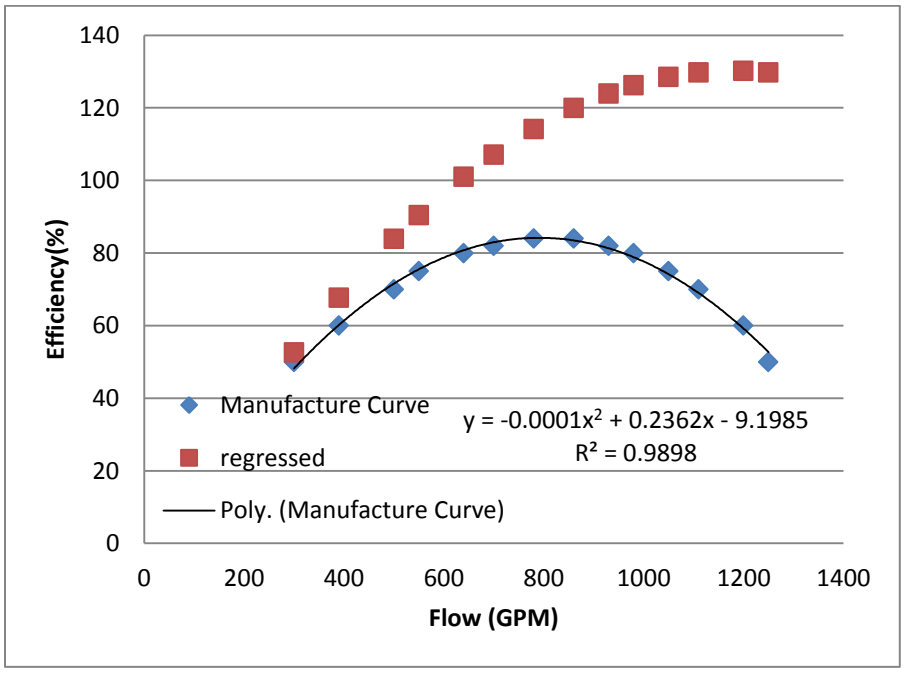

Figure A-3: Manufacture Efficiency Curve and Regressed Efficiency Curve (Model: FI6013, IN.DIA 10.375")

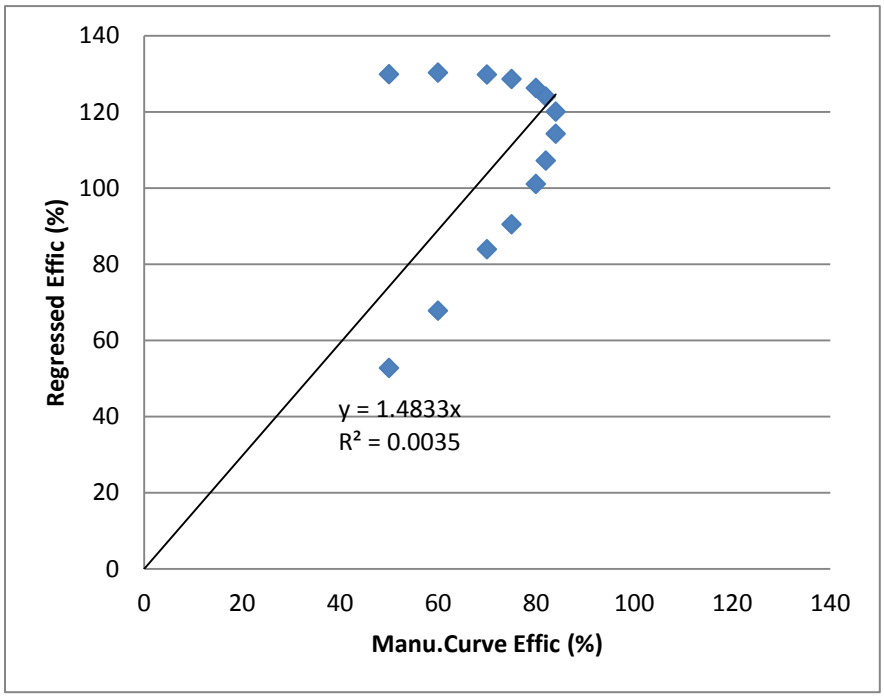

Figure A-4: Manu. Curve efficiency and regressed efficiency comparison (Model: FI6013, IN.DIA 10.375")

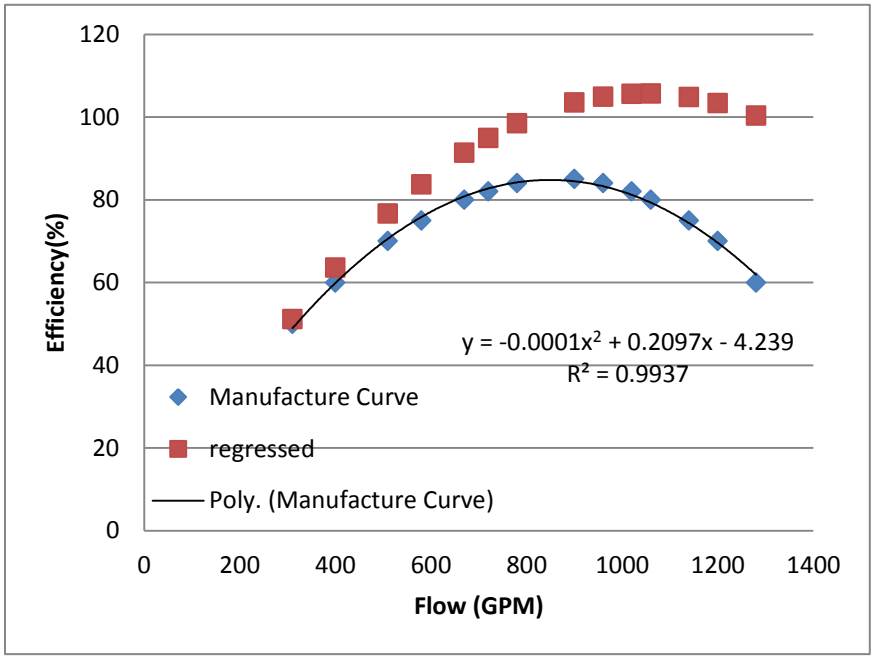

Figure A-5: Manufacture Efficiency Curve and Regressed Efficiency Curve (Model: FI6013, IN.DIA 11.25")

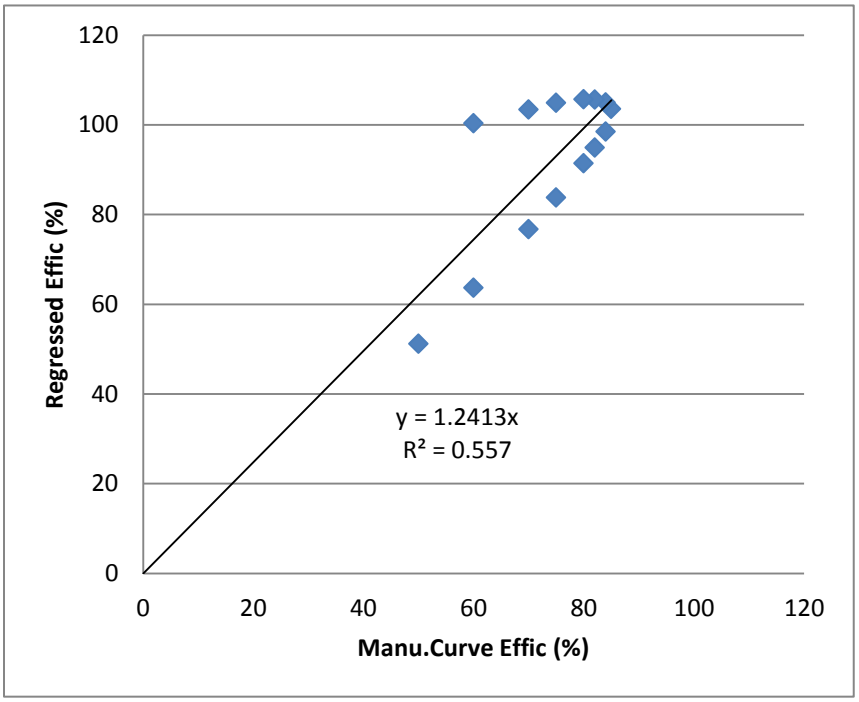

Figure A-6: Manu. Curve efficiency and regressed efficiency comparison (Model: FI6013, IN.DIA 11.25")

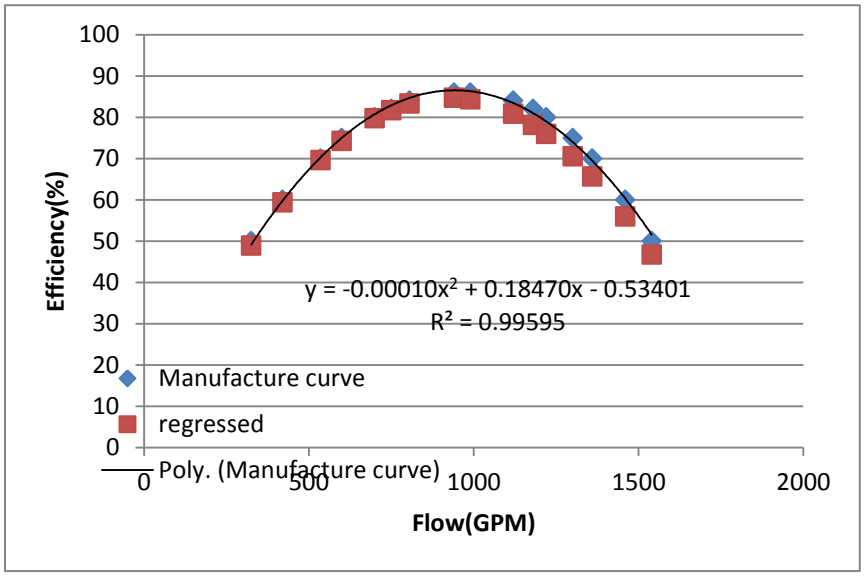

Figure A-7: Manufacture Efficiency Curve and Regressed Efficiency Curve (Model: FI6013, IN.DIA 12.125")

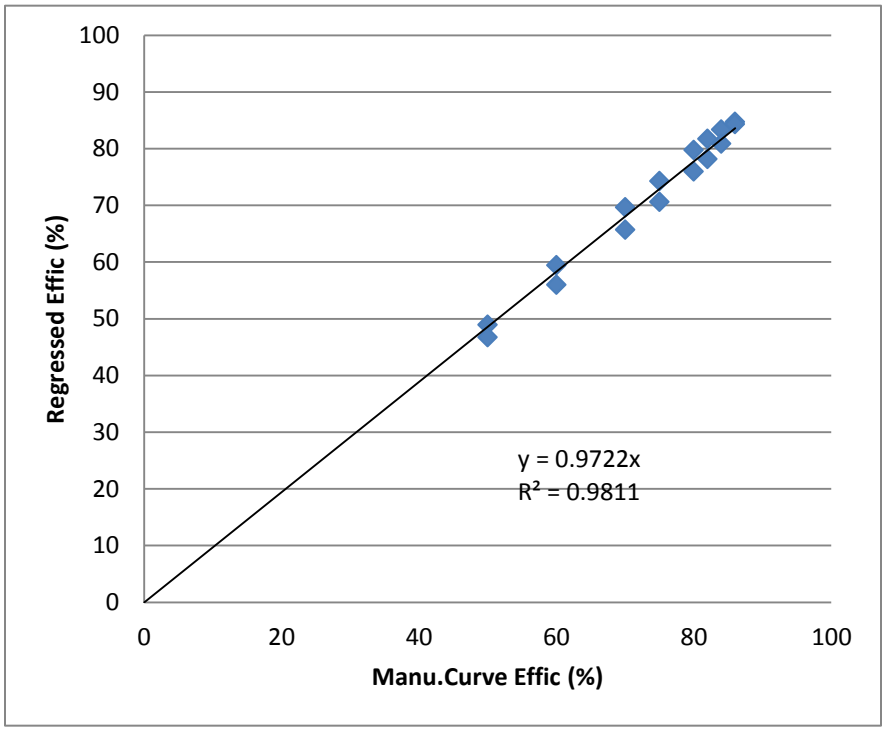

Figure A-8: Manu. Curve efficiency and regressed efficiency comparison (Model: FI6013, IN.DIA 12.125")

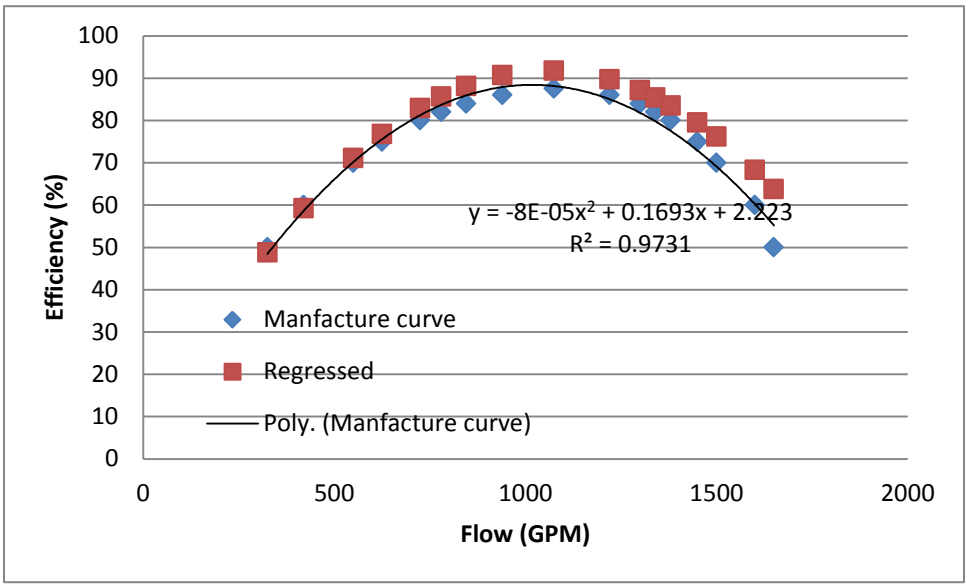

Figure A-9: Manufacture Efficiency Curve and Regressed Efficiency Curve (Model: FI6013, IN.DIA 13")

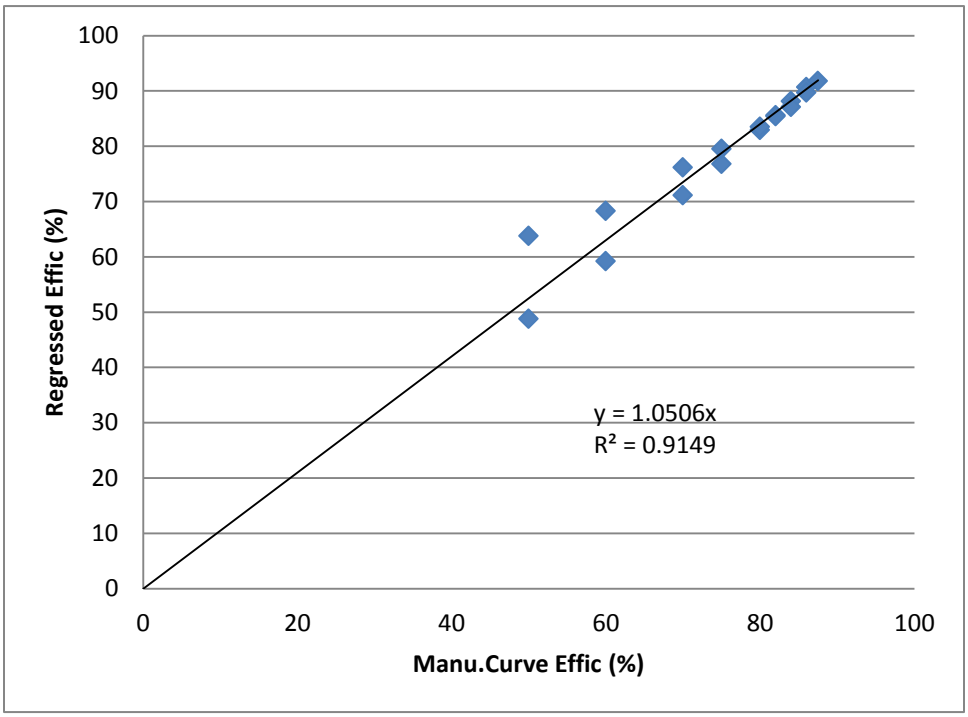

Figure A-10: Manu. Curve efficiency and regressed efficiency comparison (Model: FI6013, IN.DIA 13")

Appendix – B: Pump Power Simulation with Spreadsheet

design working point

Qdes(GPM) Hdes(fWg)

1800

	case 1	CPF configuration					
No. Pump	head (fwg)	tFlow	flow	speed	pow(hp)	tPow(hp)	system res
4	139.75044	1800	450	100%	21.90179	87.60717	4.31329E-05
		1700				87.60717	
		1600				87.60717	
		1500				87.60717	
		1400				87.60717	
		1300				87.60717	
		1200				87.60717	
		1100				87.60717	
		1000				87.60717	
		900				87.60717	
		800				87.60717	
		700				87.60717	
		600				87.60717	
		500				87.60717	
		400				87.60717	
		300				87.60717	
		200				87.60717	

$$flow = \frac{tFlow}{No.\ Pump}$$

$$head = a_0 + a_1 * flow + a_2 * flow^2$$

$$pow = b_0 + b_1 * flow + b_2 * flow^2$$

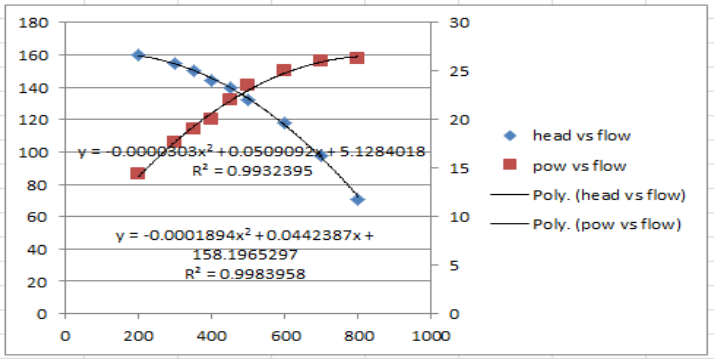

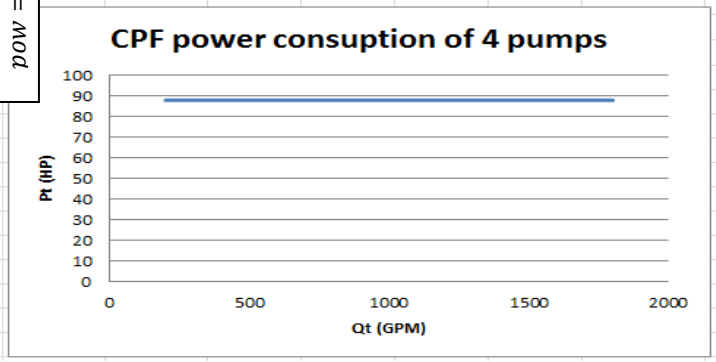

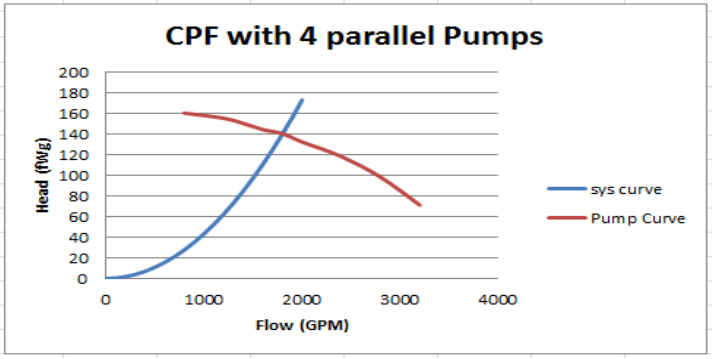

Figure B-1: CPF configuration with 4 pumps Power Consumption Simulation

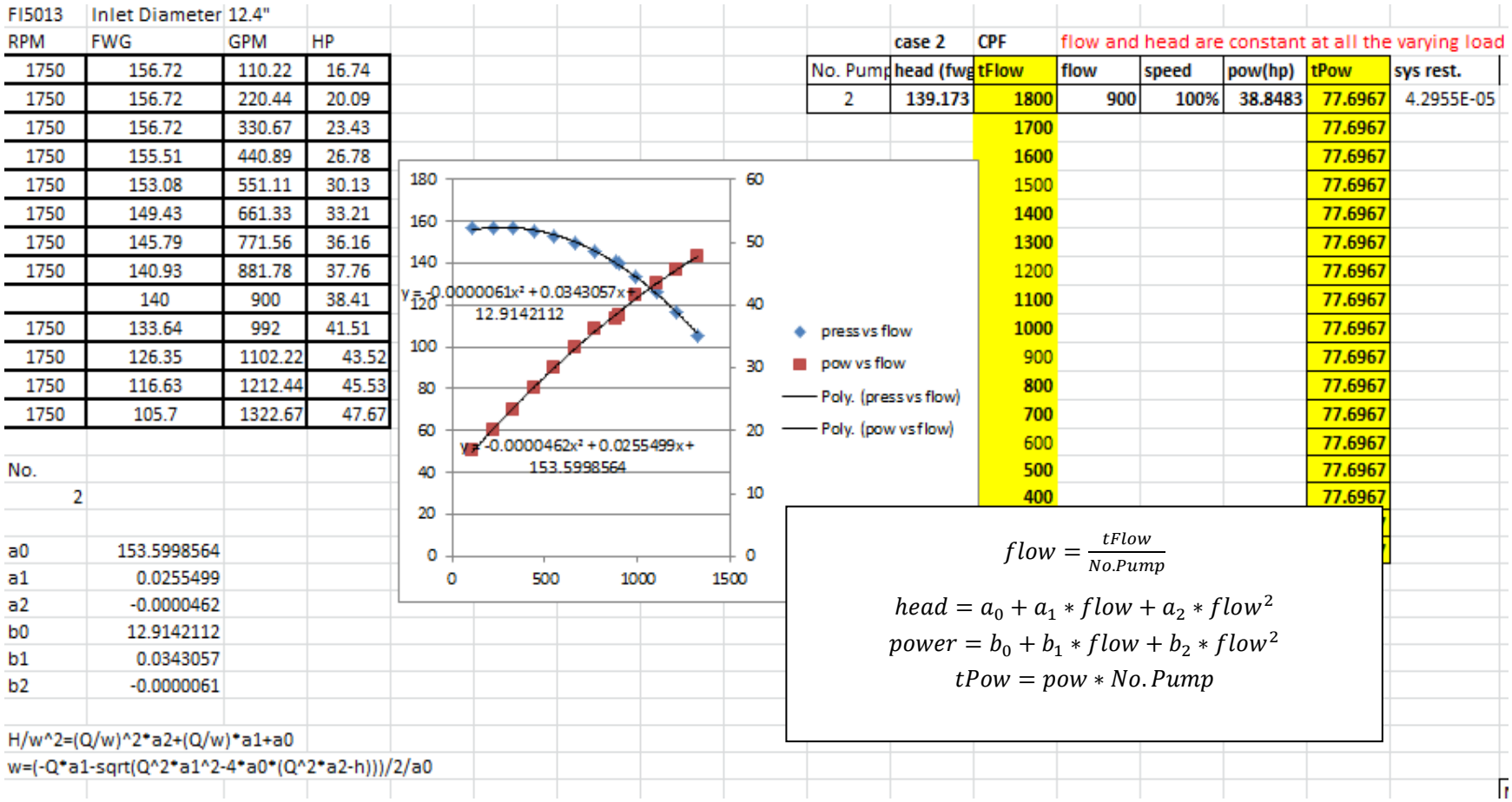

Figure B-2: CPF configuration with 2 pumps Power Consumption Simulation

Secondary side

Q	H	w1	w2	P1	P2	P1-P2	P_MAX flow	P_best effic	Q_norm	P1_norm	P2_norm
0	19.6	0.4205	0.4205	0.47717	0.95434	-0.477168804	0.477168804	0.954337608	0	0.005125336	0.010250672
100	19.842	0.41426	0.41719	0.97357	1.48337	-0.509793858	0.973572447	1.483366305	0.055555556	0.010457277	0.015933043
200	20.5679	0.42419	0.42182	1.47005	2.03816	-0.568110197	1.47004725	2.038157447	0.111111111	0.015789981	0.021892132
300	21.7778	0.44785	0.43379	2.06462	2.67502	-0.610396741	2.064619973	2.675016714	0.166666667	0.022176369	0.028732725
400	23.4716	0.48234	0.45219	2.83422	3.44481	-0.610590706	2.834224225	3.444814931	0.222222222	0.030442795	0.037001234
500	25.6494	0.52499	0.47607	3.84459	4.39467	-0.55007883	3.844590744	4.394669574	0.277777778	0.041295282	0.047203755
600	28.3111	0.57367	0.50448	5.15646	5.56942	-0.412952675	5.156463945	5.56941662	0.333333333	0.055386294	0.059821876
700	31.4568	0.62681	0.5366	6.8287	7.01267	-0.183970937	6.828695056	7.012665993	0.388888889	0.07334796	0.075324017
758.89	33.5357	0.65973	0.55696	8.0056	8.0056	-0.0000004756	8.0056032519	8.0056037275	0.421605574	0.085989294	0.085989299
800	35.0864	0.68329	0.57173	8.91957	8.76746	0.152108786	8.91956668	8.767457894	0.444444444	0.095806302	0.09417248
900	39.2	0.74228	0.6093	11.4873	10.8766	0.610668984	11.48729706	10.87662807	0.5	0.123386649	0.116827369
1000	43.7975	0.8032	0.64887	14.5902	13.383	1.207213027	13.38299155	13.38299155	0.555555556	0.156715409	0.143748567
1100	48.879	0.86562	0.69005	18.2867	16.3294	1.957318581	16.32942428	16.32942428	0.611111111	0.196420439	0.175396609
1200	54.4444	0.92924	0.73258	22.6355	19.7589	2.876599651	19.75889179	19.75889179	0.666666667	0.24313095	0.212232995
1300	60.4938	0.99381	0.77621	27.6951	23.7145	3.980682186	23.71445254	23.71445254	0.722222222	0.29747728	0.254720221
1400	67.0272	1.05915	0.82076	33.5244	28.2393	5.285190283	28.23925027	28.23925027	0.777777778	0.360090661	0.3033217
1500	74.0444	1.12513	0.86609	40.1822	33.3765	6.805739249	33.37650274	33.37650274	0.833333333	0.431603029	0.358501641
1600	81.5457	1.19164	0.91208	47.7274	39.1695	8.557932733	39.16949004	39.16949004	0.888888889	0.512646861	0.42072492
1700	89.5309	1.25859	0.95862	56.2189	45.6615	10.55736208	45.661544	45.661544	0.944444444	0.60385506	0.490456971
1800	98	1.32592	1.00565	65.7156	52.896	12.81960685	52.89603897	52.89603897	1	0.705860857	0.568163684
1350	63.7	1.02639	0.79838	30.5099	25.903	4.606906829			0.75	0.327711107	0.278227683
450	24.5	0.50279	0.4635	3.30545	3.89439	-0.588947213			0.25	0.035504262	0.041830226

a0	110.845	b0	6.41742809	a0'	110.8448151
a1	0.03285	b1	0.03319862	a1'	0.01642714
a2	-5.4E-05	b2	-0.00001264	a2'	-0.00001353

Qdes	1800	gpm
Hdes	98	gpm
Pdes	93.1	HP

Independent head ratio

0.2

w1,P1 for single pump operation

w2,P2 for 2 pump operation

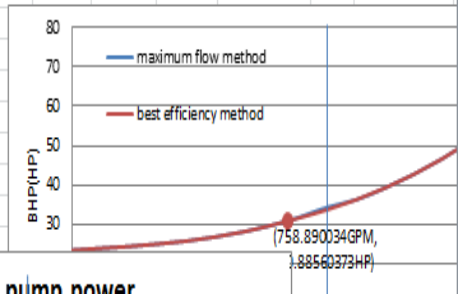

Figure B-3: PSF configuration Secondary Side Pump Power Consumption Simulation with Constant DP control Method

$$H = H_{des} * (IndependentHeadRatio + (1 - IndependentHeadRatio) * \left(\frac{Q}{Q_{des}}\right)^2)$$

$\omega 1 = \frac{-a_1 * Q + \sqrt{(a_1 * Q)^2 - 4 * a_0 * (a_2 * Q^2 - H)}}{2 * a_0}$ Speed ratio when 1 pump is in operation;

$\omega 2 = \frac{-a_1' * Q + \sqrt{(a_1' * Q)^2 - 4 * a_0' * (a_2' * Q^2 - H)}}{2 * a_0'}$ Speed ratio when 2 pumps are in operation;

$a_0' = a_0; a_1' = \frac{a_1}{N}; a_2' = a_2 / N^2$ N=2 (number of pumps in operation);

$P1 = \left(b_0 + \frac{Q}{\omega 1} * b_1 + \left(\frac{Q}{\omega 1}\right)^2 * b_2\right) * \omega 1^3$ Power consumption when 1 pump is in operation;

$P2 = \left(b_0 + \frac{Q}{2 * \omega 2} * b_1 + \left(\frac{Q}{2 * \omega 2}\right)^2 * b_2\right) * \omega 2^3 * 2$ Power consumption when 2 pumps are in operation;

Figure B-4: Equations utilized for PSF configuration Secondary Side Pump Power Consumption Simulation with Constant DP control Method

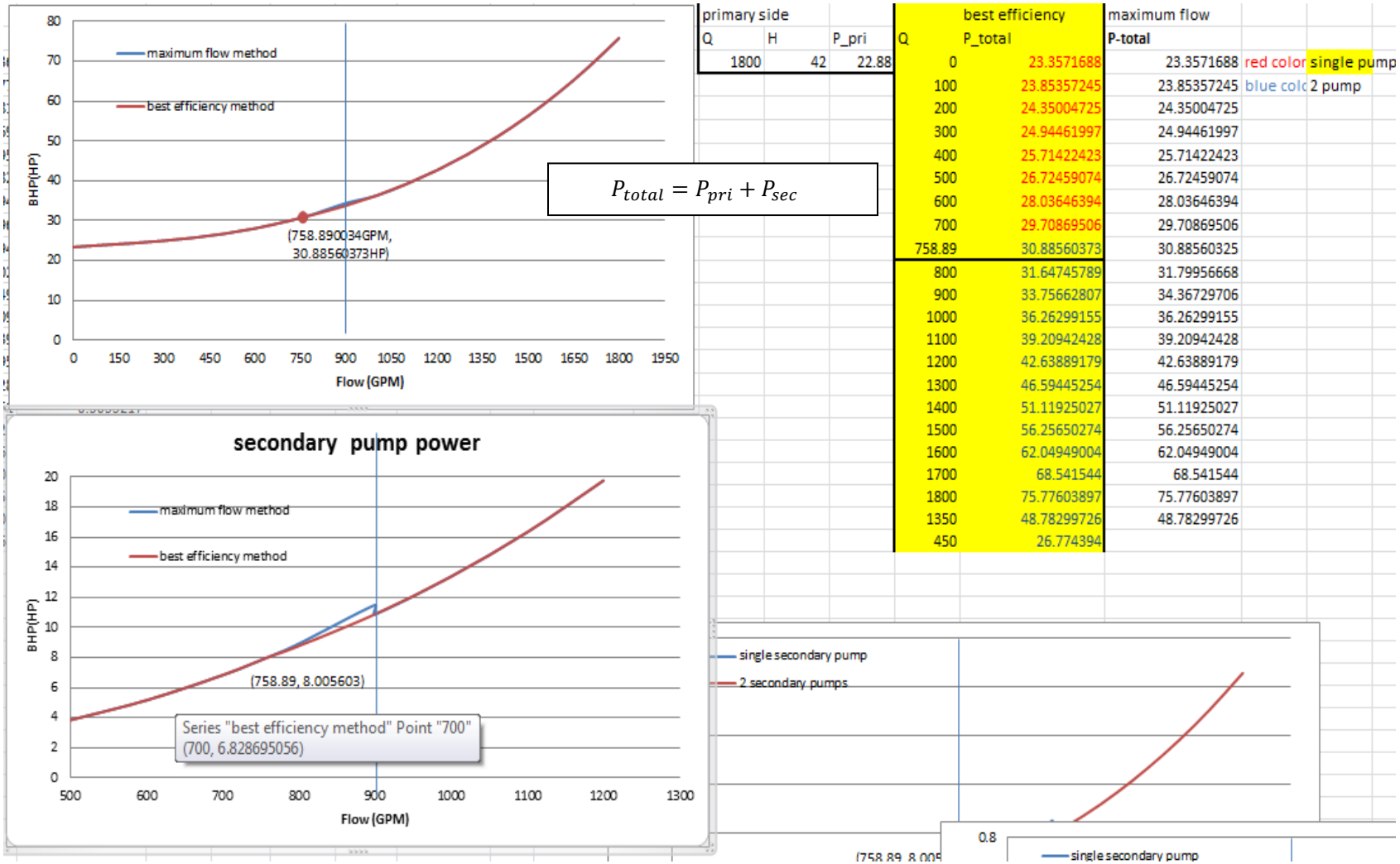

primary side			best efficiency		maximum flow	
Q	H	P_pri	Q	P_total	P-total	
1800	42	22.88	0	23.3571688	23.3571688	red color single pump
			100	23.85357245	23.85357245	blue colo 2 pump
			200	24.35004725	24.35004725	
			300	24.94461997	24.94461997	
			400	25.71422423	25.71422423	
			500	26.72459074	26.72459074	
			600	28.03646394	28.03646394	
			700	29.70869506	29.70869506	
			758.89	30.88560373	30.88560325	
			800	31.64745789	31.79956668	
			900	33.75662807	34.36729706	
			1000	36.26299155	36.26299155	
			1100	39.20942428	39.20942428	
			1200	42.63889179	42.63889179	
			1300	46.59445254	46.59445254	
			1400	51.11925027	51.11925027	
			1500	56.25650274	56.25650274	
			1600	62.04949004	62.04949004	
			1700	68.541544	68.541544	
			1800	75.77603897	75.77603897	
			1350	48.78299726	48.78299726	
			450	26.774394		

Figure B-5: PSF configuration total Pump Power Consumption Simulation with Constant DP control Method

Q	H	w1	w2	P1	P2	P1-P2	
0	19.6	0.35722	0.35722	0.58866	1.17732	-0.588661696	
100	19.9716	0.35651	0.35749	0.99947	1.6076	-0.608129491	
200	21.0864	0.37013	0.36633	1.50451	2.14576	-0.641248059	
300	22.9444	0.39585	0.38287	2.19637	2.85325	-0.656877909	
400	25.5457	0.431	0.406	3.16236	3.79237	-0.630007008	
500	28.8901	0.47321	0.43453	4.48775	5.02652	-0.538769212	
600	32.9778	0.5206	0.46738	6.25746	6.62021	-0.36275639	
700	37.8086	0.5718	0.50366	8.55669	8.63896	-0.082263738	
723.254	39.0385	0.58414	0.51251	9.17637	9.17637	-0.0000000009	
800	43.3827	0.62583	0.54264	11.4711	11.1491	0.322019703	
900	49.7	0.68198	0.58376	15.0867	14.2176	0.869147191	C
1000	56.7605	0.73977	0.62659	19.4899	17.9119	1.577986762	
1100	64.5642	0.79882	0.67079	24.7672	22.2999	2.467267892	
1200	73.1111	0.85888	0.7161	31.0052	27.4496	3.555614929	
1300	82.4012	0.91973	0.76232	38.2909	33.4293	4.861572031	
1400	92.4346	0.98123	0.80928	46.711	40.3074	6.403621955	
1500	103.211	1.04326	0.85688	56.3527	48.1525	8.200200234	
1600	114.731	1.10574	0.905	67.3028	57.0331	10.26970589	
1700	126.994	1.16858	0.95356	79.6485	67.0179	12.63050953	
1800	140	1.23174	1.0025	93.4767	78.1758	15.30095949	A
1350	87.325	0.95041	0.78571	42.3537	36.7518	5.601932203	B
450	27.125	0.45135	0.41966	3.77483	4.36856	-0.593731655	D

				N	2	
a0	153.5998564	b0	12.9142112	a0'	153.599856	
a1	0.0255499	b1	0.0343057	a1'	0.01277495	
a2	-0.0000462	b2	-0.0000061	a2'	-0.00001155	

Qdes	1800	gpm	red color	single pump
Hdes	140	gpm	blue color	2 pump

Independent head ratio

0.14

w1,P1 for single pump operation

w2,P2 for 2 pump operation

Q	best effic P_total	max flow P_total
0	0.58866	0.58866
100	0.99947	0.99947
200	1.50451	1.50451
300	2.19637	2.19637
400	3.16236	3.16236
500	4.48775	4.48775
600	6.25746	6.25746
700	8.55669	8.55669
723.254	9.17637	9.17637
800	11.1491	11.4711
900	14.2176	15.0867
1000	17.9119	17.9119
1100	22.2999	22.2999
1200	27.4496	27.4496
1300	33.4293	33.4293
1400	40.3074	40.3074
1500	48.1525	48.1525
1600	57.0331	57.0331
1700	67.0179	67.0179
1800	78.1758	78.1758
		36.7518

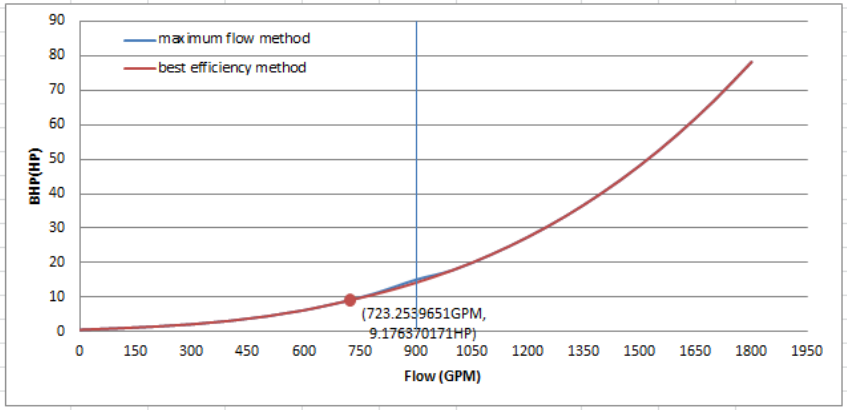

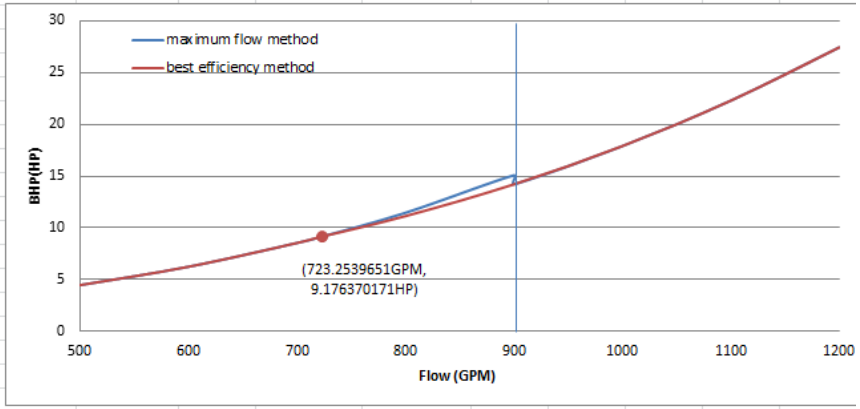

Figure B-6: VPF configuration Pump Power Consumption Simulation with Constant DP control Method

$$H = H_{des} * (z_{des} + (1 - z_{des}) * \left(\frac{Q}{Q_{des}}\right)^2)$$

$\omega 1 = \frac{-a_1 * Q + \sqrt{(a_1 * Q)^2 - 4 * a_0 * (a_2 * Q^2 - H)}}{2 * a_0}$ Speed ratio when 1 pump is in operation;

$\omega 2 = \frac{-a_1' * Q + \sqrt{(a_1' * Q)^2 - 4 * a_0' * (a_2' * Q^2 - H)}}{2 * a_0'}$ Speed ratio when 2 pumps are in operation;

$a_0' = a_0; a_1' = \frac{a_1}{N}; a_2' = a_2/N^2$ N=2 (number of pumps in operation);

$P1 = \left(b_0 + \frac{Q}{\omega 1} * b_1 + \left(\frac{Q}{\omega 1}\right)^2 * b_2\right) * \omega 1^3$ Power consumption when 1 pump is in operation;

$P2 = \left(b_0 + \frac{Q}{2 * \omega 2} * b_1 + \left(\frac{Q}{2 * \omega 2}\right)^2 * b_2\right) * \omega 2^3 * 2$ Power consumption when 2 pumps are in operation;

Figure B-7: equations utilized in VPF configuration Pump Power Consumption Simulation with Constant DP control Method

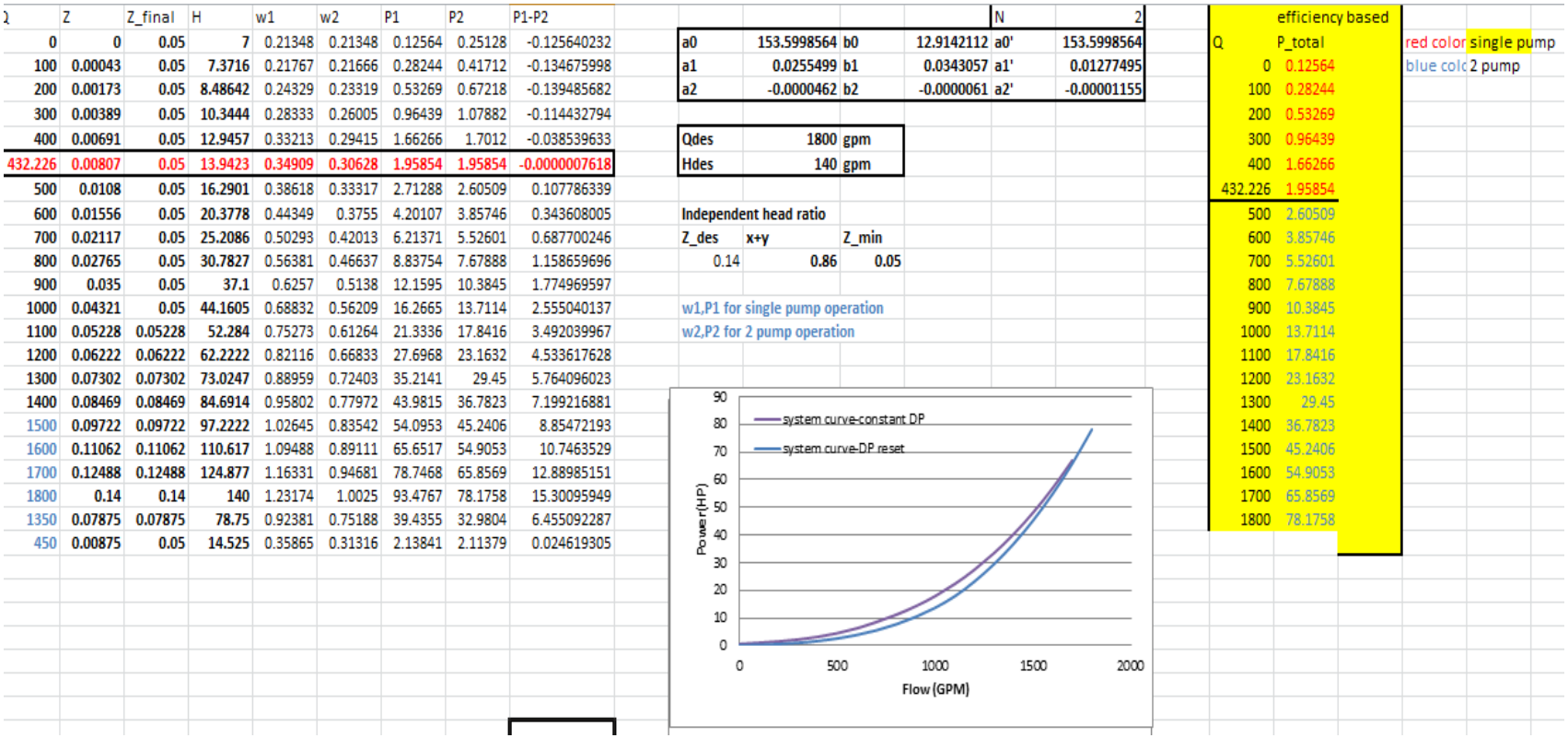

Q	Z	Z_final	H	w1	w2	P1	P2	P1-P2
0	0	0.05	7	0.21348	0.21348	0.12564	0.25128	-0.125640232
100	0.00043	0.05	7.3716	0.21767	0.21666	0.28244	0.41712	-0.134675998
200	0.00173	0.05	8.48642	0.24329	0.23319	0.53269	0.67218	-0.139485682
300	0.00389	0.05	10.3444	0.28333	0.26005	0.96439	1.07882	-0.114432794
400	0.00691	0.05	12.9457	0.33213	0.29415	1.66266	1.7012	-0.038539633
432.226	0.00807	0.05	13.9423	0.34909	0.30628	1.95854	1.95854	-0.0000007618
500	0.0108	0.05	16.2901	0.38618	0.33317	2.71288	2.60509	0.107786339
600	0.01556	0.05	20.3778	0.44349	0.3755	4.20107	3.85746	0.343608005
700	0.02117	0.05	25.2086	0.50293	0.42013	6.21371	5.52601	0.687700246
800	0.02765	0.05	30.7827	0.56381	0.46637	8.83754	7.67888	1.158659696
900	0.035	0.05	37.1	0.6257	0.5138	12.1595	10.3845	1.774969597
1000	0.04321	0.05	44.1605	0.68832	0.56209	16.2665	13.7114	2.555040137
1100	0.05228	0.05228	52.284	0.75273	0.61264	21.3336	17.8416	3.492039967
1200	0.06222	0.06222	62.2222	0.82116	0.66833	27.6968	23.1632	4.533617628
1300	0.07302	0.07302	73.0247	0.88959	0.72403	35.2141	29.45	5.764096023
1400	0.08469	0.08469	84.6914	0.95802	0.77972	43.9815	36.7823	7.199216881
1500	0.09722	0.09722	97.2222	1.02645	0.83542	54.0953	45.2406	8.85472193
1600	0.11062	0.11062	110.617	1.09488	0.89111	65.6517	54.9053	10.7463529
1700	0.12488	0.12488	124.877	1.16331	0.94681	78.7468	65.8569	12.88985151
1800	0.14	0.14	140	1.23174	1.0025	93.4767	78.1758	15.30095949
1350	0.07875	0.07875	78.75	0.92381	0.75188	39.4355	32.9804	6.455092287
450	0.00875	0.05	14.525	0.35865	0.31316	2.13841	2.11379	0.024619305

				N	2
a0	153.5998564	b0	12.9142112	a0'	153.5998564
a1	0.0255499	b1	0.0343057	a1'	0.01277495
a2	-0.0000462	b2	-0.0000061	a2'	-0.00001155

Qdes	1800	gpm
Hdes	140	gpm

Independent head ratio

Z_des	x+y	Z_min
0.14	0.86	0.05

w1,P1 for single pump operation

w2,P2 for 2 pump operation

Q	efficiency based P_total
0	0.12564
100	0.28244
200	0.53269
300	0.96439
400	1.66266
432.226	1.95854
500	2.60509
600	3.85746
700	5.52601
800	7.67888
900	10.3845
1000	13.7114
1100	17.8416
1200	23.1632
1300	29.45
1400	36.7823
1500	45.2406
1600	54.9053
1700	65.8569
1800	78.1758

red color single pump

blue colo 2 pump

Figure B-8: VPF configuration Pump Power Consumption Simulation with DP Reset control Method

$$z = \left(\frac{Q}{Q_{des}}\right)^2 * z_{des}$$

$$z\_final = max\{z, z_{min}\}$$

$$H = H_{des} * (z_{final} + (1 - z_{des}) * \left(\frac{Q}{Q_{des}}\right)^2)$$

$\omega 1 = \frac{-a_1 * Q + \sqrt{(a_1 * Q)^2 - 4 * a_0 * (a_2 * Q^2 - H)}}{2 * a_0}$ Speed ratio when 1 pump is in operation;

$\omega 2 = \frac{-a_1' * Q + \sqrt{(a_1' * Q)^2 - 4 * a_0' * (a_2' * Q^2 - H)}}{2 * a_0'}$ Speed ratio when 2 pumps are in operation;

$a_0' = a_0; a_1' = \frac{a_1}{N}; a_2' = a_2/N^2$ N=2 (number of pumps in operation);

$P1 = \left(b_0 + \frac{Q}{\omega 1} * b_1 + \left(\frac{Q}{\omega 1}\right)^2 * b_2\right) * \omega 1^3$ Power consumption when 1 pump is in operation;

$P2 = \left(b_0 + \frac{Q}{2 * \omega 2} * b_1 + \left(\frac{Q}{2 * \omega 2}\right)^2 * b_2\right) * \omega 2^3 * 2$ Power consumption when 2 pumps are in operation;

Figure B-9: equations utilized in VPF configuration Pump Power Consumption Simulation with DP Reset control Method

Appendix – C: WNCC Trending Data Plots

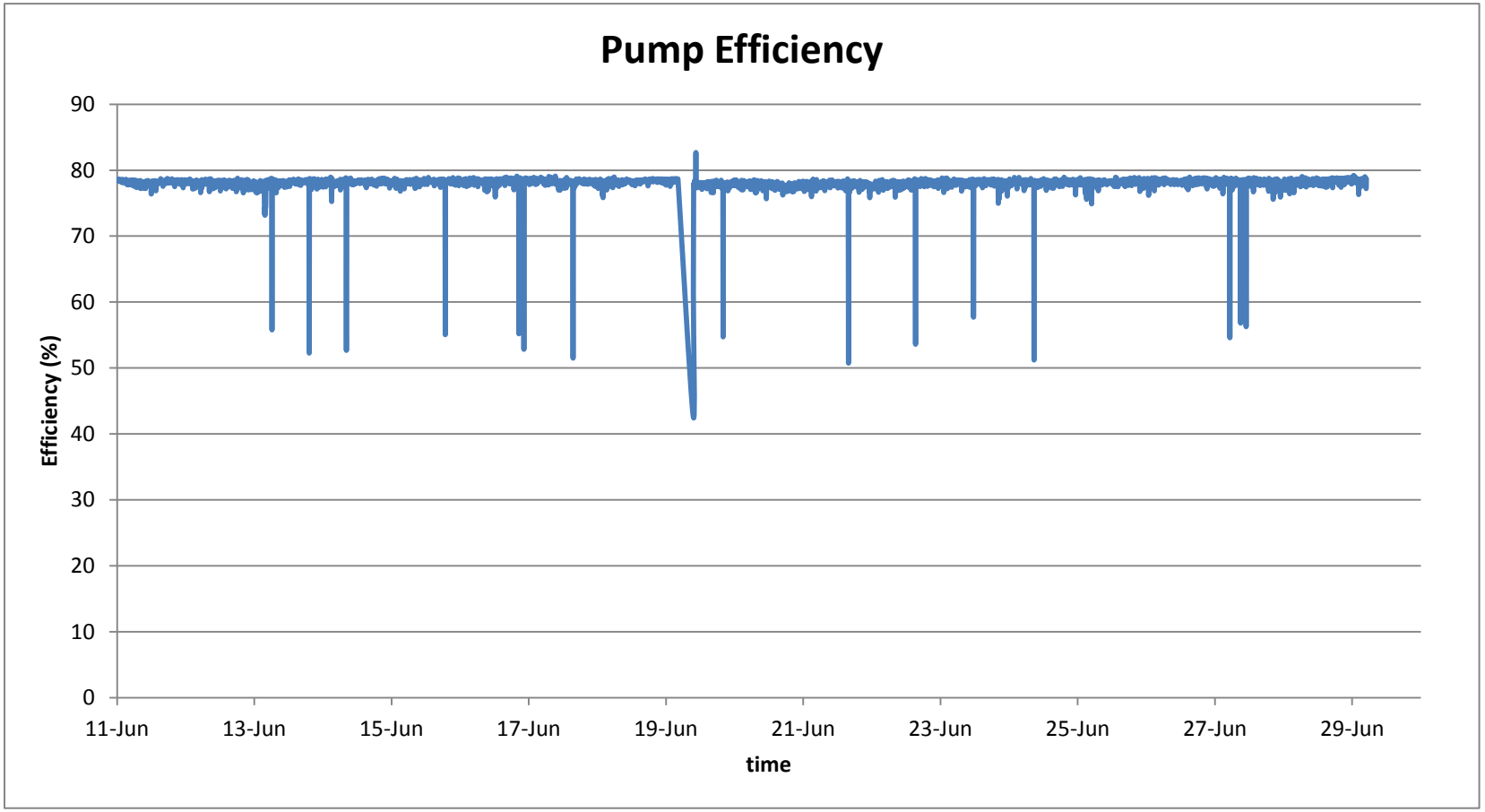

Figure C-1: pump system efficiency trending data plot during Jun 11th to Jun 29th with pump controller for WNCC

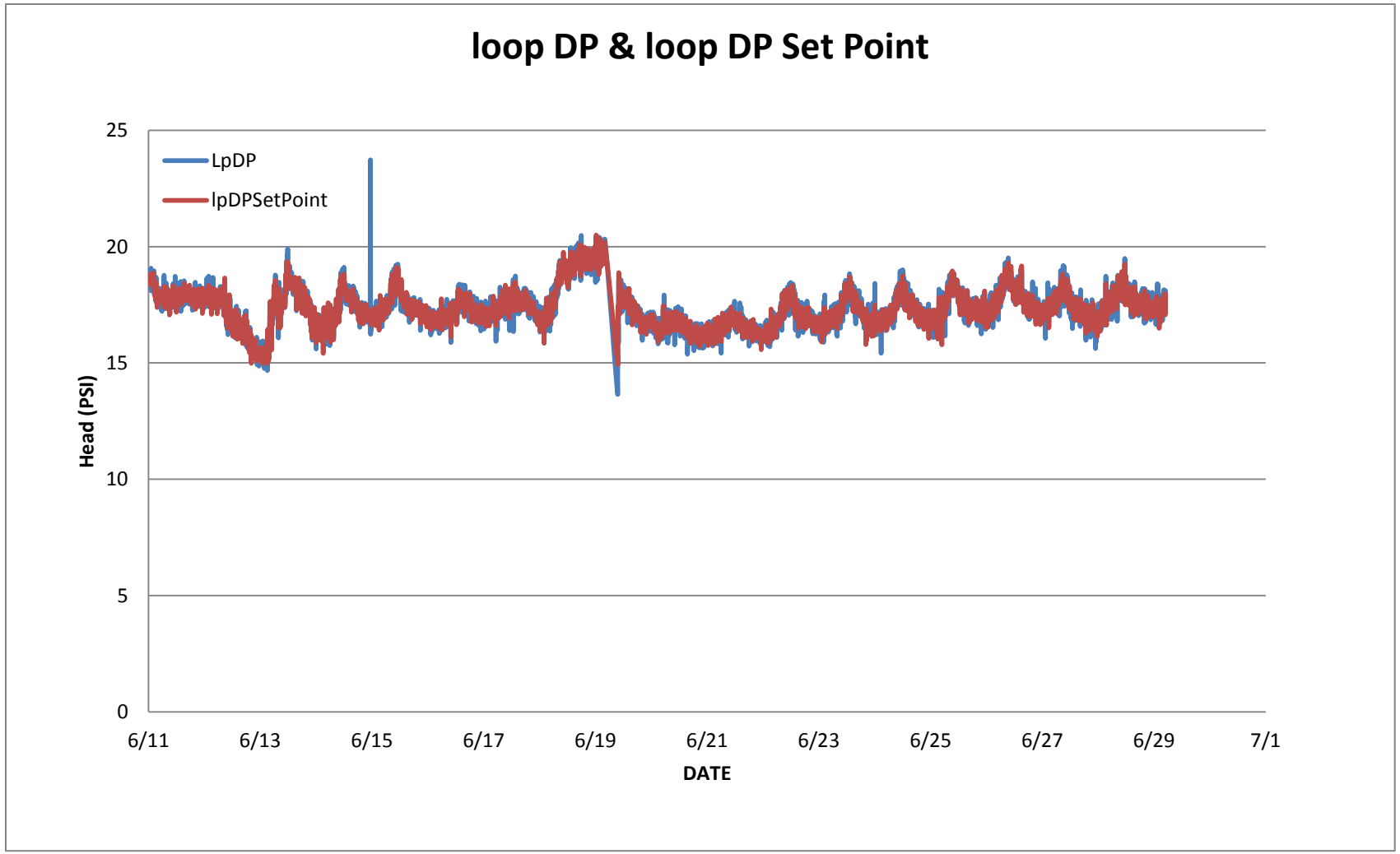

Figure C-2: loop DP & its set point trending data plot during Jun 11th to Jun 29th with pump controller for WNCC

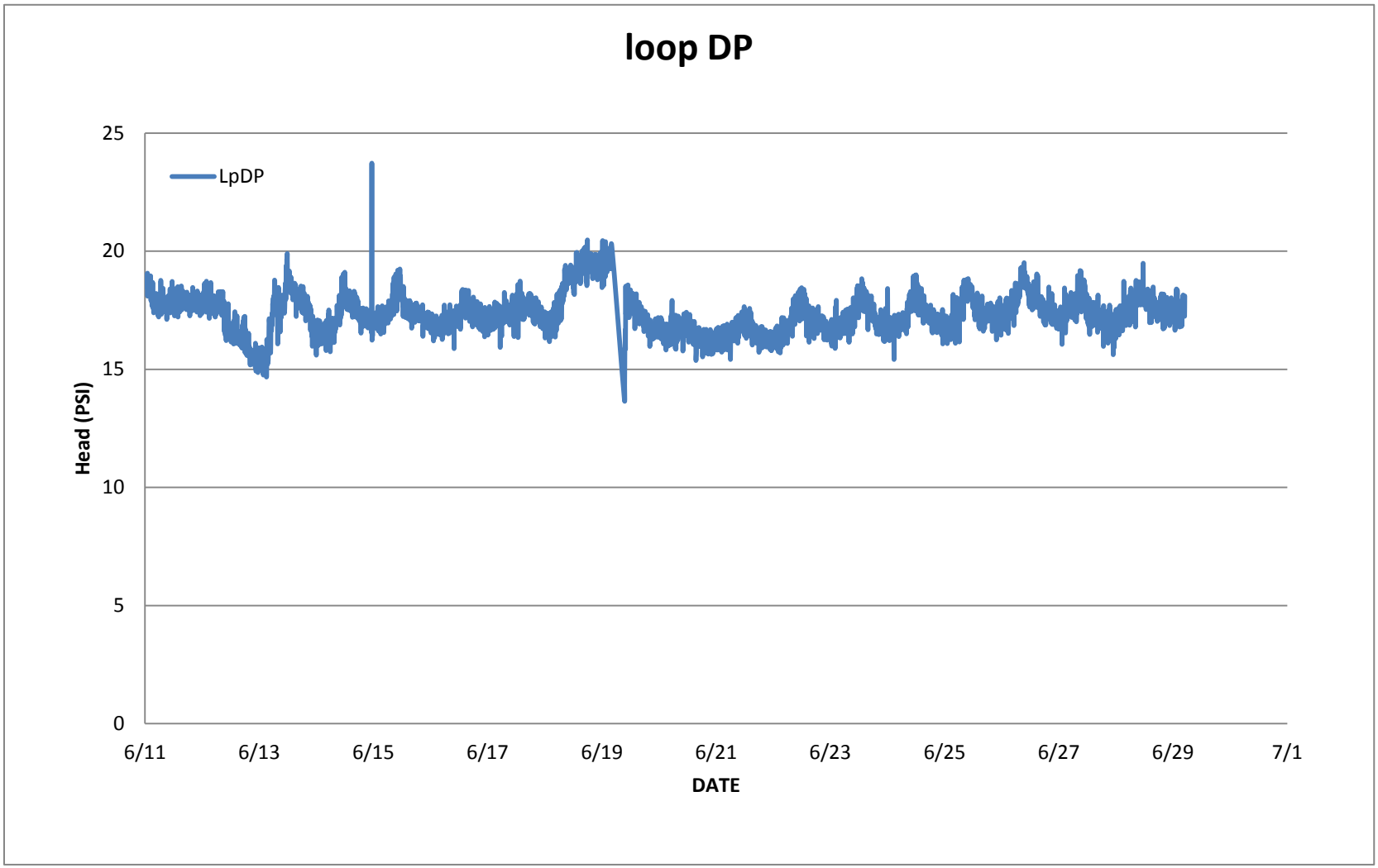

Figure C-3: Loop DP trending data plot during Jun 11th to Jun 29th with Pump Controller for WNCC

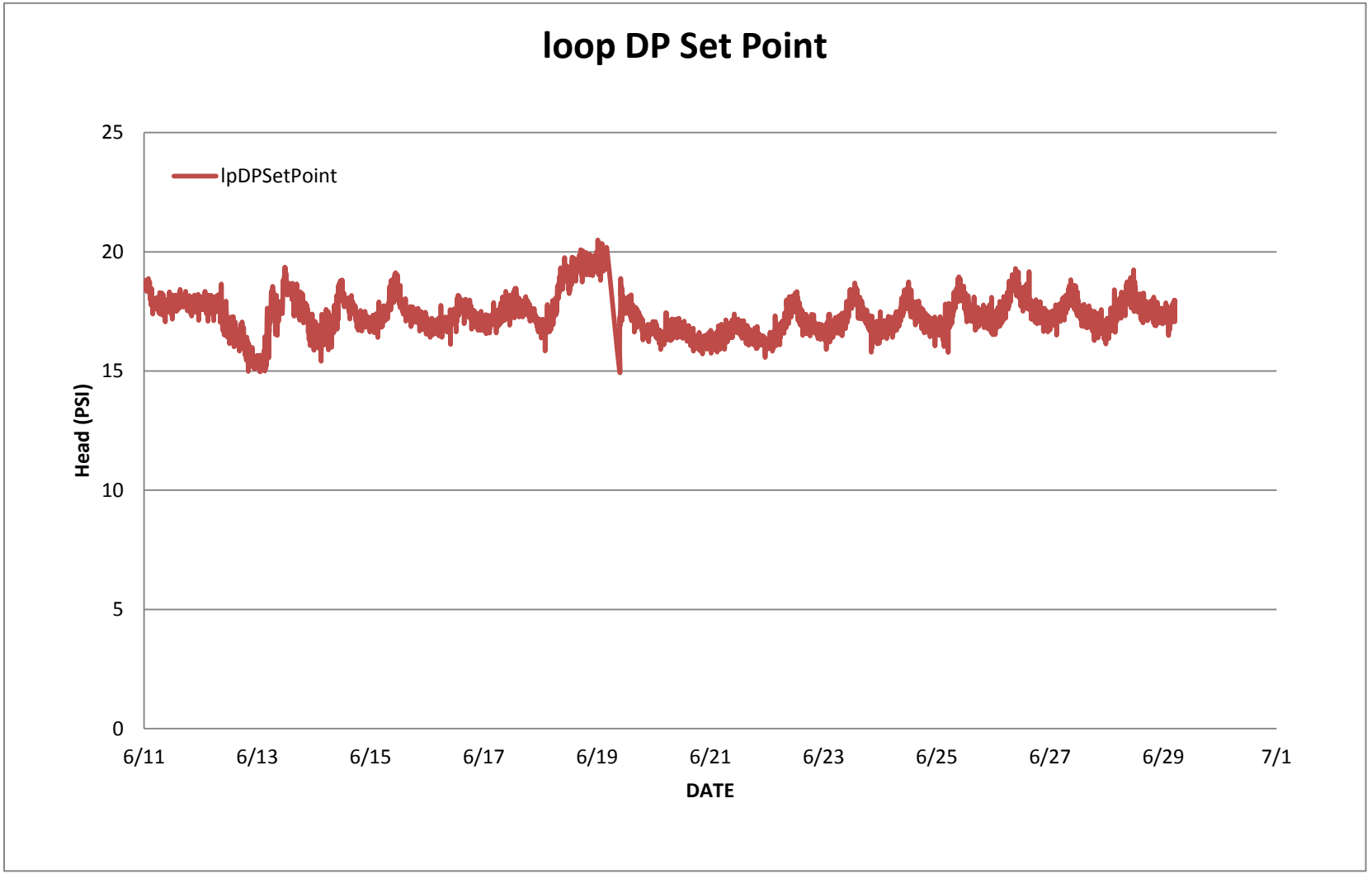

Figure C-4: loop DP set point trending data plot during Jun 11th to Jun 29th with Pump Controller for WNCC

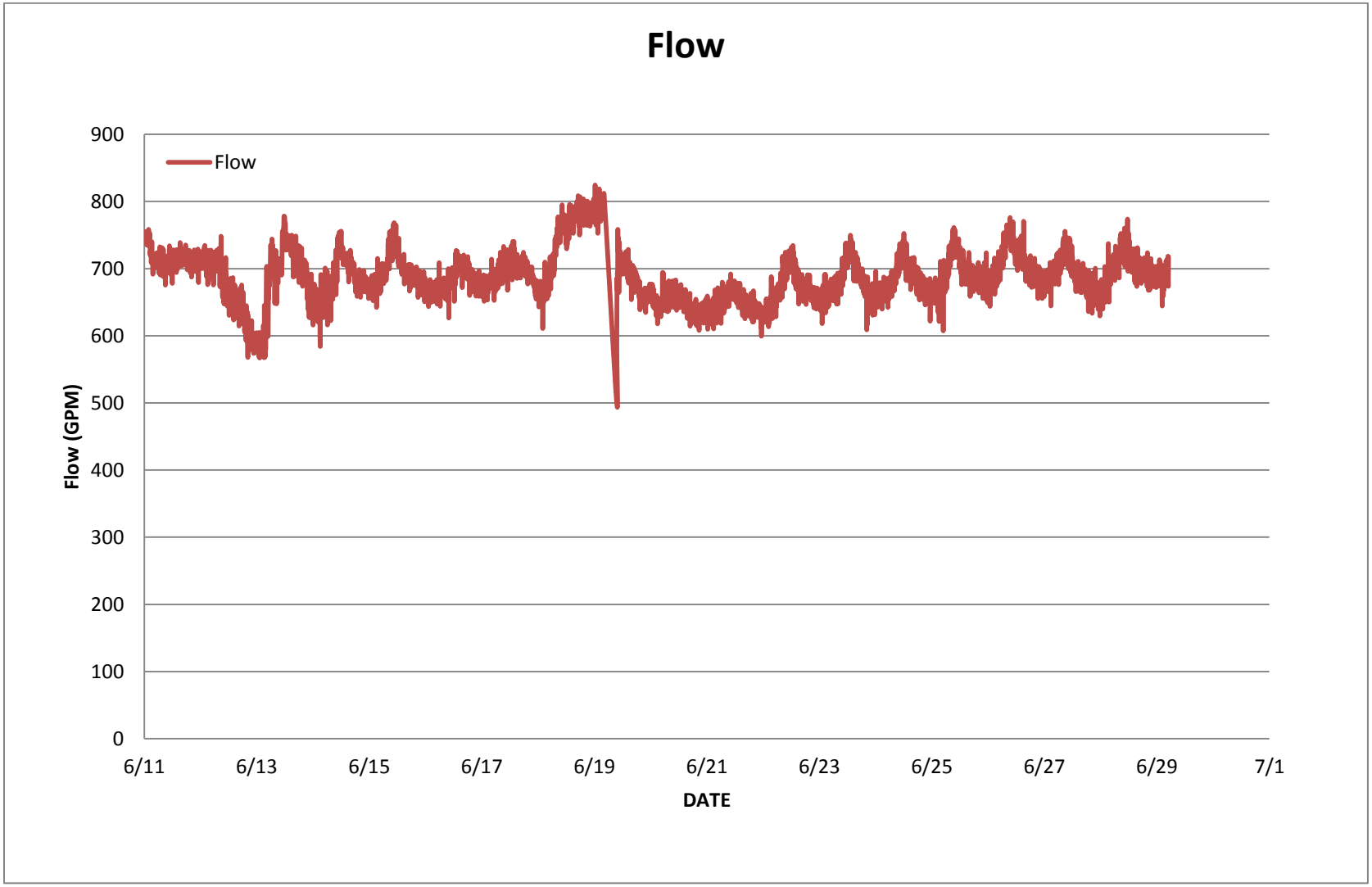

Figure C-5: Flow trending data plot during Jun 11th to Jun 29th with pump controller for WNCC

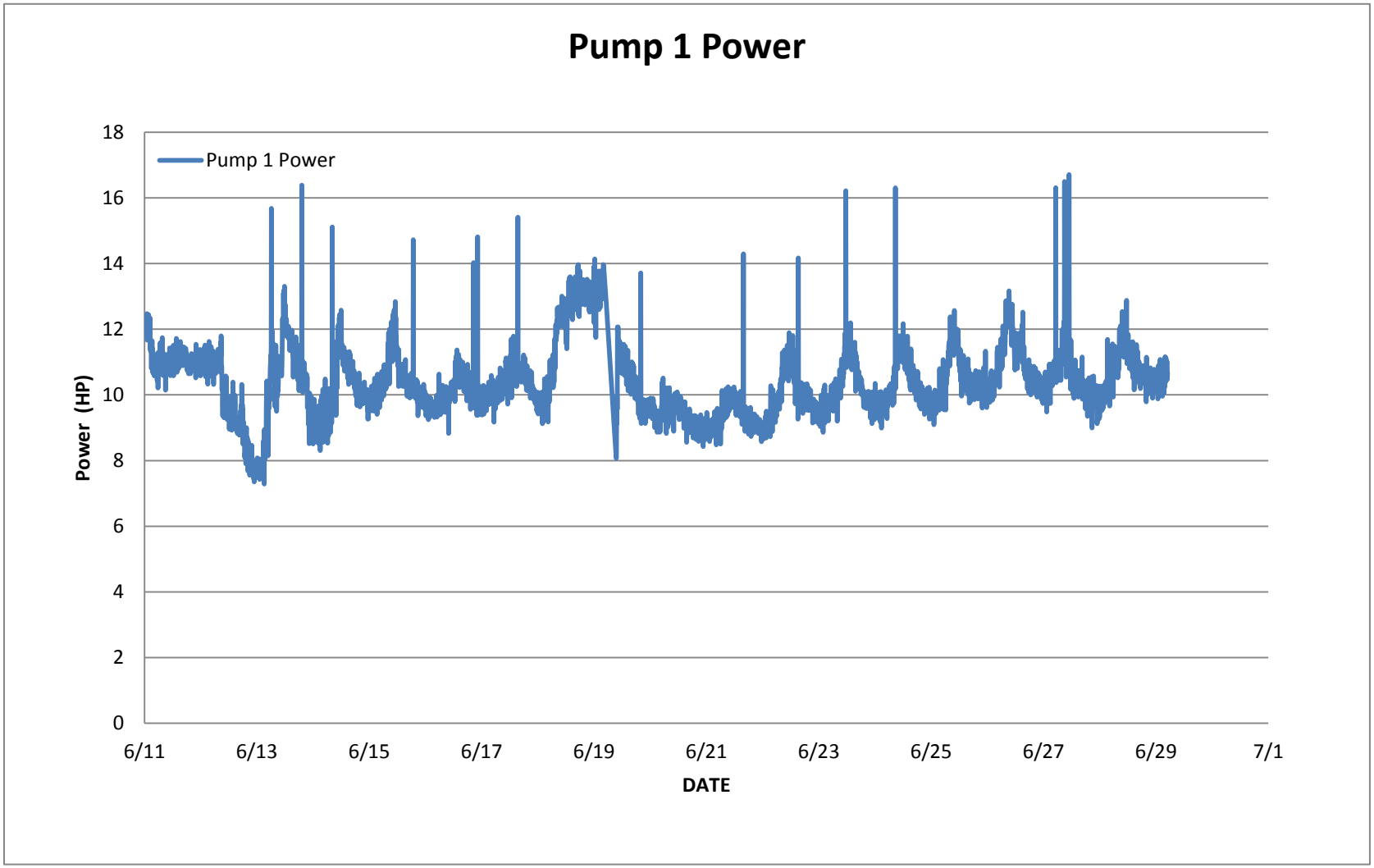

Figure C-6: P-1 Power trending data plot during Jun 11th to Jun 29th with pump controller for WNCC

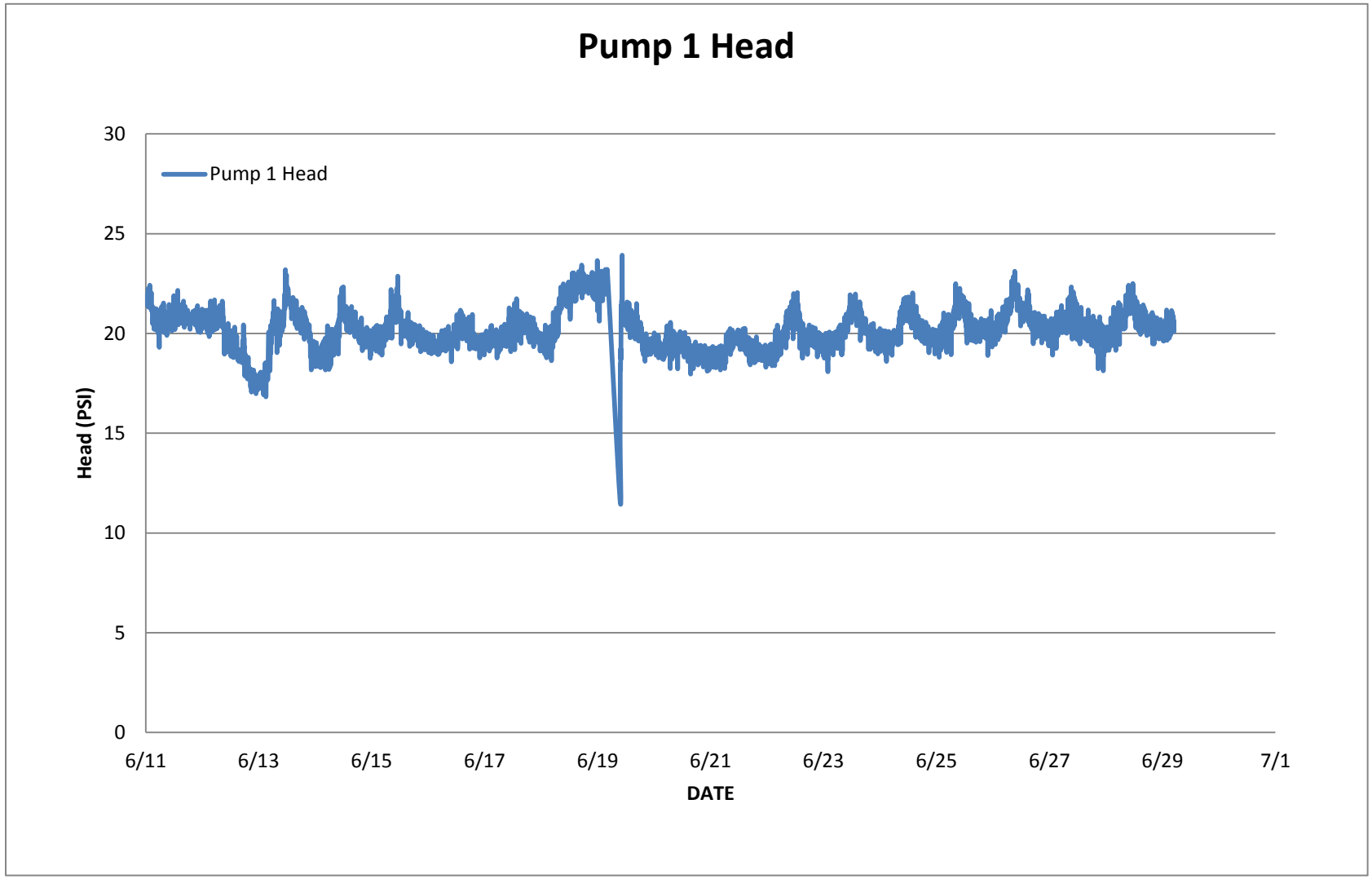

Figure C-7: Pump 1 Head trending data plot during Jun 11th to Jun 29th with pump controller for WNCC

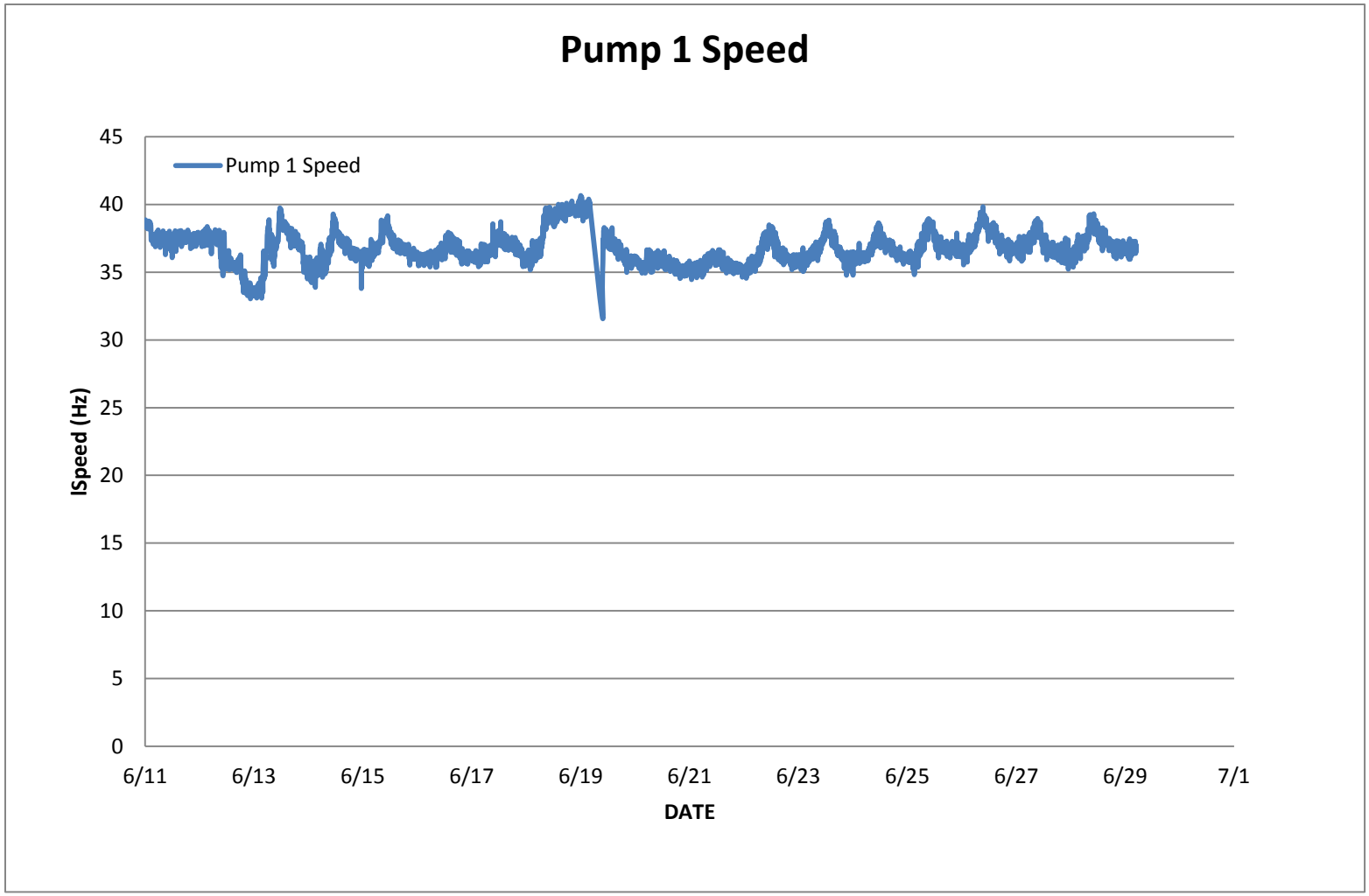

Figure C-8: Pump 1 Speed trending data plot during Jun 11th to Jun 29th with pump controller for WNCC

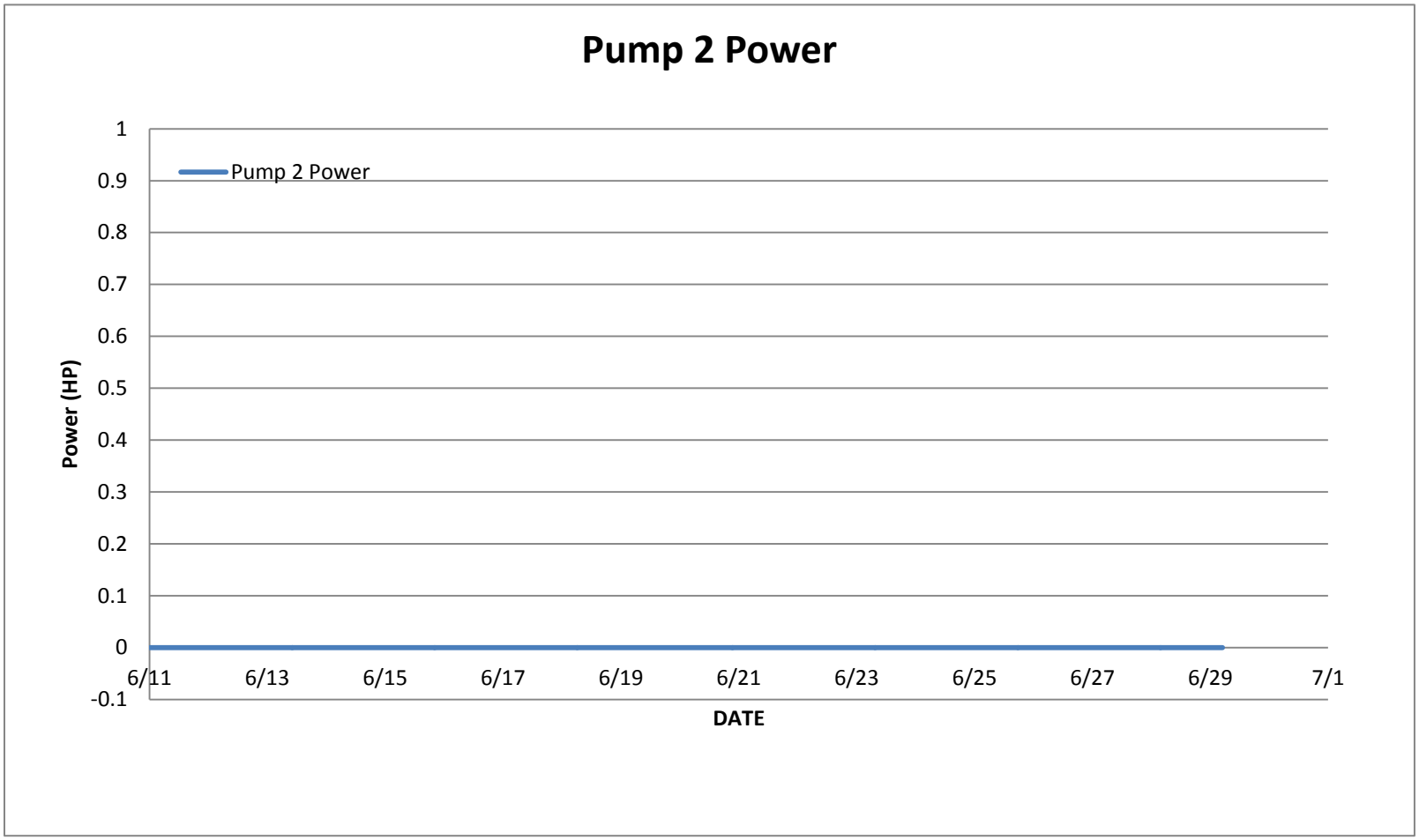

Figure C-9: Pump 2 Power trending data plot during Jun 11th to Jun 29th with pump controller for WNCC

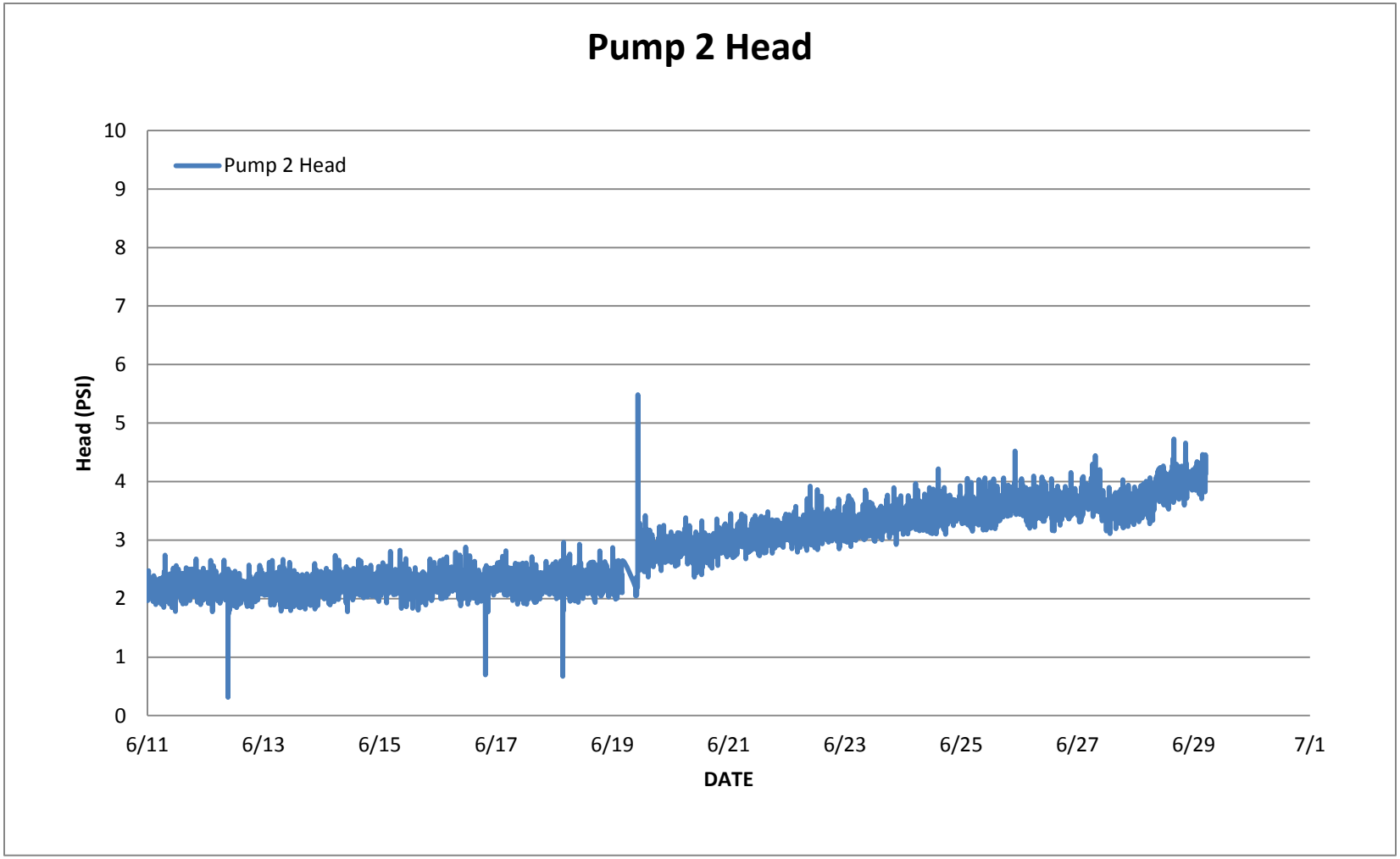

Figure C-10: Pump 2 Head trending data plot during Jun 11th to Jun 29th with pump controller for WNCC

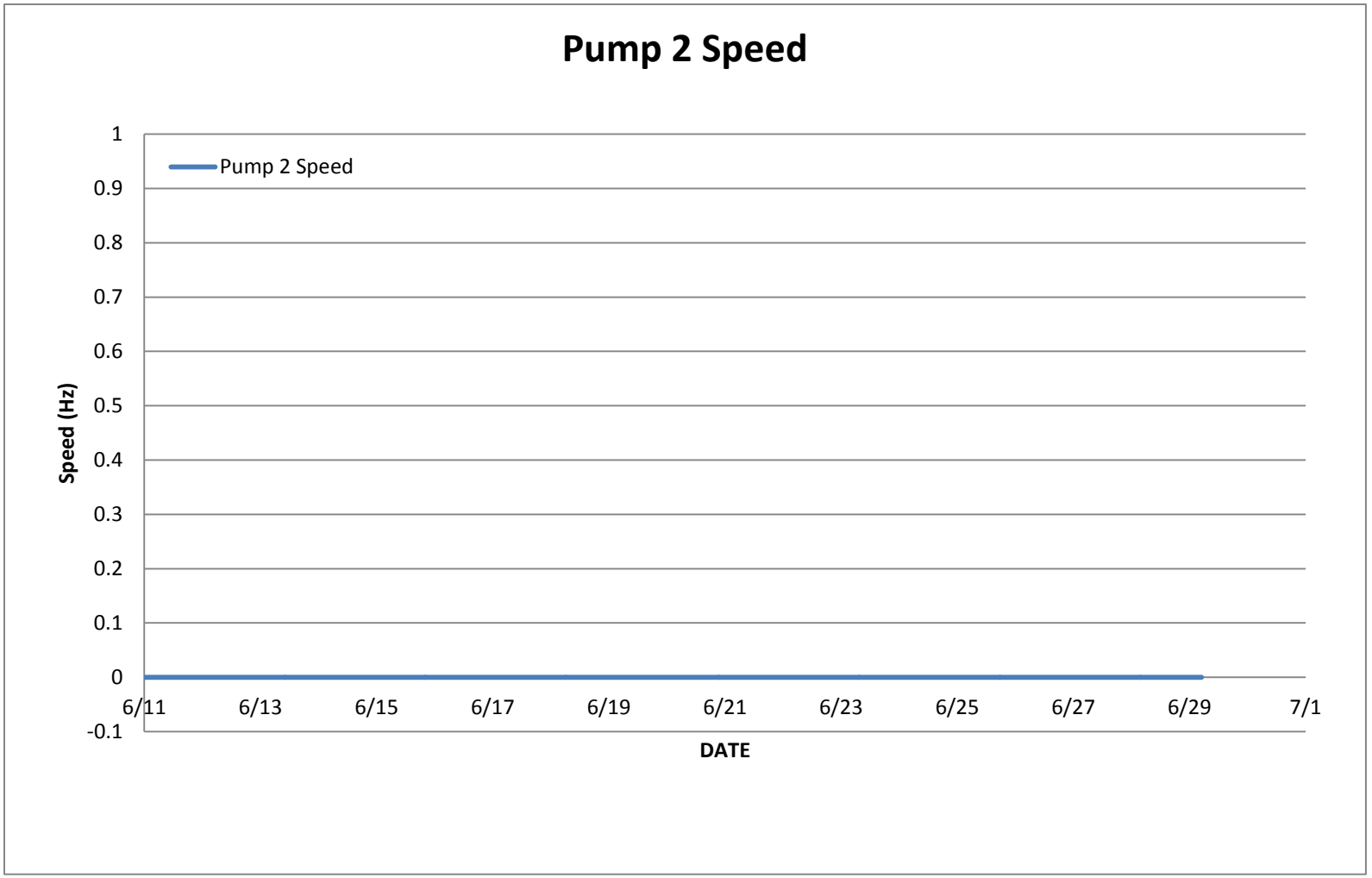

Figure C-11: Pump 2 Speed trending data plot during Jun 11th to Jun 29th with pump controller for WNCC

Appendix – D: Monthly Pump Power Consumption Prediction for WNCC

65F												
Month starting	CDD	% Estimated	GPM	Z	psi to fwg	2.31	vfd effic	0.95				
7/1/2011	295	0.5		0.861			motor effi	0.945				
8/1/2011	326	0.7		lpmin	10	a0	153.5999	b0	12.91421			
9/1/2011	110	1		lpmax	60	a1	0.02555	b1	0.034306			
10/1/2011	37	0.9		Qdes	1800	a2	-4.6E-05	b2	-6.1E-06			
11/1/2011	0	0.8										
12/1/2011	0	0.7										
1/1/2012	0	0.7										
2/1/2012	0	0.5		LPDP(psi)	P1DP(psi)	P1DP(fwg	P1SPD	P1PWR(HI	P1PWR(kV	with motor	with VFD	
3/1/2012	20	0.5	46.6	10.03358	11.6534	26.91935	0.415556	1.197545	0.893369	0.95	0.94	
4/1/2012	34	0.4	79.3	10.09703	11.7271	27.0896	0.41566	1.381482	1.030585	1.09	1.08	
5/1/2012	95	0.2	221.6	10.75754	12.49424	28.86169	0.432135	2.332111	1.739755	1.84	1.83	
6/1/2012	295	0.3	688.0							7.762	8.17	
7/1/2012	321	0.3	748.6	18.64904	21.65974	50.03401	0.643565	11.87913	8.861829	9.38	9.33	
8/1/2012	277	0.4	646.0	16.44047	19.09462	44.10857	0.590926	8.899339	6.638907	7.03	6.99	
9/1/2012	127	0.4	296.2	11.35383	13.1868	30.4615	0.450035	2.994177	2.233656	2.36	2.35	
10/1/2012	22	0.5	51.3	10.04063	11.66159	26.93826	0.415482	1.223421	0.912672	0.97	0.96	
11/1/2012	3	0.4								avg	3.96	
12/1/2012	1	0.3										
1/1/2013	0	0.2										
2/1/2013	0	0.5										

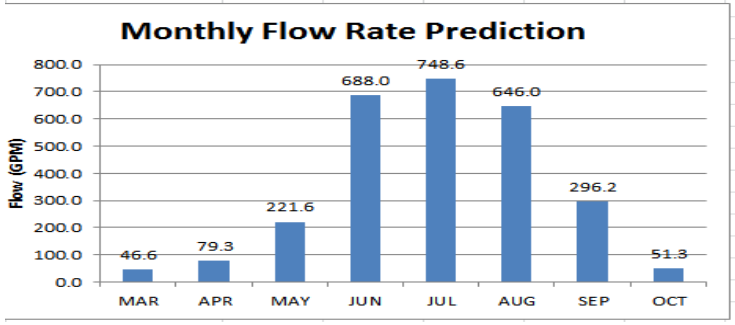

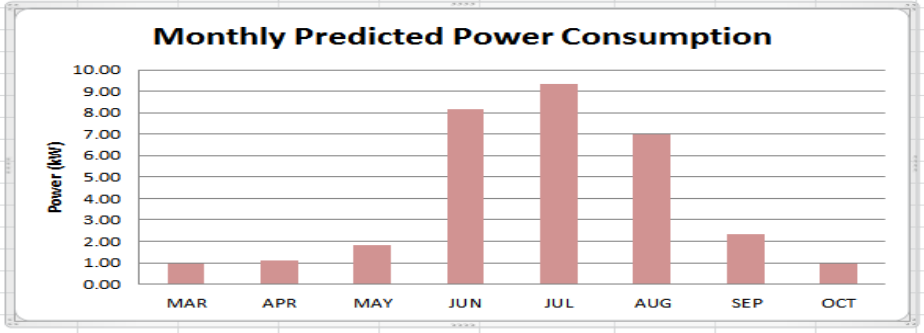

Figure D-1: Monthly Power Consumption Prediction Procedure for cooling in WNCC